Breakthroughs in Photonics 2009

Coherent Photon Sources · Ultrafast Photonics · Nonlinear Photonics
Terahertz Photonics · Nano-Photonics · Silicon Photonics
Photonics Materials · Bio-Photonics · Magneto-Photonics
Photovoltaics and Sensors · Integrated Photonics Systems

IEEE photonics SOCIETY

IEEE

Photo provided by Getty Images.
Photographer: David Fairfield

Breakthroughs in Photonics 2009

Table of Contents

Photonics Materials and Engineered Photonic Structures

Bio-Photonics

Magneto-Photonics

Photovoltaics and Sensors

Integrated Photonic Systems

Editorial

Breakthroughs in Photonics 2009

As founding Editor-in-Chief, I am pleased to introduce *Breakthroughs in Photonics*: an annual feature of the IEEE PHOTONICS JOURNAL. *Breakthroughs in Photonics* is intended to highlight major accomplishments across the broad spectrum of Photonics Science and Technology within the year. This Special Section is also intended to draw the attention of readers and authors to the topics that are within the scope of the journal.

Breakthroughs in Photonics 2009 contains 17 invited peer-reviewed briefs written by world-renowned experts. These briefs cover progress in the areas of ***Coherent Photon Sources, Ultrafast Photonics, Nonlinear Photonics, Terahertz Photonics, Nano-Photonics, Silicon Photonics, Bio-Photonics, Magneto-Photonics, Photonic Materials and Engineered Nano-structures, Photovoltaics and Sensors, and Integrated Photonics Systems***. These selected topics represent a subset of the much broader and intense activity in the generation, control, and utilization of radiation that takes place worldwide.

Assembling this Special Section has truly been a team effort. I would like to extend my gratitude to the authors for contributing with insightful and complete reviews and to the Editorial Board for their active participation in identifying critical areas across the field of Photonics and helping with recruitment of invited speakers. Last, I would like to thank the Editorial Staff and the IEEE for helping structure this annual Special Section in the IEEE PHOTONICS JOURNAL.

Carmen S. Menoni, *Editor-In-Chief*

Mid-Infrared Lasers

Timothy J. Carrig, *Senior Member, IEEE*, and Andrew M. Schober

(Invited Paper)

Lockheed Martin Coherent Technologies, Louisville, CO 80027 USA

DOI: 10.1109/JPHOT.2010.2044653
1943-0655/$26.00 ©2010 IEEE

Manuscript received January 21, 2010. Current version published April 23, 2010. Corresponding author: T. J. Carrig (e-mail: Tim.Carrig@lmco.com).

Abstract: We review breakthroughs in the area of mid-infrared laser development. We summarize 2009 research across a broad range of mid-infrared laser technologies, including bulk solid-state lasers, fiber lasers, and nonlinear optics for the generation of infrared light between 2 and 8 μm.

Index Terms: Solid-state lasers, laser crystals, infrared lasers, nonlinear crystals, fiber lasers, MIR devices.

1. Introduction

This paper discusses recent worldwide progress developing solid-state lasers and nonlinear optical devices in the mid-infrared (MIR) spectral region. For the purposes of this review, we choose to generously define the MIR as from $\sim$2 to 8 μm. This review encompasses bulk solid-state and fiber lasers but does not include semiconductor laser sources. Advances in the development of laser and nonlinear materials are also described.

The MIR spectral region is important for a variety of scientific, medical, and remote-sensing applications. For instance, a number of chemicals have characteristic absorption features in the 2- to 4-μm band, making MIR laser sources desirable for applications such as trace gas sensing and breath analysis and devices such as laser scalpels. The MIR region also contains atmospheric windows with very high optical transmission and low aerosol scattering which, when combined with the relatively high eye safety of MIR sources, makes MIR lasers useful for wind field profiling and free-space optical communications. Additionally, some novel applications described in the literature in 2009 include the generation of coherent X-rays [1], a 1.5-W tunable frequency comb with idler output from 2.8 to 4.8 μm [2], and a spectrometer for sub-Doppler resolution molecular absorption spectroscopy [3].

MIR laser source research continues because existing devices often fail to meet the size, weight, power, efficiency, or cost requirements of many commercial and military users. Challenges include development of low optical loss materials, limited optical pump sources, and a smaller industrial base for components than at wavelengths such as 1.5 μm.

2. Crystalline and Poly-Crystalline Solid-State Lasers

Bulk laser development research centered around Tm^{3+} and Ho^{3+} lasers in garnet, tungstate and fluoride hosts, and Cr^{2+}-doped chalcogenide lasers. Tm lasers were of particular interest with a single-frequency, Tm:YAG nonplanar ring oscillator reported that output over 800 mW [4]. A broadly

tunable, 1.847 to 2.069 μm, continuous-wave (CW) Tm:$NaY(WO_4)_2$ laser with $\sim$400-mW peak output power [5] and a Tm:$KLu(WO_4)_2$ laser, passively mode locked using carbon nanotubes, that produced 10-ps pulses at 1.950 μm [6], were also demonstrated. Additionally, the investigation of CW lasing in Tm:$GdLiF_4$ was conducted with tunable output from 1.826 to 2.054 μm approaching 1 W power [7]. CW and Q-switched operation of diode-pumped Tm:$LiLuF_4$ slab lasers was reported with an output of 10 W in CW mode and 8 W at 1-kHz pulse repetition frequency (PRF) with 315-ns duration pulses in pulsed mode [8].

Work also continued on the development of materials that transfer energy from Tm to Ho with advances including demonstrations of both the first CW [9] and passive mode-locked [10] operation of Tm, Ho:$KY(WO_4)_2$. Passive Q-switched mode locking of alphabet (i.e., triple doped, with flashlamp-pumped Cr^{3+} ions acting as a sensitizer for Tm, which then transfers energy to Ho) $Y_3Sc_2Al_2O_{12}$ was also reported [11].

Singly doped Ho lasers, resonantly pumped by Tm lasers, were also of interest with a $\sim$10-W output power, 10-kHz PRF, Ho:LuAG laser [12]; a CW, Ho:Lu_2SiO_5 laser [13]; and an injection-seeded, 1-kHz PRF, $\sim$6-mJ output pulse energy Ho:YLF laser [14] reported. Direct pumping of Ho:LuAG, with InGaAsP diodes, was also demonstrated [15].

Research with broadly tunable Cr:ZnSe lasers continued with an emphasis on finding practical pump sources. 2009 results include demonstrations of a $\sim$10-W CW laser pumped by a Tm fiber laser [16] and a 1.8-W laser pumped by a semiconductor disk laser [17]. Using Tm fiber laser pump sources, a Kerr-lens mode-locked Cr:ZnSe laser producing 95-fs pulses [18] and a passively mode-locked Cr:ZnSe laser producing 130-fs pulses [19] were reported. Cr:ZnS material, which is similar in properties to Cr:ZnSe, was demonstrated in a 10-W room-temperature laser pumped by an Er fiber laser [20].

Laser gain media research included studies of emission and gain in glass ceramics containing Tm, Ho:BaF_2 nanocrystals [21] for 2-μm lasing and theoretical and experimental investigations of 3-μm laser action in Er:YLF [22]. Additionally, studies of optical bistability [23] and thermal lensing [24] in Tm,Ho:YLF and Tm:YLF, respectively, were reported.

3. Fiber Lasers and Fiber Nonlinear Optics

Silica fiber laser research included the development of Tm, Ho, and Er lasers. Of particular interest were high-power demonstrations including a 885-W, multimode laser [25] and a 600-W Tm fiber amplifier chain [26] operating at 2.04 μm. We expect that in 2010, the first kilowatt-class Tm fiber lasers will be reported. The 100-W milestone was also demonstrated in Tm fiber lasers with $>$ 100 nm of wavelength tuning [27] and with pulsed operation [28].

A number of single-frequency Tm fiber lasers and amplifiers were demonstrated, including a 1.95-μm CW laser with less than 3-kHz linewidth [29], a 1950-nm Q-switched laser [30], a tunable, 0.3-nm linewidth laser that operated from 1.981 to 2.095 μm [31], and a 20-W, 100-kHz-linewidth, polarization-maintaining amplifier [32]. Additionally, a picosecond-class mode-locked laser was demonstrated using a fiber less than 1 m in length [33], and a 750-fs Tm:fiber laser was mode locked using a carbon nanotube saturable absorber [34].

Advances with Er fiber lasers around 2.8 μm include the demonstration of a highly stable, 5-W laser with optical efficiency greater than 30% [35]. Reported Ho fiber laser work included the demonstration of gain-switched [36] and Q-switched [37] lasers operating at 80-kHz PRF, as well as a Tm fiber-laser-pumped Ho fiber laser with 4.3 W of output power [38].

Also of interest were reports of 3-μm fluoride fiber lasers, including the report of a 24-W Er laser [39] and a 2.94-μm laser based on Ho to Pr energy transfer pumped at 1.15 μm by InGaAs diodes [40].

In addition to widespread work in traditional fiber lasers, new chalcogenide microstructured fibers for MIR generation were reported [41]–[43]. Novel MIR optical fibers are being developed with high transparency in the MIR and offer promise for supercontinuum generation, Raman lasers, and parametric mixers. An example was the generation of 10.5 W of supercontinuum, from 1 to 4 μm, in fluoride fiber [44].

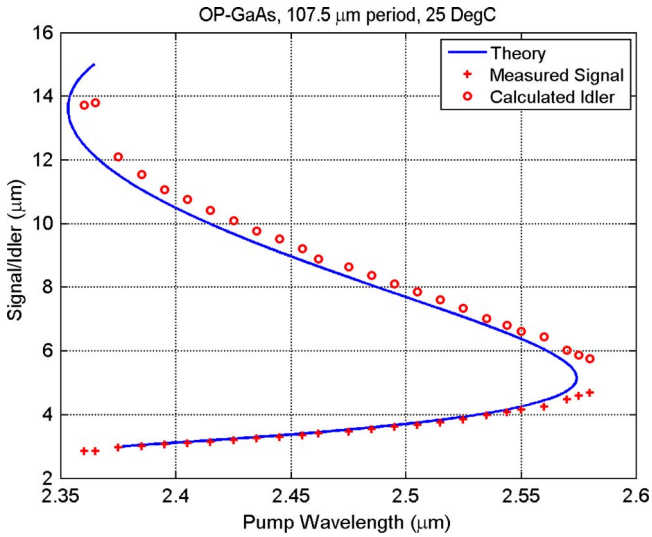

Fig. 1. Demonstration of tunable infrared generation in an OP-GaAs OPO pumped by a broadly tunable Cr:ZnSe laser. Solid line is the Sellmeier prediction, crosses represent measured signal wavelengths, and circles indicate calculated idler wavelengths. A single OP-GaAs OPO is capable of generating idler wavelengths between 3 and 14 μm with tuning of the Cr:ZnSe pump laser from 2.36 to 2.58 μm.

4. Nonlinear Optics

Parametric mixing, via oscillators, amplifiers, or difference-frequency mixers, continues to be an important technology for the generation of MIR light at wavelengths or output powers inaccessible via direct solid-state or semiconductor sources. Periodically poled $LiNbO_3$ (PPLN) is the material of choice for many of these applications. For instance, in 2009, PPLN devices have been utilized for waveform generation for MIR optical communications [45] and in the generation of light for trace gas detection [46], [47]. Supporting these uses, refined Sellmeier equations were reported for 5% MgO-doped periodically poled $LiNbO_3$ [48].

With the ability to design for wide gain bandwidth, parametric devices are particularly well suited for ultrafast applications. Recent demonstrations of short-pulse ultrafast optical parametric oscillators (OPOs) include phase-stabilized synchronously pumped parametric oscillators [2]. Additionally, optical parametric chirped pulsed amplification, utilizing MgO:PPLN, was used to generate 2-cycle pulses at 2.1 μm [49] and 2.2 μm [50], as well as 1-μJ, 8- to 9-cycle MIR pulses [51], [52].

NLO materials research included progress developing novel materials such as $CdSiP_2$, $LiInSe_2$, GaSSe compounds, $BaMgF_4$, and quasi-phase-matched (QPM) GaAs. $CdSiP_2$ is of high interest because of its ability to be pumped at near-infrared wavelengths such as 1 and 1.5 μm, transparency through the MIR, and the ability to grow and fabricate samples with high optical quality [53]. $LiInSe_2$ can be pumped at 1 μm without two-photon absorption and has generated 282 μJ at 6.2 μm [54]. GaSSe compounds were also investigated for 1-μm pumping without two-photon absorption [55]. Similarly, $BaMgF_4$ offers high transparency from the ultraviolet through the long infrared, with quasi-phase-matching achievable through the whole transparent wavelength region and birefringent phase-matching possible in a more limited region spanning 0.573 to 5.634 μm [56].

Work with GaAs included a demonstration of room-temperature direct-plate bonding [57]. It was reported that bonding of ZnSe and GaP plates had also been achieved. QPM GaAs remains of high interest because of its high nonlinear coefficient, broad transparency, and attractive thermal and phase-matching properties. Fig. 1 shows a recently measured tuning curve, demonstrating that a tunable Cr:ZnSe laser pumping an orientation-patterned GaAs (OP-GaAs) OPO can provide continuous tuning from 3 to 14 μm using a single laser/OPO source [58]. In addition to continued improvement in QPM device growth processes and material quality [59], [60], QPM GaAs was shown to exhibit polarization-diverse frequency mixing [61] and has been demonstrated in a 20–50-kHz

PRF OPO pumped by a Ho:YAG laser [62]. Demonstrated output was 2.85 W with 46% conversion efficiency.

New QPM microstructured devices in silicon waveguides were also reported [63]. Although calculated conversion to 6 μm in guided-wave devices was estimated in this work, we await publication of experimental results from this new material.

5. Conclusion

To conclude, 2009 saw significant activity in the field of MIR laser development. This research will continue in 2010 due to the on-going need for improved laser sources at these wavelengths.

References

[1] H. Xiong, H. Xu, Y. Fu, J. Yao, B. Zeng, W. Chu, Y. Cheng, Z. Xu, E. Takahashi, K. Midorikawa, X. Liu, and J. Chen, "Generation of a coherent x ray in the water window region at 1 kHz repetition rate using a mid-infrared pump source," *Opt. Lett.*, vol. 34, no. 11, pp. 1747–1749, Jun. 2009.

[2] F. Adler, K. C. Cossel, M. J. Thorpe, I. Hartl, M. E. Fermann, and J. Ye, "Phase-stabilized, 1.5 W frequency comb at 2.8–4.8 μm," *Opt. Lett.*, vol. 34, no. 9, pp. 1330–1332, May 2009.

[3] M. Abe, K. Takahata, and H. Sasada, "Sub-Doppler resolution 3.4 μm spectrometer with an efficient difference-frequency-generation source," *Opt. Lett.*, vol. 34, no. 11, pp. 1744–1746, Jun. 2009.

[4] C. Gao, M. Gao, Y. Zhang, Z. Lin, and L. Zhu, "Stable single-frequency output at 2.01 μm from a diode-pumped monolithic double diffusion-bonded Tm:YAG nonplanar ring oscillator at room temperature," *Opt. Lett.*, vol. 34, no. 19, pp. 3029–3031, Oct. 2009.

[5] M. Rico, J. M. Cano-Torres, M. D. Serrano, C. Cascales, and C. Zaldo, "Tunable continuous-wave near 2-μm laser operation in Tm^{3+} in$NaY(WO_4)_2$ single crystal," presented at the Advanced Solid-State Photon. Conf., Denver, CO, Feb. 1–4, 2009.

[6] W. B. Cho, A. Schmidt, J. H. Kim, S. Y. Choi, S. Lee, F. Rotermund, U. Griebner, G. Steinmeyer, V. Petrov, X. Mateos, M. C. Pujol, J. J. Carvajal, M. Aguilo, and F. Diaz, "Passive mode-locking of a Tm-doped bulk laser near 2 μm using a carbon nanotube saturable absorber," *Opt. Exp.*, vol. 17, no. 13, pp. 11 007–11 012, Jun. 2009.

[7] N. Coluccelli, G. Galzerano, F. Cornacchia, A. Di Lieto, M. Tonelli, and P. Laporta, "High-efficiency diode-pumped Tm:$GdLiF_4$ laser at 1.9 μm," *Opt. Lett.*, vol. 34, no. 22, pp. 3559–3561, Nov. 2009.

[8] X. Cheng, S. Zhang, J. Xu, H. Peng, and Y. Heng, "High-power diode-end-pumped Tm:$LiLuF_4$ slab lasers," *Opt. Exp.*, vol. 17, no. 17, pp. 14 895–14 901, Aug. 2009.

[9] A. A. Lagatsky, F. Fusari, C. T. A. Brown, W. Sibbett, S. V. Kurilchik, V. E. Kisel, A. S. Yasukevich, N. V. Kuleshov, and A. A. Pavlyuk, "Efficient continuous-wave, 2-μm Tm,Ho:$KY(WO_4)_2$ laser," presented at the Advanced Solid-State Photon. Conf., Denver, CO, Feb. 1–4, 2009.

[10] A. A. Lagatsky, F. Fusari, S. Calvez, J. A. Gupta, V. E. Kisel, N. V. Kuleshov, C. T. A. Brown, M. D. Dawson, and W. Sibbett, "Passive mode locking of a Tm,Ho:$KY(WO_4)_2$ laser around 2 μm," *Opt. Lett.*, vol. 34, no. 17, pp. 2587–2589, Sep. 2009.

[11] I. A. Denisov, N. A. Skoptsov, M. S. Gaponenko, A. M. Malyarevich, K. V. Yumashev, and A. A. Lipovskii, "Passive mode locking of 2.09 μm Cr, Tm,Ho:$Y_3Sc_2Al_3O_{12}$ laser using PbS quantum-dot-doped glass," *Opt. Lett.*, vol. 34, no. 21, pp. 3403–3405, Nov. 2009.

[12] X. Duan, B. Yao, G. Li, Y. Ju, Y. Wang, and G. Zhao, "High efficient actively Q-switched Ho:LuAG laser," *Opt. Exp.*, vol. 17, no. 24, pp. 21 691–21 697, Nov. 2009.

[13] B.-Q. Yao, Z.-P. Yu, X.-M. Duan, Z.-M. Jiang, Y.-J. Zhang, Y.-Z. Wang, and G.-J. Zhao, "Continuous-wave laser action around 2-μm in Ho^{3+}:Lu_2SiO_5," *Opt. Exp.*, vol. 17, no. 15, pp. 12 582–12 587, Jul. 2009.

[14] Y. Bai, J. Yu, M. Petros, P. Petzar, B. Trieu, H. Lee, and U. Singh, "High repetition rate and frequency stabilized Ho:YLF laser for CO_2 differential absorption lidar," presented at the Advanced Solid-State Photon. Conf., Denver, CO, Feb. 1–4, 2009.

[15] N. P. Barnes, F. Amzajerdian, D. J. Reichle, G. Busch, and P. Leisher, "1.88 μm InGaAsP pumped, room temperature Ho:LuAG laser," presented at the Conf. Lasers Electro-Optics, Baltimore, MD, May 31–Jun. 5, 2009.

[16] I. S. Moskalev, V. V. Fedorov, S. B. Mirov, P. A. Berry, and K. L. Schepler, "12-watt CW polycrystalline Cr^{2+}:ZnSe laser pumped by a Tm-fiber laser," presented at the Conf. Lasers Electro-Optics, Baltimore, MD, May 31–Jun. 5, 2009.

[17] N. Hempler, J.-M. Hopkins, B. Rosener, M. Rattunde, J. Wagner, V. V. Fedorov, I. S. Moskalev, S. B. Mirov, and D. Burns, "Semiconductor disk laser pumped Cr^{2+}:ZnSe lasers," *Opt. Exp.*, vol. 17, no. 20, pp. 18 136–18 141, Sep. 2009.

[18] M. N. Cizmeciyan, H. Cankaya, A. Kurt, and A. Sennaroglu, "Kerr-lens mode-locked femtosecond Cr^{2+}:ZnSe laser at 2420 nm," *Opt. Lett.*, vol. 34, no. 20, pp. 3056–3058, Oct. 2009.

[19] E. Slobodtchikov, "The progress in near and mid-IR ultrafast laser systems at Q-peak," presented at the Directed Energy Professional Society Ultrafast Workshop, Newton, MA, 2009.

[20] I. S. Moskalev, V. V. Fedorov, and S. B. Mirov, "10-watt, pure continuous-wave, polycrystalline Cr^{2+}:ZnS laser," *Opt. Exp.*, vol. 17, no. 4, pp. 2048–2056, Feb. 2009.

[21] W. J. Zhang, Q. Y. Zhang, Q. J. Chen, Q. Qian, Z. M. Yang, J. R. Qiu, P. Huang, and Y. S. Wang, "Enhanced 2.0 mm emission and gain coefficient of transparent glass ceramic containing BaF_2:Ho^{3+},Tm^{3+} nanocrystals," *Opt. Exp.*, vol. 17, no. 23, pp. 20 952–20 958, Nov. 2009.

[22] M. V. Inochkin, V. V. Nazarov, D. Y. Sachkov, L. V. Khloponin, and V. Y. Khramov, "Dynamics of the lasing spectrum of a 3-mm Er:YLF laser with semiconductor pumping," *J. Opt. Technol.*, vol. 76, no. 11, pp. 720–724, Nov. 2009.

[23] X. Zhang, L. Li, Y. Zheng, and Y. Wang, "Formation mechanism of optical bistability in end-pumped quasi-three-level Tm, Ho:YLF lasers," *J. Opt. Soc. Amer. B*, vol. 26, no. 12, pp. 2434–2439, Dec. 2009.
[24] O. N. Eremeikin, N. A. Egorov, N. G. Zakharov, A. P. Savikin, and V. V. Sharkov, "Investigating a thermal lens in a Tm: YLF crystal under intense diode pumping," *J. Opt. Technol.*, vol. 76, no. 11, pp. 676–679, Nov. 2009.
[25] P. F. Moulton, G. A. Rines, E. V. Slobodtchikov, K. F. Wall, G. Frith, B. Samson, and A. L. G. Carter, "Tm-doped fiber lasers: Fundamentals and power scaling," *IEEE J. Sel. Topics Quantum Electron.*, vol. 15, no. 1, pp. 85–92, Jan./Feb. 2009.
[26] G. D. Goodno, L. D. Book, and J. E. Rothenberg, "Single-frequency, single-mode emission at 2040 nm from a 600-W thulium-doped fiber amplifier chain," presented at the Advanced Solid-State Photon. Conf., Denver, CO, Feb. 1–4, 2009.
[27] T. S. McComb, V. Sudesh, L. Shah, R. A. Sims, and M. C. Richardson, "Widely-tunable (> 100 nm) continuous-wave narrow-linewidth high-power thulium fiber laser," *Proc. SPIE*, vol. 7193, pp. 719 31I-1–719 31I-8, 2009.
[28] D. Creeden, P. A. Budni, and P. A. Ketteridge, "Pulsed Tm-doped fiber lasers for mid-IR frequency conversion," *Proc. SPIE*, vol. 7195, pp. 719 50X-1–719 50X-5, 2009.
[29] J. Geng, Q. Wang, T. Luo, S. Jiang, and F. Amzarjerdian, "Single-frequency narrow-linewidth Tm-doped fiber laser using silicate glass fiber," *Opt. Lett.*, vol. 34, no. 22, pp. 3493–3495, Nov. 2009.
[30] J. Geng, Q. Wang, J. Smith, T. Luo, F. Amzajerdian, and S. Jiang, "All-fiber Q-switched single-frequency Tm-doped laser near 2 μm," *Opt. Lett.*, vol. 34, no. 23, pp. 3713–3715, Dec. 2009.
[31] V. Sudesh, T. McComb, R. Sims, L. Shah, and M. Richardson, "High power, tunable, CW, narrow line thulium fiber laser for ranging applications," presented at the Advanced Solid-State Photon. Conf., Denver, CO, Feb. 1–4, 2009.
[32] T. Ehrenreich, V. Khitrov, G. Frith, J. Farroni, K. Farley, K. Tankala, A. Carter, S. Christensen, B. Samson, D. Machewirth, G. Goodno, L. Book, and J. Rothenberg, "High efficiency 20 W single frequency PM fiber amplifier at 2037 nm," presented at the Advanced Solid-State Photon. Conf., Denver, CO, Feb. 1–4, 2009.
[33] Q. Wang, J. Geng, T. Luo, and S. Jiang, "Mode-locked 2 μm laser with highly thulium-doped silicate fiber," *Opt. Lett.*, vol. 34, no. 23, pp. 3616–3618, Dec. 2009.
[34] K. Kieu and F. W. Wise, "Soliton thulium-doped fiber laser with carbon nanotube saturable absorber," *IEEE Photon. Technol. Lett.*, vol. 21, no. 3, pp. 128–130, Feb. 2009.
[35] M. Bernier, D. Faucher, N. Caron, and R. Vallee, "Highly stable and efficient erbium-doped 2.8 μm all fiber laser," *Opt. Exp.*, vol. 17, no. 19, pp. 16 941–16 946, Sep. 2009.
[36] K. S. Wu, D. Ottaway, J. Munch, D. G. Lancaster, S. Bennetts, and S. D. Jackson, "Gain-switched holmium-doped fibre laser," *Opt. Exp.*, vol. 17, no. 23, pp. 20 872–20 877, Nov. 2009.
[37] D. G. Lancaster and S. D. Jackson, "In-fiber resonantly pumped Q-switched holmium fiber laser," *Opt. Lett.*, vol. 34, no. 21, pp. 3412–3414, Nov. 2009.
[38] C. Kim, J. Peppers, V. V. Fedorov, and S. B. Mirov, "Mid-IR electroluminesence of Cr:ZnSe crystals co-doped with donor and acceptor impurities," presented at the Conf. Lasers Electro-Optics, Baltimore, MD, May 31–Jun. 5, 2009.
[39] S. Tokita, M. Murakami, S. Shimizu, M. Hashida, and S. Sakabe, "Liquid-cooled 24 W mid-infrared Er:ZBLAN fiber laser," *Opt. Lett.*, vol. 34, no. 20, pp. 3062–3064, Oct. 2009.
[40] S. D. Jackson, "High-power and highly efficient diode-cladding-pumped holmium-doped fluoride fiber laser operating at 2.94 μm," *Opt. Lett.*, vol. 34, no. 15, pp. 2327–2329, Aug. 2009.
[41] M. Szpulak and S. Fevrier, "Chalcogenide As_2S_3 suspended core fiber for mid-IR wavelength conversion based on degenerate four-wave mixing," *IEEE Photon. Technol. Lett.*, vol. 21, no. 13, pp. 884–886, Jul. 2009.
[42] J. S. Sanghera, L. B. Shaw, and I. D. Aggarwal, "Chalcogenide glass-fiber-based mid-IR sources and applications," *IEEE J. Sel. Topics Quantum Electron.*, vol. 15, no. 1, pp. 114–119, Jan./Feb. 2009.
[43] Z. G. Lian, Q. Q. Li, D. Furniss, T. M. Benson, and A. B. Seddon, "Solid microstructured chalcogenide glass optical fibers for the near- and mid-infrared spectral regions," *IEEE Photon. Technol. Lett.*, vol. 21, no. 24, pp. 1804–1806, Dec. 2009.
[44] Z. Xu, C. Xia, M. N. Islam, F. L. Terry, M. J. Freeman, A. Zakel, and J. Mauricio, "10.5 watts time-averaged power mid-IR supercontinuum generation with direct pulse pattern modulation," presented at the Conf. Lasers Electro-Optics, Baltimore, MD, May 31–Jun. 5, 2009.
[45] K.-D. Buchter, H. Herrmann, C. Langrock, M. M. Fejer, and W. Sohler, "All-optical Ti:PPLN wavelength conversion modules for free-space optical transmission links in the mid-infrared," *Opt. Lett.*, vol. 34, no. 4, pp. 470–472, Feb. 2009.
[46] M. Raybaut, T. Schmid, A. Godard, A. K. Mohamed, M. Lefebvre, F. Marnas, P. Flamant, A. Bohman, P. Geiser, and P. Kaspersen, "High-energy single-longitudinal mode nearly diffraction-limited optical parametric source with 3 MHz frequency stability for CO_2 DIAL," *Opt. Lett.*, vol. 34, no. 13, pp. 2069–2071, Jul. 2009.
[47] M. F. Witinski, J. B. Paul, and J. G. Anderson, "Pump-enhanced difference-frequency generation at 3.3 μm," *Appl. Opt.*, vol. 48, no. 13, pp. 2600–2606, May 2009.
[48] P. Brand, B. Boulanger, P. Segonds, Y. Petit, C. Felix, B. Menaert, T. Taira, and H. Ishizuki, "Angular quasi-phase-matching experiments and determination of accurate Sellmeier equations for 5%MgO:PPLN," *Opt. Lett.*, vol. 34, no. 17, pp. 2578–2580, Sep. 2009.
[49] X. Gu, G. Marcus, Y. Deng, T. Metzger, C. Teisset, N. Ishii, T. Fuji, A. Baltuska, R. Butkus, V. Pervak, H. Ishizuki, T. Taira, T. Kobayashi, R. Kienberger, and F. Krausz, "Generation of carrier-envelope-phase-stable 2-cycle 740-μJ pulses at 2.1-μm carrier wavelength," *Opt. Exp.*, vol. 17, no. 1, pp. 62–69, Jan. 2009.
[50] J. Moses, S.-W. Huang, K.-H. Hong, O. D. Mucke, E. L. Falcao-Filho, A. Benedick, F. O. Ilday, A. Dergachev, J. A. Bolger, B. J. Eggleton, and F. X. Kartner, "Highly stable ultrabroadband mid-IR optical parametric chirped-pulse amplifier optimized for superfluoresence suppression," *Opt. Lett.*, vol. 34, no. 11, pp. 1639–1641, Jun. 2009.
[51] C. Heese, C. Erny, M. Haag, L. Gallman, and U. Keller, "1 mJ from a high repetition rate femtosecond optical parametric chirped-pulse amplifier in the mid-infrared," presented at the Conf. Lasers Electro-Optics, Baltimore, MD, May 31–Jun. 5, 2009.
[52] O. Chalus, P. K. Bates, M. Smolarski, and J. Biegert, "Mid-IR short-pulse OPCPA with micro-Joule energy at 100 kHz," *Opt. Exp.*, vol. 17, no. 5, pp. 3587–3594, Mar. 2009.

[53] P. Schunemann, K. T. Zawilski, T. Pollak, V. Petrov, and D. E. Zelmon, "$CdSiP_2$: A new nonlinear optical crystal for 1- and 1.5-micron-pumped mid-IR generation," presented at the Advanced Solid State Photonics, Denver, CO, Feb. 1–4, 2009.
[54] G. Marchev, A. Tyazhev, V. Vedenyapin, D. Kolker, A. Yelisseyev, S. Lobanov, L. Isanenko, J.-J. Zondy, and V. Petrov, "Nd:YAG pumped nanosecond optical parametric oscillator based on $LiInSe_2$ with tunability extending from 4.7 to 8.7 μm," *Opt. Exp.*, vol. 17, no. 16, pp. 13 441–13 446, Aug. 2009.
[55] V. L. Panyutin, A. I. Zagumennyi, A. F. Zerrouk, F. Noack, and V. Petrov, "GaS_xSe_{1-x} compounds for nonlinear optics," presented at the Conf. Lasers Electro-Optics, Baltimore, MD, May 31–Jun. 5, 2009.
[56] E. G. Villora, K. Shimamura, K. Sumiya, and H. Ishibashi, "Birefringent- and quasi phase-matching with $BaMgF_4$ for vacuum-UV/UV and mid-IR all solid-state lasers," *Opt. Exp.*, vol. 17, no. 15, pp. 12 362–12 378, Jul. 2009.
[57] M. Kawaji, K. Imura, T. Yaguchi, and I. Shoji, "Fabrication of quasi-phase-matched devices by use of the room-temperature-bonding technique," presented at the Advanced Solid-State Photon. Conf., Denver, CO, Feb. 1–4, 2009.
[58] A. M. Schober, S. Ashby, M. Stone, and J. Marquardt, private communication, Dec. 2009.
[59] P. G. Schunemann, L. A. Pomeranz, Y. E. Young, L. Mohnkern, and A. Vera, "Recent advances in all-epitaxial growth and properties of orientation-patterned gallium arsenide (OP-GaAs)," presented at the Conf. Lasers Electro-Optics, Baltimore, MD, May 31–Jun. 5, 2009.
[60] R. D. Peterson, D. Whelan, D. Bliss, and C. Lynch, "Improved material quality and OPO performance in orientation-patterned GaAs," *Proc. SPIE*, vol. 7197, pp. 719709-1–719709-8, 2009.
[61] P. S. Kuo, K. L. Vodopyanov, and M. M. Fejer, "Polarization-diverse parametric processes in Zincblende crystals," presented at the Conf. Lasers Electro-Optics, Baltimore, MD, May 31–Jun. 5, 2009.
[62] C. Kieleck, M. Eichorn, A. Hirth, D. Faye, and E. Lallier, "High-efficiency 20–50 kHz mid-infrared orientation-patterned GaAs optical parametric oscillator pumped by a 2 μm holmium laser," *Opt. Lett.*, vol. 34, no. 3, pp. 262–264, Feb. 2009.
[63] N. K. Hon, K. K. Tsia, D. R. Solli, and B. Jalali, "Periodically-poled silicon," presented at the Conf. Lasers Electro-Optics, Baltimore, MD, May 31–Jun. 5, 2009.

Interband Mid-IR Semiconductor Lasers

L. J. Mawst

(Invited Paper)

Department of Electrical Computer Engineering, University of Wisconsin-Madison, Madison, WI 53706 USA

DOI: 10.1109/JPHOT.2010.2043727
1943-0655/$26.00 ©2010 IEEE

Manuscript received January 21, 2010; revised February 15, 2010. Current version published April 23, 2010. Corresponding author: L. J. Mawst (e-mail: mawst@engr.wisc.edu).

Abstract: Significant advances in the room-temperature (RT) continuous-wave (CW) output power of both type-I quantum-well (QW) active-layer lasers and interband cascade lasers have been reported within the 3–4-μm wavelength region in 2009. Recent developments on the growth of highly strained QWs and low-defect-density lattice-mismatched materials also demonstrate potential for realizing high-performance mid-infrared (IR) lasers on conventional substrates such as Si, GaAs, and InP.

Index Terms: Semiconductor lasers, mid-infrared lasers.

Semiconductor lasers employing interband transitions of a quantum-well (QW) active region have made significant strides in terms of output power, wavelength extension, and in the development of lattice-mismatched materials and device structures in 2009. High-performance room-temperature (RT) continuous-wave (CW) operation from devices based on QW interband transitions have now been realized in the important 3–4-μm wavelength region. Interband devices generally exhibit significantly lower operating voltages and lower threshold current densities compared with intersubband quantum cascade lasers. However, challenges remain to reduce the strong temperature sensitivity of the threshold current and efficiency in such devices, as well as further increasing the CW output powers.

Of all semiconductor lasers, interband devices employing type-I InGaAsSb QWs on a GaSb substrate have demonstrated the highest performance in the 2–3-μm emission wavelength range. High-power (1-cm) arrays have been demonstrated at 2.2 μm with 15-W CW output powers and 23% wallplug efficiency [1]. Ultralow threshold current densities, J_{th}, have also been reported; J_{th} as low as 74 A/cm^2 for a 5-mm cavity length at 2.65 μm [2]. By contrast, extending RT CW operation to wavelengths of 3 μm and beyond has been more difficult, as a result of poor active region carrier confinement (in particular, hole confinement) in the highly (compressively) strained InGaAsSb QW active region. The use of a quinternary AlInGaAsSb separate confinement heterostructure (SCH) region was introduced by Grau *et al.* in 2005, resulting in the first report of type-I QW lasers operating with wavelengths as long as 3.26 μm at 50 °C under pulsed operation [3]. The quinternary SCH results in increased valence band offset leading to improved hole confinement to the QW active region as well as more homogeneous electron injection among the QWs [3]–[9]. In 2008, employing the quinternary SCH approach led to the first report by Hosoda *et al.* of appreciable power levels (> 100 mW) under RT CW operation at 3 μm [4]. In 2009, optimization of the optical waveguide width and composition, as well as a reduction of free-carrier losses, in structures with an AlInGaAsSb SCH region led to significant improvement in the CW output powers; 600 mW at 2.7 μm [5], 310 mW at 3 μm [6], 190 mw at 3.1 μm, 160 mW at 3.2 μm, and 50 mW at 3.32 μm [7].

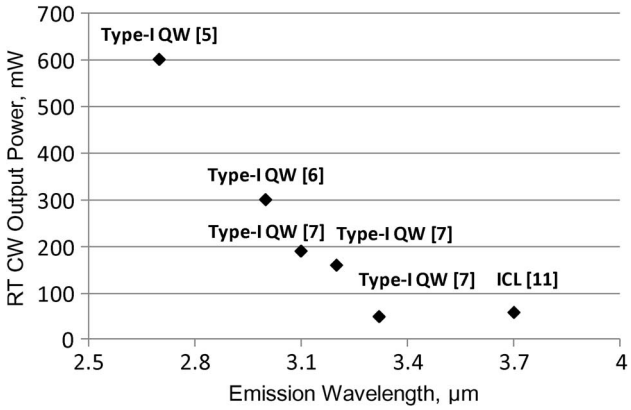

Fig. 1. Maximum RT CW output powers reported in 2009 for interband lasers in the 2.7–4.0-μm range.

A larger range of emission wavelengths in the 3–4-μm spectral region is accessible using a type-II QW, W configuration, interband cascade active region. The first CW operation above RT at 3.75 μm from such devices was reported in 2008 using a 5-stage active region Interband Cascade Laser (ICL) design [10]. Further optimized devices with low internal losses ($\sim$6 cm^{-1}) were reported in 2009, leading to a 50% increase in efficiency at 300 K compared with previous devices, enabling input power densities below 1 KW/cm^2 [11]. Record CW output power (59 mW) at 3.7 μm was reported from such devices with a wallplug efficiency as high as 3.4% [11]. The increased CW output powers (see Fig. 1) now open the door for the practical implementation of both the type-I QW and ICL devices to a variety of applications including medical diagnostics and therapy, gas sensing, and material processing. Further increases in the CW output powers can be expected if thermal management can be improved. For example, a novel approach of using highly doped InAs plasmon waveguides for ICL structures was reported by Tian *et al.* in 2009 and significant reductions in thermal resistance over conventional InAs/AlSb superlattice cladding layers were reported [12].

While highest performance interband lasers in the 2–4-μm wavelength region currently employ GaSb substrates, there is strong motivation to move away from this less mature material system toward a more conventional GaAs or InP platform. Advantages of such a strategy include; significantly lower cost (also larger diameter substrates are available), access to a more mature processing technology, better thermal conductivity and straightforward regrowth of buried-heterostructure-type devices for improved thermal management. Extending the emission wavelengths into the mid-infrared (IR) on an InP substrate by employing highly strained InGaAs(Sb) type-I multiple QWs (MQWs) [13]–[17] encounter difficulties for wavelengths $> \sim$2 μm. Through the use of the InAs/InGaAs type-I MQW active region grown at very low temperatures to inhibit strain relaxation, the emission wavelength has was extended to 2.33 μm in 2008 [18]–[20]. In 2009, RT PL at 2.52 μm was reported from MOCVD grown highly strained InAs QWs on InP substrates employing tertiary-butylarsine (TBA), an arsenic source which efficiently decomposes at low growth temperatures [21]. Furthermore, recently reported design studies indicate employing a highly strained In(Ga)As/GaAsSb type-II QW holds potential for extending emission wavelengths near 3 μm [22]. The addition of nitrogen into InAs was reported by de la Mare *et al.*, allowing for RT PL emission near 4 μm from InAsN grown by molecular-beam epitaxy (MBE) on GaAs [23]. An alternate approach to employing a highly strained active region is to utilize a *virtual* substrate with a larger lattice constant and low threading dislocation density, allowing for the growth of relaxed lattice-mismatched materials with low dislocation densities. Compositionally graded metamorphic buffer layers (MBLs) or very thick relaxed single composition buffer layers can produce such a virtual substrate. In 2009, Nash *et al.* reported that the use of a MBE grown high-Al-content $Al_zIn_{1-z}Sb$ interface layer and 8-μm-thick $Al_xIn_{1-x}Sb$ cladding layer was effective in defect reduction, allowing 3.3-μm-emitting GaInSb QW lasers on GaAs substrates which operate up to 219 K under pulsed operation [24]. However, there are few reports of employing MBL structures on InP substrates for the realization of mid-IR

lasers [25]. In 2009, Kirch *et al.* reported MOCVD-grown QW lasers emitting in the mid-IR spectral region employing $InAs_yP_{1-y}$ MBL structures on InP substrates [24]. Pulsed laser operation was reported near 2.45 μm from InAs QW active region devices with threshold current densities as low as 290 A/cm^2 [26]. Optimized device designs employing InPSb cladding layers and an InAsP SCH increase the active region carrier confinement, potentially allowing for RT operation in the 3-μm wavelength region.

In 2009, significant progress on the use of MBE grown interfacial misfit (IMF) arrays has also been reported to reduce threading dislocations in lattice-mismatched devices grown on both GaAs [27] and Si [28], [29] substrates. Unlike the relatively thick MBL, the dislocations in the IMF self-arrange in a periodic array configuration and the strain is relieved primarily in a very thin interface layer. In 2009, Tatebayashi *et al.*, reported GaSb-based lasers grown on Si substrates employing the IMF growth which demonstrate $J_{th} \sim 2$ KA/cm^2 (77 K) from lasers emitting at 1.62 μm under pulsed operation [28]. Pulsed laser operation near 2.2 μm was also reported by Rodriguez *et al.* in 2009 employing the IMF growth on Si substrates, with threshold current densities in the 4–8-KA/cm^2 range [29]. Employing the IMF growth on GaAs substrates, CW operation at 2.2 μm up to 50 °C was also reported by Rodriguez *et al.* with threshold current densities significantly lower ($J_{th} \sim 1.5$ KA/cm^2 at 20 °C) than the Si substrate based devices [27]. While the threshold current densities of lattice-mismatched devices are still significantly higher than that of state-of-the-art devices grown on a GaSb substrate, significant progress has been made in 2009 to establish the potential for this technology, provided further reduction in defect densities can be achieved through improved material growth.

References

[1] M. T. Kelemen, J. Gilly, M. Haag, J. Biesenbach, M. Rattunde, and J. Wagner, "Diode laser arrays for 1.8 to 2.3 μm wavelength range," in *Proc. SPIE Int. Soc. Opt. Eng.—Novel In-Plane Semiconductor Lasers VIII*, Jan. 2009, vol. 7230, p. 72301K.

[2] K. Kashani-Shirazi, K. Vizbaras, A. Bachmann, S. Arafin, and M.-C. Amann, "Low-threshold strained quantum-well GaSb-based lasers emitting in the 2.5- to 2.7-μm wavelength range," *IEEE Photon. Technol. Lett.*, vol. 21, no. 16, pp. 1106–1109, Aug. 2009.

[3] M. Grau, C. Lin, O. Dier, C. Lauer, and M.-C. Amann, "Room-temperature operation of 3.26 μm GaSb-based type-I lasers with quinternary AlGaInAsSb barriers," *Appl. Phys. Lett.*, vol. 87, no. 24, p. 241104, Dec. 2005.

[4] T. Hosoda, G. Belenky, L. Shterengas, G. Kipshidze, and M. V. Kisin, "Continuous-wave room temperature operated 3.0 μm type I GaSb-based lasers with quinternary AlInGaAsSb barriers," *Appl. Phys. Lett.*, vol. 92, no. 9, p. 091106, Mar. 2008.

[5] J. Chen, G. Kipshidze, L. Shterengas, T. Hosoda, Y. Wang, D. Donetsky, and G. Belenky, "2.7-μm GaSb-based diode lasers with quinary waveguide," *IEEE Photon. Technol. Lett.*, vol. 21, no. 16, pp. 1112–1115, Jul. 2009.

[6] L. Shterengas, G. Kipshidze, T. Hosoda, J. Chen, and G. Belenky, "Diode lasers emitting at 3 μm with 300 mW of continuous-wave output power," *Electron. Lett.*, vol. 45, no. 18, pp. 942–943, Aug. 2009.

[7] G. Belenky, G. Kipshidze, T. Hosoda, J. Chen, D. Wang, and L. Shterengas, "GaSb-based laser diodes operating within the spectra range of 2–3 μm," in *Proc. Adv. WOFE*, Rincon, Puerto Rico, Dec. 13–16, 2009.

[8] J. A. Gupta, P. J. Barrios, G. C. Aers, P. Waldron, and C. Storey, "Room-temperature continuous-wave operation of type-I GaSb-based lasers at 3.1 μm," *Electron. Lett.*, vol. 45, no. 16, pp. 835–837, Jul. 2009.

[9] P. Kluczynski, S. Lundqvist, S. Belahsene, and Y. Rouillard, "Tunable-diode-laser spectroscopy of C2H2 using a 3.03 μm GaInAsSb/AlGaInAsSb distributed-feedback laser," *Opt. Lett.*, vol. 34, pp. 3767–3769, 2009.

[10] M. Kim, C. L. Canedy, W. W. Bewley, C. S. Kim, J. R. Lindle, J. Abell, I. Vurgaftman, and J. R. Meyer, "Interband cascade laser emitting at $\lambda = 3.75$ μm in continuous wave above room temperature," *Appl. Phys. Lett.*, vol. 92, no. 19, p. 191110, May 2008.

[11] I. Vurgaftman, C. L. Canedy, C. S. Kim, M. Kim, W. W. Bewley, J. R. Lindle, J. Abell, and J. R. Meyer, "Mid-infrared interband cascade lasers operating at ambient temperatures," *New J. Phys.*, vol. 11, p. 125015, Dec. 2009.

[12] Z. Tian, R. Q. Yang, T. D. Mishima, M. B. Santos, and M. B. Johnson, "Plasmon-waveguide interband cascade lasers near 7.5 μm," *IEEE Photon. Technol. Lett.*, vol. 21, no. 21, pp. 1588–1591, Nov. 2009.

[13] S. Forouhar, A. Larsson, A. Ksendzov, R. J. Lang, N. Tothill, and M. D. Scott, "Room-temperature operation of MOCVD-grown GaInAs/InP strained-layer multiquantum-well lasers in 1.8 μm range," *Electron. Lett.*, vol. 28, no. 10, pp. 945–947, May 1992.

[14] O. Matsuyuki, S. Kenji, and K. Yasuhiro, "Metalorganic vapor phase epitaxical growth and 1.5 μm laser fabrication using ethyldimethylindium, tertiarybutylphosphine, and tertiarybutylarsine," *Appl. Phys. Lett.*, vol. 60, no. 10, pp. 1217–1219, Mar. 1992.

[15] M. Mitsuhara, M. Ogasawara, M. Oishi, H. Sugiura, and K. Kasaya, "2.05 μm wavelength InGaAs-InGaAs distributed-feedback multiquantum-well lasers with 10-mW output power," *IEEE Photon. Technol. Lett.*, vol. 11, no. 1, pp. 33–35, Jan. 1999.

[16] T. Sato, K. Mitsuhara, T. Watanabe, K. Kasaya, T. Takeshita, and Y. Kondo, "2.1 μm-wavelength InGaAs multiple-quantum-well distributed feedback lasers grown by MOVPE using Sb surfactant," *IEEE J. Sel. Topics Quantum Electron.*, vol. 13, no. 5, pp. 1079–1083, Sep./Oct. 2007.
[17] T. Sato, M. Mitsuhara, T. Watanabe, and Y. Kondo, "Surfactant-mediated growth of InGaAs multiple-quantum-well lasers emitting at 2.1 μm by metalorganic vapor phase epitaxy," *Appl. Phys. Lett.*, vol. 87, no. 21, p. 211903, Nov. 2005.
[18] T. Sato, M. Mitsuhara, and Y. Kondo, "2.33 μm-wavelength InAs/InGaAs multiple-quantum-well lasers grown by MOVPE," *Electron. Lett.*, vol. 43, no. 21, pp. 1143–1145, Oct. 2007.
[19] T. Sato, M. Mitsuhara, N. Nunoya, T. Fujisawa, K. Kasaya, F. Kano, and Y. Kondo, "2.33 μm-wavelength distributed feedback lasers with InAs/InGaAs multiple-quantum wells on InP substrates," *IEEE Photon. Technol. Lett.*, vol. 20, no. 12, pp. 1045–1047, Jun. 2008.
[20] T. Sato, M. Mitsuhara, T. Kakitsuka, T. Fujisawa, and Y. Kondo, "Metalorganic vapor phase epitaxial growth of InAs/InGaAs multiple quantum well structures on InP substrates," *IEEE J. Sel. Topics Quantum Electron.*, vol. 14, no. 4, pp. 992–997, Jul./Aug. 2008.
[21] S. Kim, J. Kirch, and L. Mawst, "Highly strained InAs quantum wells on InP substrates for mid-IR emission," *J. Cryst. Growth*, Dec. 11, 2009, to be published.
[22] J. Y. T. Huang, L. J. Mawst, T. F. Kuech, X. Song, S. E. Babcock, C. S. Kim, I. Vurgaftman, J. R. Meyer, and A. L. Holmes, Jr., "Design and characterization of strained InGaAs/GaAsSb Type-II 'W' quantum wells on InP substrates for mid-IR emission," *J. Phys. D, Appl. Phys.*, vol. 42, no. 2, p. 025108, Dec. 2009.
[23] M. de la Mare, Q. Zhuang, A. Krier, A. Patanè, and S. Dhar, "Growth and characterization of InAsN/GaAs dilute nitride semiconductor alloys for the midinfrared spectral range," *Appl. Phys. Lett.*, vol. 95, no. 3, p. 031110, Jul. 2009.
[24] G. R. Nash, S. J. B. Przeslak, S. J. Smith, G. de Valicourt, A. D. Andreev, P. J. Carrington, M. Yin, A. Krier, S. D. Coomber, L. Buckle, M. T. Emeny, and T. Ashley, "Midinfrared GaInSb/AlGaInSb quantum well laser diodes operating above 200 K," *Appl. Phys. Lett.*, vol. 94, no. 9, p. 091111, Mar. 2009.
[25] A. Krier, D. Chubb, S. E. Krier, M. Hopkinson, and G. Hill, "Light sources for wavelengths > 2 μm grown by MBE on InP using a strain relaxed buffer," *Proc. Inst. Elect. Eng.—Optoelectron.*, vol. 145, no. 5, pp. 292–296, Oct. 1998.
[26] J. Kirch, T. Garrod, S. Kim, J. H. Park, J. C. Shin, L. J. Mawst, T. F. Kuech, X. Song, S. E. Babcock, I. Vurgaftman, J. R. Meyer, and T.-S. Kuan, "$InAs_yP_{1-y}$ metamorphic buffer layers on InP substrates for mid-IR diode lasers," *J. Cryst. Growth*, Dec. 29, 2009, to be published.
[27] J. B. Rodriguez, L. Cerutti, and E. Tournié, "GaSb-based, 2.2 μm type-I laser fabricated on GaAs substrate operating continuous wave at room temperature," *Appl. Phys. Lett.*, vol. 94, no. 2, p. 023506, Jan. 2009.
[28] J. Tatebayashi, A. Jallipalli, M. N. Kutty, S. Huang, K. Nunna, G. Balakrishnan, L. R. Dawson, and D. L. Huffaker, "Monolithically integrated III-Sb-based laser diodes grown on Miscut Si substrates," *IEEE J. Sel. Topics Quantum Electron.*, vol. 15, no. 3, pp. 716–723, May 2009.
[29] J. B. Rodriguez, L. Cerutti, P. Grech, and E. Tournié, "Room-temperature operation of a 2.25 μm electrically pumped laser fabricated on a silicon substrate," *Appl. Phys. Lett.*, vol. 94, no. 6, p. 061124, Feb. 2009.

Compact Plasma-Based Soft X-Ray Lasers

Jorge J. Rocca

(Invited Paper)

National Science Foundation Engineering Research Center for Extreme Ultraviolet Science and Technology, Department of Electrical and Computer Engineering and Department of Physics, Colorado State University, Fort Collins, CO 80535 USA

DOI: 10.1109/JPHOT.2010.2045491
1943-0655/$26.00 ©2010 IEEE

Manuscript received February 17, 2010. Current version published April 23, 2010. Corresponding author: J. J. Rocca (e-mail: rocca@engr.colostate.edu).

Abstract: This paper reviews the major accomplishments in the demonstration of plasma-based soft x-ray lasers in 2009. Advances in shaping the plasma density and increasing the pump power have enabled the engineering of table-top laser systems operating at wavelengths as short as 10.9 nm and with stable and significant average power for use in applications.

Index Terms: Coherent sources, extreme ultraviolet, soft X-ray lasers.

The generation of intense soft X-ray (SXR) and X-ray laser radiation is attracting much attention. A separate article in this issue discusses recent progress in the generation of extremely bright X-ray laser pulses by the injection of energetic electron beams created in linear accelerators into alternating magnet structures [1]. Two such free-electron lasers are now in operation as single-user facilities: one at wavelengths as short as 6 nm [2] and the other for the first time at kiloelectronvolt photon energies [3]. Simultaneously, significant progress has been made in the generation of intense SXR laser beams by much more compact devices that use dense plasmas as the gain media. In these lasers, spontaneous emission generated by the plasma, or an externally generated coherent seed, are amplified by stimulated emission in a population inversion created between energy levels of plasma ions. A gain in plasmas was demonstrated at wavelengths as short as $\lambda = 3.56$ nm many years ago using fusion-class laser facilities to heat the plasma [4]. Advances produced by tailoring the plasma density profile, creating larger transient population inversions [5], and increasing the pump energy deposition [6], [7] have allowed the engineering of these lasers into tabletop-size devices that can be "taken" to the application site. During the past few years, several groups have been active in the development of SXR sources operating at a 5–10-Hz repetition rate with stable output for extended periods of time for applications [8]–[14]. Gain-saturated output has been demonstrated for wavelengths down to 13.2 nm [9]. At longer wavelengths (e.g., 46.9 nm), plasma heating by fast capillary discharges have allowed the development of desktop-size lasers [15]. The challenge for these tabletop plasma-based lasers has been and continues to be the extension of their range of operation to shorter wavelengths and the increase of their brightness and average power.

During the past year, the wavelength of gain-saturated tabletop lasers has been extended to 10.9 nm by amplification of spontaneous emission in nickel-like tellurium ions in a plasma generated at a 1-Hz repetition rate by the irradiation of a solid tellurium target with pulses from a Ti:Sapphire laser [16]. Laser output pulses of up to 2 μJ were obtained, and an average power of $\sim$1 μW was generated. This is a level of average power that can enable applications such as ultrahigh-resolution zone-plate imaging. For example, in 2009, a tabletop nickel-like cadmium $\lambda = 13.2$ nm SXR-laser-based

microscope was used for actinic imaging of extreme ultraviolet lithography masks that will be used in the fabrication of the generation of the future generation of computer processors [17].

The average power of these plasma-based SXR lasers is in part limited by the maximum repetition rate of the lasers drivers used to heat the plasmas. High-energy Ti:Sapphire lasers, which are the most common types of laser drivers used to pump these short wavelength lasers, are limited to repetition rates of typically 10 Hz, while often-used Nd:glass pump lasers operate at an even lower repetition rate. Advances in diode-pumped solid-state lasers open the opportunity to develop optical laser drivers that will allow plasma-based SXR lasers to greatly increase their repetition rate and, therefore, their average power. Different groups are developing diode-pumped solid-state lasers for this purpose [18], [19]. In 2009, the first all-diode-pumped SXR laser was reported. Lasing was achieved at $\lambda = 18.9$ nm in a molybdenum plasma heated by a diode-pumped chirped pulse amplification laser based on cryo-cooled Yb:YAG amplifiers [16]. This new type of SXR laser has the potential to operate at an order of magnitude larger repetition rate (e.g., 100 Hz). With the complementary goals of driving shorter wavelength lasers and increasing the SXR laser pulse energy, higher energy pump laser facilities that operate at a lower repetition rate (0.1 Hz) have also been recently developed [20], [21].

Rapid progress has also been achieved in improving the beam characteristics of plasma-based SXR lasers. Injection-seeding of SXR laser amplifiers with high harmonic (HH) pulses have been shown to generate intense fully phase coherent SXR pulses with lower divergence, shorter pulsewidth, and defined polarization. In 2004, injection seeding of the $\lambda = 32.8$ nm Ni-like Kr in a gas cell ionized by optical field ionization with the 25th harmonic of a Ti:Sapphire laser generated a saturated beam with excellent wavefront qualities [22]. Our group demonstrated the saturated amplification of HH seed pulses in significantly denser plasma amplifiers created by heating solid targets, which can readily reach shorter wavelengths and have an increased bandwidth that can support the amplification of femtosecond pulses [23]–[25]. Using this technique, fully phase-coherent laser beams at wavelengths as low as $\lambda = 13.2$ nm were generated [24], [25]. During the past year, several papers reported results of the characterization [26], [27] and modeling [28]–[30] of these new injection-seeded SXR lasers.

There is also significant interest in reducing the pulse duration of tabletop SXR lasers to extend their application to a wide range of ultrafast dynamic studies. Transient inversions created by rapid heating of plasmas with intense picosecond optical laser pulses have generated SXR laser pulses with duration between 2–10 ps [29], [31], [32]. High-repetition-rate transient inversion lasers produced by grazing incidence pumping have been measured to generate pulse durations of about 5 ps [33]. In all these self-seeded SXR lasers, the pulse duration was determined by the duration of the gain. The recent demonstration of injection-seeded with HHs [22], [24], [25], [33] creates a fundamentally new regime for the generation of short SXR laser pulses in which the pulsewidth is governed by the amplifier bandwidth and is independent of the gain duration. As mentioned above, of particular interest are the SXR plasma amplifiers created by laser irradiation of solid targets [23]–[25] in which the high density of the laser gain media results in broader laser line bandwidths that can support the generation of SXR pulsewidths in the 0.1–1-ps range. In 2009, the first measurement of the pulsewidth of an injection-seeded SXR laser was reported to yield (1.13 ± 0.47) ps, which is the shortest reported to date for a plasma amplifier [33]. The experiment was preformed, seeding the 32.6-nm line of Ne-like Ti with the 25th harmonic of a Ti: Sapphire laser. The results were found to be in agreement with model simulations that predict that intense femtosecond SXR laser pulses will result from injection seeding denser plasma amplifiers.

References

[1] K. A. Nugent, W. Barletta, and S. V. Milton, "X-ray free electron lasers," *IEEE Photon. J.*, vol. 2, no. 2, pp. 221–224, Apr. 2010.
[2] FLASH, *Deutsches Elektronen-Synchrotron*. [Online]. Available: http://flash.desy.de/
[3] SLAC, *Linac Coherent Light Source*. [Online]. Available: http://lcls.slac.stanford.edu/
[4] B. J. Macgowan, L. B. Dasilva, D. J. Fields, C. J. Keane, J. A. Koch, R. A. London, D. L. Matthews, S. Maxon, S. Mrowka, A. L. Osterheld, J. H. Scofield, G. Shimkaveg, J. E. Trebes, and R. S. Walling, "Short wavelength X-ray laser research at the Lawrence-Livermore-National-Laboratory," *Phys. Fluids B: Plasma Phys.*, vol. 4, no. 7, pp. 2326–2337, Jul. 1992.

[5] P. V. Nickles, V. N. Shlyaptsev, M. Kalachnikov, M. Schnürer, I. Will, and W. Sandner, "Short pulse X-ray laser at 32.6 nm based on transient gain in Ne-like titanium," *Phys. Rev. Lett.*, vol. 78, no. 14, pp. 2748–2751, Apr. 1997.
[6] R. Keenan, J. Dunn, P. K. Patel, D. F. Price, R. F. Smith, and V. N. Shlyaptsev, "High-repetition-rate grazing-incidence pumped X-ray laser operating at 18.9 nm," *Phys. Rev. Lett.*, vol. 94, no. 10, p. 103901, Mar. 2005.
[7] B. M. Luther, Y. Wang, M. A. Larotonda, D. Alessi, M. Berrill, M. C. Marconi, J. J. Rocca, and V. N. Shlyaptsev, "Saturated high-repetition-rate 18.9-nm tabletop laser in nickellike molybdenum," *Opt. Lett.*, vol. 30, no. 2, pp. 165–167, Jan. 2005.
[8] Y. Wang, M. A. Larotonda, B. M. Luther, D. Alessi, M. Berrill, V. N. Shlyaptsev, and J. J. Rocca, "Demonstration of high-repetition-rate tabletop soft-X-ray lasers with saturated output at wavelengths down to 13.9 nm and gain down to 10.9 nm," *Phys. Rev. A, Gen. Phys.*, vol. 72, no. 5, p. 053807, Nov. 2005.
[9] J. J. Rocca, Y. Wang, M. A. Larotonda, B. M. Luther, M. Berrill, and D. Alessi, "Saturated 13.2 nm high-repetition-rate laser in nickellike cadmium," *Opt. Lett.*, vol. 31, no. 1, p. 129, Jan. 2006.
[10] S. Sebban, T. Mocek, D. Ros, L. Upcraft, P. Balcou, R. Haroutunian, G. Grillon, B. Rus, A. Klisnick, A. Carillon, G. Jamelot, C. Valentin, A. Rousse, J. P. Rousseau, L. Notebaert, M. Pittman, and D. Hulin, "Demonstration of a Ni-like Kr optical-field-ionization collisional soft X-ray laser at 32.8 nm," *Phys. Rev. Lett.*, vol. 89, no. 25, p. 253 901, Dec. 2002.
[11] M. C. Chou, P. H. Lin, C. A. Lin, J. Y. Lin, J. Wang, and S. Y. Chen, "Dramatic enhancement of optical-field-ionization collisional-excitation X-ray lasing by an optically preformed plasma waveguide," *Phys. Rev. Lett.*, vol. 99, no. 6, p. 063904, Aug. 2007.
[12] H. T. Kim, I. W. Choi, N. Hafz, J. H. Sung, T. J. Yu, K. H. Hong, T. M. Jeong, Y. C. Noh, D. K. Ko, K. A. Janulewicz, J. Tummler, P. V. Nickles, W. Sandner, and J. Lee, "Demonstration of a saturated Ni-like Ag X-ray laser pumped by a single profiled laser pulse from a 10-Hz Ti:Sapphire laser system," *Phys. Rev. A, Gen. Phys.*, vol. 77, no. 2, p. 023807, Feb. 2008.
[13] F. Lindau, O. Lundh, A. Persson, K. Cassou, S. Kazamias, D. Ros, F. Ple, G. Jamelot, A. Klisnick, S. de Rossi, D. Joyeux, B. Zielbauer, D. Ursescu, T. Kuhl, and C. G. Wahlstrom, "Quantitative study of 10 Hz operation of a soft X-ray laser-energy stability and target considerations," *Opt. Express*, vol. 15, no. 15, pp. 9486–9493, Jul. 2007.
[14] D. Zimmer, B. Zielbauer, M. Pittman, O. Guilbaud, J. Habib, S. Kazamias, D. Ros, V. Bagnoud, and T. Kuehl, "Optimization of a tabletop high-repetition-rate soft X-ray laser pumped in double-pulse single-beam grazing incidence," *Opt. Lett.*, vol. 35, no. 4, pp. 450–452, Feb. 2010.
[15] S. Heinbuch, M. Grisham, D. Martz, and J. J. Rocca, "Demonstration of a desk-top size high repetition rate soft X-ray laser," *Opt. Express*, vol. 13, no. 11, pp. 4050–4055, May 2005.
[16] D. Alessi, D. H. Martz, Y. Wang, M. Berrill, B. M. Luther, and J. J. Rocca, "Gain-saturated 10.9 nm tabletop laser operating at 1 Hz repetition rate," *Opt. Lett.*, vol. 35, no. 3, pp. 414–416, Feb. 2010.
[17] F. Brizuela, Y. Wang, C. A. Brewer, F. Pedaci, W. Chao, E. H. Anderson, Y. Liu, K. A. Goldberg, P. Naulleau, P. Wachulak, M. C. Marconi, D. T. Attwood, J. J. Rocca, and C. S. Menoni, "Microscopy of extreme ultraviolet lithography masks with 13.2 nm tabletop laser illumination," *Opt. Lett.*, vol. 34, no. 3, pp. 271–273, Feb. 2009.
[18] F. J. Furch, B. A. Reagan, B. M. Luther, A. H. Curtis, S. P. Meehan, and J. J. Rocca, "Demonstration of an all-diode-pumped soft X-ray laser," *Opt. Lett.*, vol. 34, no. 21, pp. 3352–3354, Nov. 2009.
[19] J. Tummler, R. Jung, H. Stiel, P. V. Nickles, and W. Sandner, "High-repetition-rate chirped-pulse-amplification thin-disk laser system with joule-level pulse energy," *Opt. Lett.*, vol. 34, no. 9, pp. 1378–1380, May 2009.
[20] D. Ros, O. Guilbaud, S. Kazamias, M. Pittman, J.-C. Lagron, B. Zielbauer, J. Habib, J.-P. Chambaret, G. Mourou, K. Cassou, B. Cros, G. Maynard, P. Zeitoun, S. Sebban, J. Gautier, A. Klisnick, S. de Rossi, S. Jacquemot, P. Audebert, B. Rus, D. Zimmer, and T. Kühl, "Perspectives of XUV sources development on LASERIX facility, ILE, and ELI," in *Proc. SPIE—Soft X-Ray Lasers and Applications VIII*, J. Dunn and G. J. Tallents, Eds., 2009, vol. 7451, p. 74510A.
[21] T. Kawachi, M. Kishimoto, M. Kado, Y. Ochi, N. Hasegawa, M. Tanaka, M. Nishikino, M. Ishino, T. Imazono, T. Ohba, T. Kaihori, M. Koike, K. Namikawa, T. Suemoto, K. Terakawa, T. Tomita, N. Sarukura, H. Nishimura, A. Y. Faenov, S. Bulanov, and H. Daido, "Source development and novel applications of X-ray lasers for probing materials," in *Proc. SPIE—Soft X-Ray Lasers and Applications VIII*, J. Dunn and G. J. Tallents, Eds., 2009, vol. 7451, p. 745 107.
[22] P. Zeitoun, G. Faivre, S. Sebban, T. Mocek, A. Hallou, M. Fajardo, D. Aubert, P. Balcou, F. Burgy, D. Douillet, S. Kazamias, G. de Lacheze-Murel, T. Lefrou, S. le Pape, P. Mercere, H. Merdji, A. S. Morlens, J. P. Rousseau, and C. Valentin, "A high-intensity highly coherent soft X-ray femtosecond laser seeded by a high harmonic beam," *Nature*, vol. 431, no. 7007, pp. 426–429, Sep. 2004.
[23] Y. Wang, E. Granados, M. A. Larotonda, M. Berrill, B. M. Luther, D. Patel, C. S. Menoni, and J. J. Rocca, "High-brightness injection-seeded soft-X-ray-laser amplifier using a solid target," *Phys. Rev. Lett.*, vol. 97, no. 12, p. 123 901, Sep. 2006.
[24] Y. Wang, E. Granados, F. Pedaci, D. Alessi, B. M. Luther, M. Berrill, and J. J. Rocca, "Phase-coherent, injection-seeded, table-top soft-X-ray lasers at 18.9 nm and 13.9 nm," *Nat. Photon.*, vol. 2, no. 2, pp. 94–98, Feb. 2008.
[25] F. Pedaci, Y. Wang, M. Berrill, B. Luther, E. Granados, and J. J. Rocca, "Highly coherent injection-seeded 13.2 nm tabletop soft X-ray laser," *Opt. Lett.*, vol. 33, no. 5, pp. 491–493, Mar. 2008.
[26] J. J. Rocca, F. J. Furch, B. A. Reagan, Y. Wang, D. Alessi, D. H. Martz, B. M. Luther, M. Berrill, S. Domingue, C. D. Kemp, F. Pedaci, V. N. Shlyaptsev, M. C. Marconi, and C. S. Menoni, "Progress in the development of compact high-repetition rate soft X-ray lasers: Gain saturation at 10.9 nm and first demonstration of an all-diode-pumped soft X-ray laser," in *Proc. SPIE—Soft X-Ray Lasers and Applications VIII*, J. Dunn and G. J. Tallents, Eds., 2009, vol. 7451, p. 745106-1.
[27] J. P. Goddet, S. Sebban, J. Gautier, P. Zeitoun, C. Valentin, F. Tissandier, T. Marchenko, G. Lambert, M. Ribières, D. Douillet, T. Lefrou, G. Iaquaniello, F. Burgy, G. Maynard, B. Cros, B. Robillard, T. Mocek, J. Nejdl, M. Kozlova, and K. Jakubczak, "Aberration-free laser beam in the soft X-ray range," *Opt. Lett.*, vol. 34, no. 16, pp. 2438–2440, Aug. 2009.
[28] K. A. Janulewicz, C. M. Kim, H. T. Kim, H. C. Kang, K. T. Kim, and J. Lee, "X-ray laser research and applications at c-FAST," in *Proc. SPIE—Soft X-Ray Lasers and Applications VIII*, J. Dunn and G. J. Tallents, Eds., 2009, vol. 7451, p. 74510P.
[29] A. Klisnick, O. Larroche, F. de Dortan, J. Habib, and O. Guilbaud, "Simulations of ASE and seeded transient X-ray lasers using the COLAX code," in *Proc. SPIE—Soft X-Ray Lasers and Applications VIII*, J. Dunn and G. J. Tallents, Eds., 2009, vol. 7451, p. 74510U.

[30] G. J. Tallents and I. Al'miev, "Temporal and frequency output of seeded and unseeded X-ray lasers," in *Proc. SPIE—Soft X-Ray Lasers and Applications*, J. Dunn and G. J. Tallents, Eds., 2009, vol. 7451, p. 74510V.
[31] J. Dunn, R. F. Smith, R. Shepherd, R. Booth, J. Nilsen, J. R. Hunter, and V. N. Shlyaptsev, "Temporal characterization of a picosecond-laser-pumped X-ray laser for applications," in *Proc. SPIE—Soft X-Ray Lasers and Applications V*, E. E. Fill and S. Suckewer, Eds., 2003, vol. 5197, pp. 51–59.
[32] M. A. Larotonda, Y. Wang, M. Berrill, B. M. Luther, J. J. Rocca, M. M. Shakya, S. Gilbertson, and Z. H. Chang, "Pulse duration measurements of grazing-incidence-pumped high repetition rate Ni-like Ag and Cd transient soft X-ray lasers," *Opt. Lett.*, vol. 31, no. 20, pp. 3043–3045, Oct. 2006.
[33] Y. Wang, M. Berrill, F. Pedaci, M. M. Shakya, S. Gilbertson, Z. Chang, E. Granados, B. M. Luther, M. A. Larotonda, and J. J. Rocca, "Measurement of 1-ps soft-X-ray laser pulses from an injection-seeded plasma amplifier," *Phys. Rev. A, Gen. Phys.*, vol. 79, no. 2, p. 023810, Feb. 2009.

Short-Wavelength Free-Electron Lasers

Keith A. Nugent[1] **and William A. Barletta**[2,3]

(Invited Paper)

[1]Australian Research Council Centre of Excellence for Coherent X-ray Science, School of Physics, The University of Melbourne, Melbourne, Vic. 3010, Australia
[2]Department of Physics, Massachusetts Institute of Technology, Cambridge, MA 02139 USA
[3]Sincrotrone Trieste, 34149 Trieste, Italy

DOI: 10.1109/JPHOT.2010.2044654
1943-0655/$26.00 ©2010 IEEE

Manuscript received February 10, 2010. Current version published April 23, 2010. Corresponding author: K. A. Nugent (e-mail: keithan@unimelb.edu.au).

Abstract: This paper presents a short review of the development of and the motivation for short-wavelength free-electron lasers. The first observation of coherent X-ray production was reported from the Linac Coherent Light Source in April 2009.

Index Terms: X-rays, Lasers, free-electron lasers, synchrotrons.

X-ray science has been developing with remarkable rapidity in recent years. There have been exceptional increases in the coherent output of the available sources, and a great deal of work has been published on the development of coherent X-ray methods [1].

The source of many of the gains in the brightness of X-ray sources has been the improvement in the electron beam quality and the use of structured magnetic arrays (known generically as insertion devices) to improve the X-ray output from the beam.

Several proposals [2]–[4] have suggesting that the underlying developments in beam physics, accelerator technology, and insertion-device technology could lead to stimulated emission of radiation and subsequent high-gain amplification from an electron beam. The electron beam acts as a gain medium for free-to-free energy transitions and was first demonstrated in a low-gain system by Madey in 1973 [5], [6]. Such a free-electron laser (FEL) combines a linear accelerator and with a long insertion device. In an FEL, electrons pass through a magnetic structure of alternating dipoles producing X-rays which then interact with the electrons in such a manner as to further enhance the radiation output—a process known as self-amplified spontaneous emission (SASE). The high-gain SASE process was first demonstrated in 1986 [7] and extended to visible wavelengths in the last ten years or so [8], and it has led to the development of a number of FEL facilities.

Over the last five years or so, vacuum ultraviolet free to soft X-ray FELs have been operating in Hamburg, Germany (the FLASH facility) [9], and in Japan [10], with further facilities being constructed or proposed elsewhere [11]. The long term goal for X-ray science is the establishment and operation of X-ray FEL systems that can produce highly coherent beams with wavelengths in the range of 0.1 to 40 nm. The first FEL hard X-ray beam at 0.1 nm was produced at the SLAC National Accelerator Laboratory in April 2009 [12].

A high-profile, but by no means the only, motivation for the development of hard X-ray FEL facilities is that the extraordinary brightness of FEL sources will such that it might be possible to image single biomolecules without the need for crystals [13]. Conventional macromolecular crystallography, as performed at synchrotron facilities, requires the formation of a crystal of the biomolecule of interest, the acquisition of X-ray diffraction data, and the inversion of that data to

recover the molecular structure. As they will not crystallize, this relatively routine process cannot be applied to many of the most interesting biomolecules. The capacity to determine the structure of biomolecules without the need for crystallization will have a huge impact in structural biology.

There are many challenges. Imaging of a single molecule requires that the diffraction process is complete before the absorbed X-ray can measurably disrupt the structure of the molecule. Modeling has indicated that the motion of the nuclei will be negligible for time scales of less than about 10 fs [14] and that it is possible that the effects of the electronic damage may be ameliorated by suitable postprocessing [15]. As the technical problems involved in obtaining diffraction from a single molecule may be too difficult, work is also proceeding on the application of X-FEL sources to structures such as thin 2-D crystals [16]. A second important motivation for hard X-ray FELs is the investigation of the properties of matter at high-energy densities such as those that can be found in the interiors of planets.

The FEL facilities that provide ultra-high brilliance radiation at EUV to soft X-ray wavelengths are also motivated by a broad range of scientific challenges in condensed matter physics, chemistry, and biophysics. There has been a great deal of work performed on the exploration of the interaction of intense X-ray beams with atoms [17], molecules [18], and clusters [19], and the investigation of the dynamics of ultra-fast processes, such a phase transitions, is just beginning. One class of experiments at soft X-ray facilities relying on exploiting and expanding techniques of coherent imaging have the added benefit of accelerating progress toward the feasibility of imaging single biomolecules. Already, researchers have shown the possibility of recovering diffraction patterns from objects that are in the process of being destroyed by the beam [20]. Once a diffraction pattern has been obtained, then it needs to be analyzed to recover the diffracting structure. The development of high-resolution techniques of coherent diffraction imaging has received considerable recent attention [21] and has seen a number of applications in biology [22] and materials science [23], [24] using soft X-ray FELs and synchrotron light sources.

Many experiments proposed for FEL facilities require that the X-ray pulse be spatially coherent. As a SASE FEL does not contain a resonant cavity, the spatial coherence of the output beam relies on the electrons in the beam radiating as a phased array. Moreover, the intensity of the radiation varies from shot-to-shot, leading to significant work to characterize every pulse of the beam [25]. The first measurement of FEL coherence at X-ray wavelengths, reported in 2009 [26], found imperfect spatial coherence. However, methods are also emerging that allow for high-resolution coherent imaging in cases where the object is illuminated with imperfectly coherent X-ray beams [27]; therefore, moderate deviations from perfect coherence will be able to be tolerated.

As the SASE pulses have a stochastic temporal profile, the pulses are temporally partially coherent. Full-phase coherence and much narrower bandwidth can be approached by one of two methods: 1) injecting the FEL with a narrow-band fully coherent laser signal to produce a seeded FEL or 2) placing the insertion device between the mirrors of an resonator cavity to form an FEL oscillator. Indeed, many of the FELs operating today at infrared to ultraviolet wavelengths are oscillators.

The international community has been working hard, then, on the preparation for the use of the light from X-ray FELs. Narrow-bandwidth, seeded, soft X-ray FELs using various schemes of harmonically up-converting [28], [29] the laser seed are being built at Sincrotrone Trieste and at the FLASH facility at the Deutsches Elektronen-Synchrotron and are proposed for several other accelerator laboratories worldwide. Three hard X-ray projects are currently under varying stages of development: the Japanese SCSS (http://www-xfel.spring8.or.jp/), the European XFEL project (http://www.xfel.eu/), and the Linac Coherent Light Source (LCLS) in the USA (http://lcls.slac.stanford.edu/). In April 2009, the LCLS project reported the first coherent hard X-ray beam, with a performance beyond its design specifications. This is an exciting milestone. We can expect much exciting science to flow from these developments over the coming years.

References

[1] K. A. Nugent, "Coherent methods in the X-ray sciences," *Adv. Phys.*, vol. 59, no. 1, pp. 1–99, Jan. 2010.
[2] S. Reiche, P. Musumeci, C. Pellegrini, and J. B. Rosenzweig, "Development of ultra-short pulse, single coherent spike for SASE X-ray FELs," *Nucl. Instrum. Methods Phys. Res. A, Accel. Spectrom. Detect. Assoc. Equip.*, vol. 593, no. 1/2, pp. 45–48, Aug. 2008.

[3] R. Bonifacio, C. Pellegrini, and L. M. Narducci, "Collective instabilities and high-gain regime in a free-electron laser," *Opt. Commun.*, vol. 50, no. 6, pp. 373–378, Jul. 1984.
[4] K. J. Kim and M. Xie, "Self-amplified spontaneous emission for short-wavelength coherent radiation," *Nucl. Instrum. Methods Phys. Res. A, Accel. Spectrom. Detect. Assoc. Equip.*, vol. 331, no. 1–3, pp. 359–364, Jul. 1993.
[5] J. M. J. Madey, H. A. Schwettman, and W. M. Fairbank, "Free-electron laser," *IEEE Trans. Nucl. Sci.*, vol. NS-20, no. 3, pp. 980–983, Jun. 1973.
[6] J. M. J. Madey, "Stimulated emission of bremsstrahlung in a periodic magnetic field," *J. Appl. Phys.*, vol. 42, no. 5, pp. 1906–1913, Apr. 1971.
[7] T. J. Orzechowski, B. R. Anderson, J. C. Clark, W. M. Fawley, A. C. Paul, D. Prosnitz, E. T. Scharlemann, S. M. Yarema, D. B. Hopkins, A. M. Sessler, and J. S. Wurtele, "High-efficiency extraction of microwave-radiation from a tapered-wiggler free-electron laser," *Phys. Rev. Lett.*, vol. 57, no. 17, pp. 2172–2175, Oct. 1986.
[8] S. V. Milton, E. Gluskin, N. D. Arnold, C. Benson, W. Berg, S. G. Biedron, M. Borland, Y. C. Chae, R. J. Dejus, P. K. Den Hartog, B. Deriy, M. Erdmann, Y. I. Eidelmann, M. W. Hahne, Z. Huang, K. J. Kim, J. W. Lewellen, Y. Li, A. H. Lumpkin, O. Makarov, E. R. Moog, A. Nassiri, V. Sajaev, R. Soliday, B. J. Tieman, E. M. Trakhtenberg, G. Travish, I. B. Vasserman, N. A. Vinokurov, X. J. Wang, G. Wiemerslage, and B. X. Yang, "Exponential gain and saturation of a self-amplified spontaneous emission free-electron laser," *Science*, vol. 292, no. 5524, pp. 2037–2041, Jun. 2001.
[9] W. Ackermann, G. Asova, V. Ayvazyan, A. Azima, N. Baboi, J. Bahr, V. Balandin, B. Beutner, A. Brandt, A. Bolzmann, R. Brinkmann, O. I. Brovko, M. Castellano, P. Castro, L. Catani, E. Chiadroni, S. Choroba, A. Cianchi, J. T. Costello, D. Cubaynes, J. Dardis, W. Decking, H. Delsim-Hashemi, A. Delserieys, G. Di Pirro, M. Dohlus, S. Dusterer, A. Eckhardt, H. T. Edwards, B. Faatz, J. Feldhaus, K. Flottmann, J. Frisch, L. Frohlich, T. Garvey, U. Gensch, C. Gerth, M. Gorler, N. Golubeva, H. J. Grabosch, M. Grecki, O. Grimm, K. Hacker, U. Hahn, J. H. Han, K. Honkavaara, T. Hott, M. Huning, Y. Ivanisenko, E. Jaeschke, W. Jalmuzna, T. Jezynski, R. Kammering, V. Katalev, K. Kavanagh, E. T. Kennedy, S. Khodyachykh, K. Klose, V. Kocharyan, M. Korfer, M. Kollewe, W. Koprek, S. Korepanov, D. Kostin, M. Krassilnikov, G. Kube, M. Kuhlmann, C. L. S. Lewis, L. Lilje, T. Limberg, D. Lipka, F. Lohl, H. Luna, M. Luong, M. Martins, M. Meyer, P. Michelato, V. Miltchev, W. D. Moller, L. Monaco, W. F. O. Muller, O. Napieralski, O. Napoly, P. Nicolosi, D. Nolle, T. Nunez, A. Oppelt, C. Pagani, R. Paparella, N. Pchalek, J. Pedregosa-Gutierrez, B. Petersen, B. Petrosyan, G. Petrosyan, L. Petrosyan, J. Pfluger, E. Plonjes, L. Poletto, K. Pozniak, E. Prat, D. Proch, P. Pucyk, P. Radcliffe, H. Redlin, K. Rehlich, M. Richter, M. Roehrs, J. Roensch, R. Romaniuk, M. Ross, J. Rossbach, V. Rybnikov, M. Sachwitz, E. L. Saldin, W. Sandner, H. Schlarb, B. Schmidt, M. Schmitz, P. Schmuser, J. R. Schneider, E. A. Schneidmiller, S. Schnepp, S. Schreiber, M. Seidel, D. Sertore, A. V. Shabunov, C. Simon, S. Simrock, E. Sombrowski, A. A. Sorokin, P. Spanknebel, R. Spesyvtsev, L. Staykov, B. Steffen, F. Stephan, F. Stulle, H. Thom, K. Tiedtke, M. Tischer, S. Toleikis, R. Treusch, D. Trines, I. Tsakov, E. Vogel, T. Weiland, H. Weise, M. Wellhoffer, M. Wendt, I. Will, A. Winter, K. Wittenburg, W. Wurth, P. Yeates, M. V. Yurkov, I. Zagorodnov, and K. Zapfe, "Operation of a free-electron laser from the extreme ultraviolet to the water window," *Nat. Photon.*, vol. 1, no. 6, pp. 336–342, Jun. 2007.
[10] T. Shintake, H. Tanaka, T. Hara, T. Tanaka, K. Togawa, M. Yabashi, Y. Otake, Y. Asano, T. Bizen, T. Fukui, S. Goto, A. Higashiya, T. Hirono, N. Hosoda, T. Inagaki, S. Inoue, M. Ishii, Y. Kim, H. Kimura, M. Kitamura, T. Kobayashi, H. Maesaka, T. Masuda, S. Matsui, T. Matsushita, X. Marechal, M. Nagasono, H. Ohashi, T. Ohata, T. Ohshima, K. Onoe, K. Shirasawa, T. Takagi, S. Takahashi, M. Takeuchi, K. Tamasaku, R. Tanaka, Y. Tanaka, T. Tanikawa, T. Togashi, S. Wu, A. Yamashita, K. Yanagida, C. Zhang, H. Kitamura, and T. Ishikawa, "A compact free-electron laser for generating coherent radiation in the extreme ultraviolet region," *Nat. Photon.*, vol. 2, no. 9, pp. 555–559, Sep. 2008.
[11] M. Zangrando, A. Abrami, D. Bacescu, I. Cudin, C. Fava, F. Frassetto, A. Galimberti, R. Godnig, D. Giuressi, L. Poletto, L. Rumiz, R. Sergo, C. Svetina, and D. Cocco, "The photon analysis, delivery, and reduction system at the FERMI@ Elettra free electron laser user facility," *Rev. Sci. Instrum.*, vol. 80, no. 11, 113110, Nov. 2009.
[12] P. Emma *et al.,* "First lasing of the LCLS X-ray FEL at 1.5 Angstroms," in *Proc. PAC*, 2009. [Online]. Available: http://www-ssrl.slac.stanford.edu/lcls/commissioning/documents/th3pbi01
[13] R. Neutze, R. Wouts, D. van der Spoel, E. Weckert, and J. Hajdu, "Potential for biomolecular imaging with femtosecond X-ray pulses," *Nature*, vol. 406, no. 6797, pp. 752–757, Aug. 2000.
[14] Z. Jurek, G. Oszlanyi, and G. Faigel, "Imaging atom clusters by hard X-ray free-electron lasers," *Europhys. Lett.*, vol. 65, no. 4, pp. 491–497, Feb. 2004.
[15] S. P. Hau-Riege, R. A. London, H. N. Chapman, A. Szoke, and N. Timneanu, "Encapsulation and diffraction-pattern-correction methods to reduce the effect of damage in X-ray diffraction imaging of single biological molecules," *Phys. Rev. Lett.*, vol. 98, no. 19, 198302, May 2007.
[16] A. P. Mancuso, A. Schropp, B. Reime, L. M. Stadler, A. Singer, J. Gulden, S. Streit-Nierobisch, C. Gutt, G. Grubel, J. Feldhaus, F. Staier, R. Barth, A. Rosenhahn, M. Grunze, T. Nisius, T. Wilhein, D. Stickler, H. Stillrich, R. Fromter, H. P. Oepen, M. Martins, B. Pfau, C. M. Gunther, R. Konnecke, S. Eisebitt, B. Faatz, N. Guerassimova, K. Honkavaara, V. Kocharyan, R. Treusch, E. Saldin, S. Schreiber, E. A. Schneidmiller, M. V. Yurkov, E. Weckert, and I. A. Vartanyants, "Coherent-pulse 2D crystallography using a free-electron laser X-ray source," *Phys. Rev. Lett.*, vol. 102, no. 3, 035502, Jan. 2009.
[17] A. A. Sorokin, S. V. Bobashev, T. Feigl, K. Tiedtke, H. Wabnitz, and M. Richter, "Photoelectric effect at ultrahigh intensities," *Phys. Rev. Lett.*, vol. 99, no. 21, 213002, Nov. 2007.
[18] P. Johnsson, A. Rouzee, W. Siu, Y. Huismans, F. Lepine, T. Marchenko, S. Dusterer, F. Tavella, N. Stojanovic, A. Azima, R. Treusch, M. F. Kling, and M. J. J. Vrakking, "Field-free molecular alignment probed by the free electron laser in Hamburg (FLASH)," *J. Phys. B, At. Mol. Opt. Phys.*, vol. 42, no. 13, 134017, Jul. 2009.
[19] C. Bostedt, H. Thomas, M. Hoener, E. Eremina, T. Fennel, K. H. Meiwes-Broer, H. Wabnitz, M. Kuhlmann, E. Ploenjes, K. Tiedtke, R. Treusch, J. Feldhaus, A. R. B. de Castro, and T. Moller, "Multistep ionization of argon clusters in intense femtosecond extreme ultraviolet pulses," *Phys. Rev. Lett.*, vol. 100, no. 13, 133401, Apr. 2008.
[20] H. N. Chapman, A. Barty, M. J. Bogan, S. Boutet, M. Frank, S. P. Hau-Riege, S. Marchesini, B. W. Woods, S. Bajt, H. Benner, R. A. London, E. Plonjes, M. Kuhlmann, R. Treusch, S. Dusterer, T. Tschentscher, J. R. Schneider, E. Spiller, T. Moller, C. Bostedt, M. Hoener, D. A. Shapiro, K. O. Hodgson, D. Van der Spoel, F. Burmeister, M. Bergh, C. Caleman,

G. Huldt, M. M. Seibert, F. Maia, R. W. Lee, A. Szoke, N. Timneanu, and J. Hajdu, "Femtosecond diffractive imaging with a soft-X-ray free-electron laser," *Nat. Phys.*, vol. 2, no. 12, pp. 839–843, Dec. 2006.
[21] B. Abbey, K. A. Nugent, G. J. Williams, J. N. Clark, A. G. Peele, M. A. Pfeifer, M. De Jonge, and I. McNulty, "Keyhole coherent diffractive imaging," *Nat. Phys.*, vol. 4, no. 5, pp. 394–398, May 2008.
[22] X. J. Huang, J. Nelson, J. Kirz, E. Lima, S. Marchesini, H. J. Miao, A. M. Neiman, D. Shapiro, J. Steinbrener, A. Stewart, J. J. Turner, and C. Jacobsen, "Soft X-ray diffraction microscopy of a frozen hydrated yeast cell," *Phys. Rev. Lett.*, vol. 103, no. 19, 198101, Nov. 2009.
[23] A. Barty, S. Marchesini, H. N. Chapman, C. Cui, M. R. Howells, D. A. Shapiro, A. M. Minor, J. C. H. Spence, U. Weierstall, J. Ilavsky, A. Noy, S. P. Hau-Riege, A. B. Artyukhin, T. Baumann, T. Willey, J. Stolken, T. van Buuren, and J. H. Kinney, "Three-dimensional coherent X-ray diffraction imaging of a ceramic nanofoam: Determination of structural deformation mechanisms," *Phys. Rev. Lett.*, vol. 101, no. 5, 055501, Aug. 2008.
[24] B. Abbey, G. J. Williams, M. A. Pfeifer, J. N. Clark, C. T. Putkunz, A. Torrance, I. McNulty, T. M. Levin, A. G. Peele, and K. A. Nugent, "Quantitative coherent diffractive imaging of an integrated circuit at a spatial resolution of 20 nm," *Appl. Phys. Lett.*, vol. 93, no. 21, 214101, Nov. 2008.
[25] A. Barty, R. Soufli, T. McCarville, S. L. Baker, M. J. Pivovaroff, P. Stefan, and R. Bionta, "Predicting the coherent X-ray wavefront focal properties at the Linac Coherent Light Source (LCLS) X-ray free electron laser," *Opt. Exp.*, vol. 17, no. 18, pp. 15 508–15 519, Aug. 2009.
[26] A. Singer, I. A. Vartanyants, M. Kuhlmann, S. Duesterer, R. Treusch, and J. Feldhaus, "Transverse-coherence properties of the free-electron-laser FLASH at DESY," *Phys. Rev. Lett.*, vol. 101, no. 25, 254801, Dec. 2008.
[27] L. W. Whitehead, G. J. Williams, H. M. Quiney, D. J. Vine, R. A. Dilanian, S. Flewett, K. A. Nugent, A. G. Peele, E. Balaur, and I. McNulty, "Diffractive imaging using partially coherent X rays," *Phys. Rev. Lett.*, vol. 103, no. 24, 243902, Dec. 2009.
[28] L. H. Yu, L. DiMauro, A. Doyuran, W. S. Graves, E. D. Johnson, R. Heese, S. Krinsky, H. Loos, J. B. Murphy, G. Rakowsky, J. Rose, T. Shaftan, B. Sheehy, J. Skaritka, X. J. Wang, and Z. Wu, "First ultraviolet high-gain harmonic-generation free-electron laser," *Phys. Rev. Lett.*, vol. 91, no. 7, 074801, Aug. 2003.
[29] G. Stupakov, "Using the beam-echo effect for generation of short-wavelength radiation," *Phys. Rev. Lett.*, vol. 102, no. 7, 074801, Feb. 2009.

Femtosecond to Attosecond Optics

Ursula Keller

(Invited Paper)

Physics Department, Eidgenoessische Technische Hochschule Zurich, 8092 Zurich, Switzerland

DOI: 10.1109/JPHOT.2010.2047008
1943-0655/$26.00 ©2010 IEEE

Manuscript received February 12, 2010; revised March 3, 2010. Current version published April 23, 2010. Corresponding author: U. Keller (e-mail: keller@phys.ethz.ch).

Abstract: We continue to observe strong progress moving from femtosecond to attosecond optics. Attosecond pulses are now available in many different labs with additional gating techniques which somewhat relax the requirements for the pulse duration of the intense infrared laser pulses. The pulse repetition rate still sets a limit on the signal-to-noise ratio for attosecond pump-probe measurements, and therefore, other streaking techniques have resulted in time-resolved measurements with sub-10-attosecond accuracy. Recent improvements on high-power ultrafast diode-pumped solid-state and fiber lasers will offer alternative sources for megahertz attosecond pulse generation. First proof-of-principle experiments have been demonstrated.

Watching ultrafast processes in real time has been the driving force to generate increasingly shorter laser pulses. In 2009, we have seen that many more laboratories around the world can generate single attosecond pulses, as new techniques have relaxed the pulse-duration requirements from intense Ti:sapphire laser systems. The shortest pulses today are still about 80 as long and were demonstrated in 2008 [1] using intense ≈3.3-fs pulses and spectral filtering in the XUV. Previously, more pulse energy in the nanojoule regime was generated with a combination of polarization gating and a somewhat longer intense laser pulse of 5 fs generating 130-as pulses [2]. The polarization gating technique was further improved in combination with an intense two-color field which breaks the symmetry and only supports one high harmonic recombination event per cycle, which is referred to as the double-optical gating (DOG) technique. Pulses as short as 107 as with an 8-fs intense pulse have been generated [3], [4]. The requirements on the intense laser pulse have been further relaxed with the generalized DOG (GDOD) technique generating 148-as pulses, starting with much longer pulses of 28-fs duration—clearly in the many cycle regime at 800 nm [5].

A general challenge remains, however, because the signal-to-noise ratio for typical attosecond pump probe measurements is reduced by at least five orders of magnitude compared with the femtosecond regime since the pulse energy (as high as 1 nJ) comes at a much lower pulse repetition rate of 1 kHz instead of 100 MHz. To date attosecond measurements have been done in combination with streaking techniques mapping time to energy [6] or time to angular momentum (referred to as attosecond angular streaking) [7]. The latter approach has allowed for the fastest measurement that has ever been made directly in the time domain and which sets an upper limit in the tunneling delay time—even without using any attosecond pulses [8].

It is typically assumed that electrons can escape from atoms through tunneling when exposed to strong laser fields, but the timing of the process has been controversial and far too rapid to probe in detail. The Keller group has used attosecond angular streaking [7] to place an upper limit of 34 as and an intensity-averaged upper limit of 12 as on the tunneling delay time in strong field ionization of

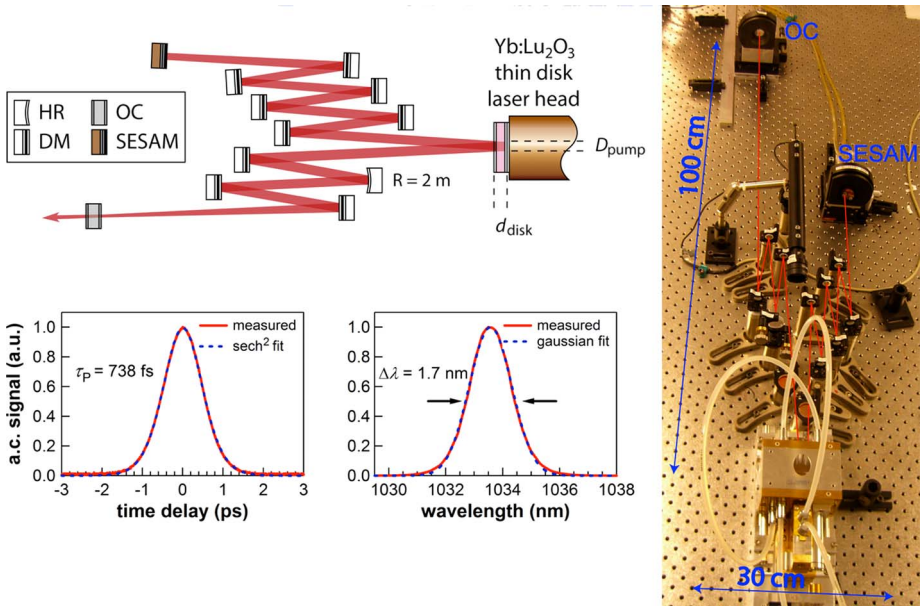

Fig. 1. SESAM mode-locked $Yb:Lu_2O_3$ thin-disk laser with 141-W average output power at a pump power of 349 W, which results in an optical-to-optical efficiency of 40%. The pulses have a time–bandwidth product of 0.35 at the full output power: which is very close to an ideal soliton pulse (i.e., 0.315), as expected from soliton mode locking. (HR: high reflector; OC: output coupler; DM: dispersive mirror; R: radius of curvature.)

a helium atom in the nonadiabatic tunneling regime [8]. To achieve this the exact timing of an intense, close-to-circular polarized laser field in the two-cycle regime was exploited—similar to the hands of a clock. This measurement is exactly based on the definition of "time" by "counting cycles"—here, a fraction of a cycle is measured. The experimental results give a strong indication that there is no real tunneling delay time, which is also confirmed with numerical simulations using the time-dependent Schrödinger equation. This measurement was done over a Keldysh parameter variation of 1.45 to 1.17 for which we could apply a small Coulomb field correction using a semiclassical picture. At higher intensities, we would expect a stronger Coulomb correction which, however, was not observed experimentally last year. This may shed some light on the ongoing discussion when simple semiclassical pictures start to break down on an atomic scale. Theory is still catching up with these new experimental results, which is a general observation in high field physics experiments. Generally, the community needs better theoretical models with valid approximations that can describe the attosecond dynamics on an atomic and molecular level. Solving the time-dependent Schrödinger equation becomes an impossible task for larger targets. Single-atom and small-molecule experiments may help to find valid approximations that can correctly predict the detailed dynamics and can reduce the numerical complexity for future models.

So far, attosecond streaking techniques have been very successful and have demonstrated that new and unexpected experimental results can be obtained when the attosecond dynamics is observed on an atomic scale. More surprises are expected, and this is what makes it exciting and motivating to push forward the frontier in time-resolved measurement techniques. However, streaking techniques have limitations, and increased efforts are being dedicated toward attosecond pulse generation in the megahertz regime and/or higher pulse energies in the kilohertz regime to ultimately allow for attosecond pump-probe measurements, where one attosecond pump pulse initiates and another time-delayed attosecond pulse probes the fast process. For example, a 100-μJ pulse energy at 5-MHz pulse repetition rates requires an average power of 500 W. Ti:sapphire lasers are not suitable for such high average power [9], and currently, the most promising femtosecond laser systems are either based on fiber laser amplifier systems, SESAM mode-locked thin-disk lasers, or optical parametric amplifiers pumped by high-average-power picosecond thin-disk lasers [10]. To

date, a femtosecond fiber CPA system has generated 830 W [11], and a passively mode-locked Yb:Lu_2O_3 thin-disk laser has generated more than 120 W of average power [12], which was recently improved further to more than 140 W with an optical-to-optical efficiency of 40%. The thin-disk laser approach requires no amplifiers, the complexity is not higher than for low-power laser oscillators (see Fig. 1), and novel Yb-doped laser materials have a great potential for sub-100-fs pulse generation [13]. In 2009, we observed the first megahertz HHG generation using high-power Yb-doped fiber CPA systems [14], and we have successfully demonstrated a lower pulse energy requirement for HHG in photonic crystal fibers [15] such that pulse energies in the tens of microjoules are sufficient for efficient HHG, which is a value easily accessible by SESAM mode-locked thin-disk lasers [16], [17].

The rapid progress in high-average-power femtosecond laser technology will continue. The development of high average photon flux, compact, tabletop ultrafast VUV/XUV sources will enable new measurements in photoelectron imaging spectroscopy, surface science, metrology, and biology and could become key instrumentations for laser accelerators and high-repetition-rate free-electron lasers (FELs). The pulse energy of low-repetition-rate systems very often has to be increased to a level where space-charge effects (i.e., electromagnetic forces between the generated charged particles within the interaction volume) start to blur the dynamics to be investigated—simply because the minimal detectable signal requires a certain average photon flux. A high photon flux but low pulse energy will also be very important for surface science and condensed matter physics using, for example, angle-resolved photoemission spectroscopy (ARPES) (e.g., in [18]). Strongly correlated electron systems with their complex physics are one of the biggest challenges in condensed-matter physics today. For example, space-charge effects have been a serious limitation for time-dependent measurements in high-T_c superconductors in the VUV regime [19]. A higher photon flux at higher repetition rates with lower pulse energies would allow for time-resolved ARPES.

References

[1] E. Goulielmakis, M. Schultze, M. Hofstetter, V. S. Yakovlev, J. Gagnon, M. Uiberacker, A. L. Aquila, E. M. Gullikson, D. T. Attwood, R. Kienberger, F. Krausz, and U. Kleineberg, "Single-cycle nonlinear optics," *Science*, vol. 320, no. 5883, pp. 1614–1617, Jun. 2008.

[2] G. Sansone, E. Benedetti, F. Calegari, C. Vozzi, L. Avaldi, R. Flammini, L. Poletto, P. Villoresi, C. Altucci, R. Velotta, S. Stagira, S. De Silvestri, and M. Nisoli, "Isolated single-cycle attosecond pulses," *Science*, vol. 314, no. 5798, pp. 443–446, Oct. 20, 2006.

[3] H. Mashiko, S. Gilbertson, C. Li, S. D. Khan, M. M. Shakya, E. Moon, and Z. Chang, "Double optical gating of high-order harmonic generation with carrier-envelope phase stabilized lasers," *Phys. Rev. Lett.*, vol. 100, no. 10, p. 103906, Mar. 2008.

[4] H. Mashiko, S. Gilbertson, M. Chini, X. M. Feng, C. X. Yun, H. Wang, S. D. Khan, S. Y. Chen, and Z. H. Chang, "Extreme ultraviolet supercontinua supporting pulse durations of less than one atomic unit of time," *Opt. Lett.*, vol. 34, no. 21, pp. 3337–3339, Nov. 2009.

[5] X. M. Feng, S. Gilbertson, H. Mashiko, H. Wang, S. D. Khan, M. Chini, Y. Wu, K. Zhao, and Z. H. Chang, "Generation of isolated attosecond pulses with 20 to 28 femtosecond lasers," *Phys. Rev. Lett.*, vol. 103, no. 18, p. 183 901, Oct. 2009.

[6] R. Kienberger, M. Hentschel, M. Uiberacker, C. Spielmann, M. Kitzler, A. Scrinzi, M. Wieland, T. Westerwalbesloh, U. Kleineberg, U. Heinzmann, M. Drescher, and F. Krausz, "Steering attosecond electron wave packets with light," *Science*, vol. 297, no. 5584, pp. 1144–1148, Aug. 2002.

[7] P. Eckle, M. Smolarski, P. Schlup, J. Biegert, A. Staudte, M. Schöffler, H. G. Muller, R. Dörner, and U. Keller, "Attosecond angular streaking," *Nat. Phys.*, vol. 4, no. 7, pp. 565–570, Jul. 2008.

[8] P. Eckle, A. Pfeiffer, C. Cirelli, A. Staudte, R. Dörner, H. G. Muller, M. Büttiker, and U. Keller, "Attosecond ionization and tunneling delay time measurements in helium," *Science*, vol. 322, no. 5907, pp. 1525–1529, Dec. 2008.

[9] T. Südmeyer, S. V. Marchese, S. Hashimoto, C. R. E. Baer, G. Gingras, B. Witzel, and U. Keller, "Femtosecond laser oscillators for high-field science," *Nat. Photon.*, vol. 2, no. 10, pp. 599–604, Oct. 2008.

[10] T. Metzger, A. Schwarz, C. Y. Teisset, D. Sutter, A. Killi, R. Kienberger, and F. Krausz, "High-repetition-rate picosecond pump laser based on a Yb:YAG disk amplifier for optical parametric amplification," *Opt. Lett.*, vol. 34, no. 14, pp. 2123–2125, Jul. 2009.

[11] T. Eidam, S. Hanf, E. Seise, T. V. Andersen, T. Gabler, C. Wirth, T. Schreiber, J. Limpert, and A. Tünnermann, "Femtosecond fiber CPA system emitting 830 W average output power," *Opt. Lett.*, vol. 35, no. 2, pp. 94–96, Jan. 2010.

[12] C. J. Saraceno, C. R. E. Baer, C. Kränkel, O. H. Heckl, M. Golling, T. Südmeyer, U. Keller, R. Peters, K. Petermann, and G. Huber, "120 W average power from a mode-locked Yb:Lu_2O_3 thin disk laser," presented at the Conf. Lasers Electro-Optics, San Jose, CA, 2010, Talk CThA4.

[13] T. Südmeyer, C. Kränkel, C. R. E. Baer, O. H. Heckl, C. J. Saraceno, M. Golling, R. Peters, K. Petermann, G. Huber, and U. Keller, "High-power ultrafast thin disk laser oscillators and their potential for sub-100-femtosecond pulse generation," *Appl. Phys. B*, vol. 97, no. 2, pp. 281–295, Oct. 2009.
[14] J. Boullet, Y. Zaouter, J. Limpert, S. Petit, Y. Mairesse, B. Fabre, J. Higuet, E. Mevel, E. Constant, and E. Cormier, "High-order harmonic generation at a megahertz-level repetition rate directly driven by an ytterbium-doped-fiber chirped-pulse amplification system," *Opt. Lett.*, vol. 34, no. 9, pp. 1489–1491, May 2009.
[15] O. H. Heckl, C. R. E. Baer, C. Kränkel, S. V. Marchese, F. Schapper, M. Holler, T. Südmeyer, J. S. Robinson, J. W. G. Tisch, F. Couny, P. Light, F. Benabid, and U. Keller, "High harmonic generation in a gas-filled hollow-core photonic crystal fiber," *Appl. Phys. B*, vol. 97, no. 2, pp. 369–373, Oct. 2009.
[16] S. V. Marchese, C. R. E. Baer, A. G. Engqvist, S. Hashimoto, D. J. H. C. Maas, M. Golling, T. Südmeyer, and U. Keller, "Femtosecond thin disk laser oscillator with pulse energy beyond the 10-microjoule level," *Opt. Express*, vol. 16, no. 9, pp. 6397–6407, Apr. 2008.
[17] J. Neuhaus, D. Bauer, J. Zhang, A. Killi, J. Kleinbauer, M. Kumkar, S. Weiler, M. Guina, D. H. Sutter, and T. Dekorsy, "Subpicosecond thin-disk laser oscillator with pulse energies of up to 25.9 microjoules by use of an active multipass geometry," *Opt. Express*, vol. 16, no. 25, pp. 20 530–20 539, Dec. 2008.
[18] Y. L. Chen, J. G. Analytis, J.-H. Chu, Z. K. Liu, S.-K. Mo, X. L. Qi, H. J. Zhang, D. H. Lu, X. Dai, Z. Fang, S. C. Zhang, I. R. Fisher, Z. Hussain, and Z.-X. Shen, "Experimental realization of a three-dimensional topological insulator, Bi_2Te_3," *Science*, vol. 325, no. 5937, pp. 178–181, Jul. 2009.
[19] J. D. Koralek, J. F. Douglas, N. C. Plumb, Z. Sun, A. V. Fedorov, M. M. Murnane, H. C. Kapteyn, S. T. Cundiff, Y. Aiura, K. Oka, H. Eisaki, and D. S. Dessau, "Laser based angle-resolved photoemission, the sudden approximation, and quasiparticle-like spectral peaks in $Bi_2Sr_2CaCu_2O_8$," *Phys. Rev. Lett.*, vol. 96, no. 1, p. 017005, Jan. 2006.

Major Accomplishments in 2009 on Slow Light

Robert W. Boyd[1] **and John R. Lowell**[2]

(Invited Paper)

[1]The Institute of Optics and Department of Physics and Astronomy, University of Rochester, Rochester, NY 14627 USA
[2]Defense Sciences Office, Defense Advanced Research Projects Agency, Arlington, VA 22203 USA

DOI: 10.1109/JPHOT.2010.2047101
1943-0655/$26.00 ©2010 IEEE

Manuscript received February 12, 2010. Current version published April 23, 2010. Corresponding author: R. W. Boyd (e-mail: boydrw@mac.com). The views, opinions, and/or findings contained in this paper are those of the authors and should not be interpreted as representing the official views or policies, either expressed or implied, of the Defense Advanced Research Projects Agency or the Department of Defense.

Abstract: We present a brief overview of recent advances in the field of "slow light," the field that studies means for controllably reducing the group velocity of light to values much smaller than its vacuum velocity, *c*. Some of the results summarized here include electrooptic modulation of single photons, all-optical switching within an atomic-vapor-filled hollow fiber, large induced phase shifts for microwave photonics, slow-light-enhanced nonlinear optical interactions, and highly controllable time delays in semiconductor optical amplifiers, parametric delay-dispersion tuners, and arrays of active microresonators.

2009 proved to be a very productive year for research on "slow light," which is the research field aimed at developing methods for controlling the velocity at which pulses of light travel in passing through material systems. The ability to control this velocity, which is known as the group velocity, holds promise for the development of many applications in the field of photonics. Just as group velocities much smaller than the speed of light in a vacuum are known as slow light, group velocities greater than c are known as fast light. Both effects can be induced under appropriate circumstances. Recent progress in this area has been summarized in a review article of Boyd and Gauthier [1].

As the field of slow light has matured over the past decade, it has become clear that there are many physical processes that can be used to modify the group velocity. In this context, it is useful to distinguish processes resulting from material properties and processes resulting from the structure of materials. In the former case, slow light results from the frequency dependence of the refractive index of a bulk material. It can be described in terms of a group index $n_g = n + \omega dn/d\omega$, where n is the usual refractive index and where the group index is defined so that the group velocity is given by c/n_g. Here, the refractive index can be either the intrinsic refractive index of the material or can be the index as modified by some sort of nonlinear optical interaction. In the latter case, however, slow light results from the modification of the velocity of light pulses as the result of a structure built into a material system; this structure could be a waveguide, a Bragg grating, or a photonic crystal.

In starting, we first describe advances in the use of slow light based on material properties. Given that there are a wide range of materials that support slow-light processes, we will first discuss the work using atomic species, followed by work that uses condensed matter systems.

The group of Harris [2] recently demonstrated the electro-optic modulation of single photons. In this paper, Stokes photons of a biphoton pair are used to set the time origin for electro-optic modulation of

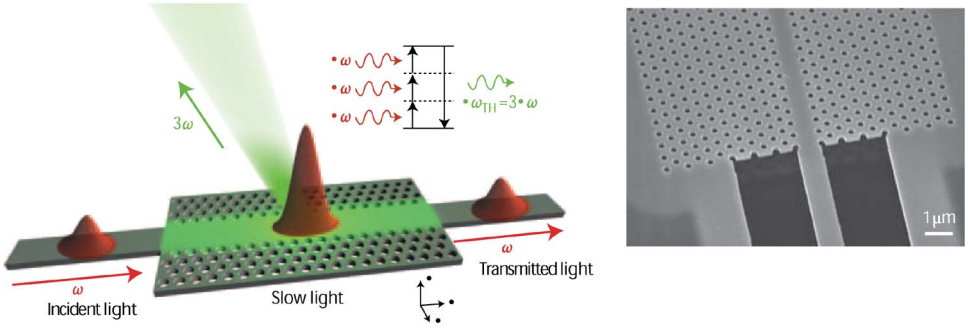

Fig. 1. Illustration of the enhancement of nonlinear optical processes through the use of slow-light methods. (a) Schematic of slow-light-enhanced third-harmonic generation (THG). The fundamental pulse at frequency ν (energy h ν) is spatially compressed in the slow-light photonic-crystal waveguide, increasing the electric field strength, while the third-harmonic signal is ejected from the wave-guide structure. (b) Scanning-electron-microscope (SEM) image of a tapered ridge waveguide coupled to a photonic-crystal waveguide etched in a thin silicon membrane. (After Corcoran *et al.*) (Reprinted by permission from Macmillan Publishers Ltd.: *Nature Photonics*, vol. 3, April 2009, © 2009. www.nature.com/naturephotonics.)

the wave function of the slowed and time-stretched, anti-Stokes photon, thereby allowing for arbitrary phase and amplitude modulation. They demonstrated conditional single-photon wave functions composed of several pulses or, instead, having Gaussian or exponential shapes. In a follow-up to this earlier work, Belthangady *et al.* [3] have presented a proof-of-principle experiment demonstrating a Fourier technique for measuring the shape of biphoton wave packets. The technique is based on the use of synchronously driven fast modulators and slow integrating detectors.

In separate work, Bajcsy *et al.* [4] have demonstrated efficient all-optical switching using slow light within a hollow fiber They demonstrated a fiber-optical switch that is activated by extremely small energies corresponding to only a few hundred optical photons per pulse. This result is achieved by simultaneously confining both photons and a small laser-cooled ensemble of atoms inside the hollow core of a single-mode photonic-crystal fiber. These workers make use of quantum optical techniques for generating slow-light propagation and for creating large nonlinear interaction between light beams. Another work, by Schmidt and Hawkins [11], demonstrated the use of waveguide structures to confine photons for interaction with atoms, although at room temperature.

Working in a semiconductor condensed matter system, Xue *et al.* [5] have reported major advances in the use of slow-light methods in the field of microwave photonics. They suggested and experimentally demonstrated a method for increasing the tunable rf phase shift of a semiconductor waveguide while at the same time enabling control of the rf power. This method is based on the use of slow- and fast-light effects in a cascade of semiconductor optical amplifiers (SOAs) combined with the use of spectral filtering to enhance the role of refractive index dynamics. A continuously tunable phase shift of approximately 240° at a microwave frequency of 19 GHz was demonstrated in a cascade of two SOAs, while maintaining an rf power change of less than 1.6 dB. The technique is scalable to more amplifiers and should allow realization of an rf phase shift of 360°.

Pesala *et al.* [6] have demonstrated a chirped pulse scheme that is highly effective in attaining large tunable time shifts via slow and fast light for an ultrashort pulse through an SOA. They show that advance can be turned into delay by simply reversing the sign of the chirp. A large continuously tunable advance-bandwidth product (ABP) of 4.7 and delay-bandwidth product (DBP) of 4.0 are achieved for negatively and positively chirped pulses, respectively, in the same device. They show that the tunable time shift is a direct result of self-phase modulation (SPM), and their theoretical simulation agrees well with their experimental results. Furthermore, their simulation results show that by proper optimization of the SOA and chirper design, a large continuously tunable DBP of 55 can be achieved.

Following up on an idea of Sharping *et al.* [7], Kurosu and Namiki [8] have demonstrated a parametric delay-dispersion tuner (PDDT) that is capable of the continuous tuning of delay and dispersion for wideband optical signals in a simultaneous and independent manner. They experimentally demonstrate a tunable delay of 22 ns for 2.6-ps return-to-zero optical signals without distortion and error-free transmissions at 43 Gb/s. They show that PDDT has a bandwidth of approximately 0.9 THz, resulting in the DBP of approximately 20 000, and that it exhibits excellent performance in terms of stability and reproducibility.

Finally, we turn to the demonstration of slow light in material structures. Recent work has emphasized how certain nonlinear optical processes can be enhanced through use of slow-light methods. For example, Corcoran *et al.* [9] have observed green light emission at the third-harmonic frequency through slow-light-enhanced third-harmonic generation in silicon photonic crystal waveguides pumped by a 1550-nm laser source, as illustrated in Fig. 1.

Moreover, Dumeige [10] has proposed theoretically the use of a short array of active microresonators to stop and manipulate light. This process uses the loss and gain to dynamically tune a short coupled-resonator delay line. The structure is made of four resonators and is optimized to avoid pulse distortion in the passive regime. The loss and gain modulations allow the resonant structure to be isolated from the access waveguide and pulses to be stored. He demonstrates via numerical simulations the pulse storing process and shows that this active delay line also induces nonlinear effects leading to pulse compression. This last property could be useful for tailoring pulse-dispersion tailoring.

In summary, extremely good progress has been made in 2009 in the area of slow-light research. Significant advances have been made both in the fundamental physics of slow light and in its engineering applications. This breadth of the field of slow light suggests why it is such an exciting area of research.

References

[1] R. W. Boyd and D. J. Gauthier, "Controlling the velocity of light pulses," *Science*, vol. 326, no. 5956, pp. 1074–1077, Nov. 2009.
[2] P. Kolchin, C. Belthangady, S. Du, G. Y. Yin, and S. E. Harris, "Electro-optic modulation of single photons," *Phys. Rev. Lett.*, vol. 101, no. 10, p. 103601, Sep. 2008.
[3] C. Belthangady, S. Du, C.-S. Chuu, G. Y. Yin, and S. E. Harris, "Modulation and measurement of time-energy entangled photons," *Phys. Rev. A, Gen. Phys.*, vol. 80, no. 3, p. 031803, Sep. 2009.
[4] M. Bajcsy, S. Hofferberth, V. Balic, T. Peyronel, M. Hafezi, A. S. Zibrov, V. Vuletic, and M. D. Lukin, "Efficient all-optical switching using slow light within a hollow fiber," *Phys. Rev. Lett.*, vol. 102, no. 20, p. 203902, May 2009.
[5] W. Xue, S. Sales, J. Capmany, and J. Mørk, "Microwave phase shifter with controllable power response based on slow- and fast-light effects in semiconductor optical amplifiers," *Opt. Lett.*, vol. 34, no. 7, pp. 929–931, Apr. 2009.
[6] B. Pesala, F. Sedgwick, A. V. Uskov, and C. Chang-Hasnain, "Greatly enhanced slow and fast light in chirped pulse semiconductor optical amplifiers: Theory and experiments," *Opt. Express*, vol. 17, no. 4, p. 2188, Feb. 2009.
[7] J. E. Sharping, Y. Okawachi, J. van Howe, C. Xu, Y. Wang, A. E. Willner, and A. L. Gaeta, "All-optical, wavelength and bandwidth preserving, pulse delay based on parametric wavelength conversion and dispersion," *Opt. Express*, vol. 13, no. 20, pp. 7872–7877, Oct. 2005.
[8] T. Kurosu and S. Namiki, "Continuously tunable 22 ns delay for wideband optical signals using a parametric delay-dispersion tuner," *Opt. Lett.*, vol. 34, no. 9, pp. 1441–1443, May 2009.
[9] B. Corcoran, C. Monat, C. Grillet, D. J. Moss, B. J. Eggleton, T. P. White, L. O'Faolain, and T. F. Krauss, "Green light emission in silicon through slow-light enhanced third-harmonic generation in photonic-crystal waveguides," *Nat. Photon.*, vol. 3, no. 4, pp. 206–210, Apr. 2009.
[10] Y. Dumeige, "Stopping and manipulating light using a short array of active microresonators," *Europhys. Lett.*, vol. 86, no. 1, p. 14003, Apr. 2009.
[11] H. Schmidt and A. R. Hawkins, "Atomic spectroscopy and quantum optics in hollow-core waveguides," *Laser Photon. Rev.*, Feb. 2010. [Online]. Available: http://www3.interscience.wiley.com/cgi-bin/fulltext/123269287/PDFSTART

Breakthroughs in Terahertz Science and Technology in 2009

Daniel Mittleman

(Invited Paper)

Rice University, Houston, TX 77005 USA

DOI: 10.1109/JPHOT.2010.2045490
1943-0655/$26.00 ©2010 IEEE

Manuscript received February 1, 2010. Current version published April 23, 2010. Corresponding author: D. Mittleman (e-mail: daniel@rice.edu).

Abstract: Terahertz science and technology continues to advance at a rapid pace. This article reviews a few of the most exciting advances from 2009, including reports in high-field THz science, imaging, and plasmonics.

Index Terms: Terahertz, sub-millimeter, far infrared.

In 2009, the field of terahertz science and technology continued to grow very rapidly. The number of peer-reviewed journal articles topped 1000, and attendance at related conferences (such as the IRMMW-THz conference series and the Optical Terahertz Science and Technology topical meeting) continues to grow. The field is highly interdisciplinary, since terahertz techniques are valuable for everything from spectroscopy to sensing. Rapid progress in source, detector, and systems technologies are matched by equally dramatic advances in materials research, photonic components, the development of new applications areas, and so on. Here, we discuss just a few of many important studies whose results were reported in 2009.

One important current research area in terahertz photonics is the quest to reach high intensity. Time-domain spectroscopy has become a standard tool for the generation and detection of single-cycle terahertz pulses, but in most cases, the pulse energy is quite low. As a result, schemes for exploiting the high temporal resolution have been mostly limited to using the terahertz as a probe, rather than as the pump pulse that can initiate a nonlinear interaction. Within the last few years, researchers have demonstrated tabletop methods for producing terahertz pulses with microjoules of energy per pulse or with peak electric fields in the 100-MV/cm range. This, in turn, has enabled new experimental capabilities in the study of terahertz-induced nonlinear optics.

In 2009, several groups reported measurements which rely on these new capabilities. Most notably, Nelson and his coworkers at the Massachusetts Institute of Technology have published the results of several terahertz-pump, terahertz-probe measurements, illustrating the new types of spectroscopic information that can be obtained. For example, in a conventional optical pump-probe measurement on a semiconductor, interband transitions give rise to a population of both electrons and holes. A time-delayed probe pulse interacts with both of these hot carrier distributions, and therefore, disentangling the dynamics of the two can be challenging. In contrast, a terahertz pump (using an n-doped sample, for example) creates only nonequilibrium electrons and not holes. The relaxation dynamics, which are measured with a time-delayed terahertz probe pulse, are therefore unambiguous [1].

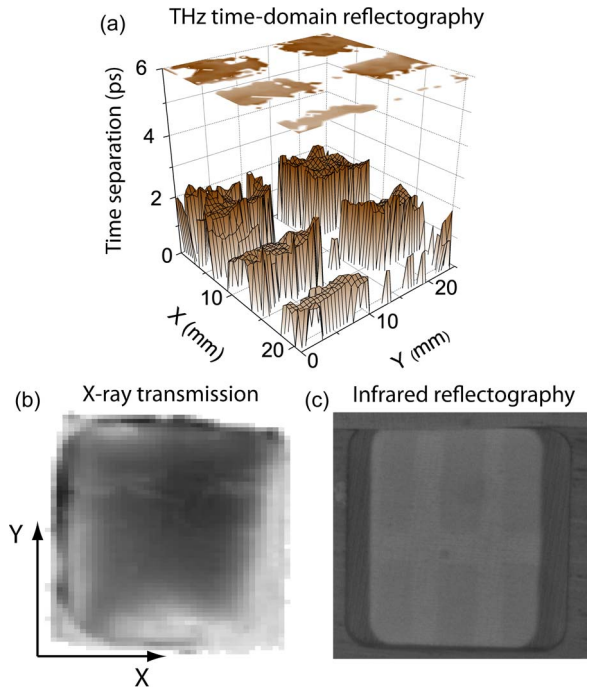

Fig. 1.

The design and construction of novel terahertz resonators continues to be a hot topic. This effort is motivated by sensing applications, in which a small shift in the resonant frequency can be correlated with the presence of a sensing target. Unlike in the optical regime, where compact high-Q resonators (e.g., $Q \sim 10^4$ or higher) are fairly routine, the state of the art in integrated terahertz resonant devices is less well developed. 2009 saw some significant progress in waveguide-integrated resonators, notably from groups at Oklahoma State University (using Bragg resonances) [2] and Rice University (using groove cavities) [3]. Perhaps the most impressive result came from the University of California at Santa Barbara, where a photonic crystal cavity was demonstrated with a Q of about 1000 [4].

Another research area making rapid progress in 2009 is terahertz plasmonics. The terahertz range lies between the range of microwaves, where surface waves at metal surfaces have been well known for over a century, and the regime of plasmonics, where the surface response of metals is strongly influenced by resonant plasmon interactions. In the terahertz range, it is natural to extend and merge these two related concepts. Using ideas from the optical plasmonics community (such as the concept of metamaterials) or from the microwave photonics community (such as waveguides based on surface waves), researchers have made important steps in the development of components and techniques for terahertz science and technology.

The field of terahertz metamaterials provides some excellent examples. Taylor and her coworkers at Los Alamos National Laboratory, along with collaborators at Sandia National Laboratory, Boston College, and Boston University, demonstrated a metamaterial-based phase modulator for terahertz radiation. Although the response is resonant, as dictated by the nature of a typical split-ring-resonator-based planar metamaterial, the modulation is broadband, since the metamaterial affects both the amplitude and the phase of the terahertz signal over a broad spectral range [5]. The Los Alamos and Sandia groups also collaborated with researchers at Rice University to demonstrate the first high-speed spatial control of a terahertz wave front using a metamaterial-based modulator [6]. This spatial light modulator could have important uses in many future terahertz applications. For example, it could replace the need for a multipixel focal plane array in a real-time terahertz imaging system.

Speaking of terahertz imaging, this area also saw several important advances, both in techniques and devices for image formation and in expanding the range of applications. A collaboration

between groups at the University of Wuppertal and the Johann Wolfgang Goethe-University Frankfurt demonstrated a focal plane array fabricated in 0.25-μm CMOS [7]. This device, operating at room temperature, exhibits impressive sensitivity for radiation at 0.65 THz and has a clear route for scaling to a large number of pixels. This low-cost solution could eliminate one of the key barriers to the widespread implementation of terahertz imaging. The goal of subwavelength resolution continues to attract a great deal of attention. Impressive results have been described by a group at Aachen University. In this paper, a surface wave propagating on a tapered wire waveguide was compressed to a region that is much smaller than the wavelength. A target, which is held in the near field of the tapered tip, was then imaged with resolution in the few micrometer range [8]. Meanwhile, the list of possible applications of terahertz imaging continues to grow. One exciting area with enormous potential is that of art conservation, which saw several important feasibility studies in 2009 [9], [10]. Fig. 1 illustrates the unique types of information that can be obtained. This and other imaging applications continue to be one of the key motivating factors in the growth of the field.

References

[1] M. C. Hoffmann, J. Hebling, H. Y. Hwang, K.-L. Yeh, and K. A. Nelson, "THz-pump/THz-probe spectroscopy of semiconductors at high field strengths," *J. Opt. Soc. Amer. B, Opt. Phys.*, vol. 26, no. 9, pp. A29–A34, 2009.
[2] S. S. Harsha, N. Laman, and D. Grischkowsky, "High-Q terahertz Bragg resonances within a metal parallel plate waveguide," *Appl. Phys. Lett.*, vol. 94, no. 9, p. 091118, Mar. 2009.
[3] R. Mendis, V. Astley, J. Liu, and D. M. Mittleman, "Terahertz microfluidic sensor based on a parallel-plate waveguide resonant cavity," *Appl. Phys. Lett.*, vol. 95, no. 17, p. 171 113, Oct. 2009.
[4] M. S. Sherwin and C. M. Yee, "High-Q terahertz microcavities in silicon photonic crystal slabs," *Appl. Phys. Lett.*, vol. 94, no. 15, p. 154 104, Apr. 2009.
[5] H.-T. Chen, W. J. Padilla, M. J. Cich, A. K. Azad, R. D. Averitt, and A. J. Taylor, "A metamaterial solid-state terahertz phase modulator," *Nat. Photon.*, vol. 3, no. 3, pp. 148–151, Mar. 2009.
[6] W. L. Chan, H.-T. Chen, A. J. Taylor, I. Brener, M. J. Cich, and D. M. Mittleman, "A spatial light modulator for terahertz beams," *Appl. Phys. Lett.*, vol. 94, no. 21, p. 213 511, May 2009.
[7] E. Öjefors, U. R. Pfeiffer, A. Lisauskas, and H. G. Roskos, "A 0.65 THz focal-plane array in a quarter-micron CMOS process technology," *IEEE J. Solid-State Circuits*, vol. 44, no. 7, pp. 1968–1976, Jul. 2009.
[8] M. Awad, M. Nagel, and H. Kurz, "Tapered Sommerfeld wire terahertz near-field imaging," *Appl. Phys. Lett.*, vol. 94, no. 5, p. 051107, Feb. 2009.
[9] K. Fukunaga, I. Hosako, I. N. Duling, and M. Picollo, "Terahertz imaging systems: A non-invasive technique for the analysis of paintings," *Proc. SPIE*, vol. 7391, pp. 739 10D-1–739 10D-9, Jul. 2009.
[10] A. L. Adam, P. C. M. Planken, S. Meloni, and J. Dik, "Terahertz imaging of hidden paint layers on canvas," *Opt. Express*, vol. 17, no. 5, pp. 3407–3416, Mar. 2009.

Nanolasers Beat the Diffraction Limit

Martin T. Hill

(Invited Paper)

Department of Electrical Engineering, Eindhoven University of Technology,
5600 MB Eindhoven, The Netherlands

DOI: 10.1109/JPHOT.2010.2044785
1943-0655/$26.00 ©2010 IEEE

Manuscript received January 25, 2010; revised February 19, 2010. Current version published April 23, 2010. Corresponding author: M. T. Hill (e-mail: M.T.Hill@tue.nl).

Abstract: Recently, a number of groups have reported a dramatic reduction in the minimum size of lasers, achieved via the use of metals to form the laser's resonant cavity. These results dispel misconceptions that the minimum laser size is limited by diffraction and dielectric cavities. Furthermore, the use of metals allows an abundance of cavity designs, providing a rich research area, the possibility of new important applications for small high-speed lasers, and new flexible and efficient coherent light emitters.

There has been a steady push to further miniaturize lasers as there are benefits similar to those seen with the shrinking dimensions of electronic components. A smaller laser requires less power and can potentially be switched on and off faster. The main thrust of research in nanolasers has been into photonic crystal cavity lasers [1]. Here, the light is confined strongly in two dimensions by what are effectively 2-D Bragg mirrors formed by making a pattern of holes in a high-refractive-index semiconductor. In all of these cavities, the refractive index differences of dielectric materials are used to confine the light. The smallest dimensions to which the optical mode of such cavities can be confined is related to the diffraction limit and is on the order of one half of the wavelength of light in the dielectric material. Furthermore, the dielectric mirror structure typically has to be many wavelengths in size, in order to be effective, implying that the total laser size is still large compared to the wavelength of light.

For a long time it was thought that diffraction effects made it impossible for lasers and other photonic devices to be smaller than about half the wavelength of the light they emitted or processed. However, it is possible to beat this "diffraction limit" by guiding light in the form of surface plasmon polaritons (SPPs) at the interface between a metal (conductor) and a dielectric (nonconducting) material such as air [2], [3]. The minimum size scales of structures employing this form of light confinement is related to the penetration depth of light into the metal, which is typically of the order of tens of nanometers.

An SPP is a light wave trapped at the metal/dielectric interface due to its interaction with conduction electrons at the metal surface. Unfortunately, the oscillating conduction electrons dissipate energy through collisions with the metal's atomic lattice. This energy dissipation leads to high optical losses; therefore, SPPs can only travel short distances, limiting the size and complexity of plasmonic circuits.

Until recently, many researchers doubted if it would be possible to overcome the losses in plasmonic or metallic waveguides and cavities with the currently available optical gain materials. Thus, nanolasers would always be based on dielectrics and limited by diffraction in size. Only recently have metallic nanocavity lasers showed that lasers can be made with a truly small overall size and a tightly confined optical mode [4].

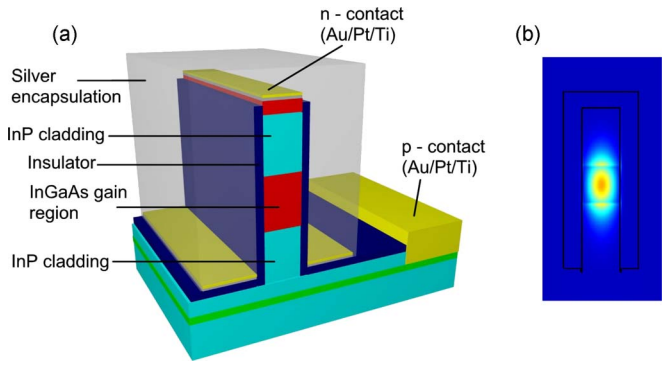

Fig. 1. A number of groups have made metallic or plasmonic nano-lasers in 2009. (a) One approach that has been pursued by several groups [5], [6] is to encapsulate a semiconductor heterostructure pillar in an insulator and a low optical loss metal such as silver or aluminium. Such an approach is particularly suitable for electrical pumping of the laser. (b) The optical mode in such structures is trapped on the InGaAs gain region in the center of the pillar due to refractive index differences.

In 2009, there were a number of significant steps forward in the field of metallic/plasmonic nanolasers, both in the further miniaturization and in moving these devices closer to applications. For electrically pumped metallic/semiconductor nanolasers, it was demonstrated that lasing at near infrared wavelengths is possible in metal–insulator–metal (MIM) waveguide structures, which can tightly confine light far below the diffraction limit [5] (see Fig. 1). The total insulator and semiconductor width of the MIM waveguide was about half the diffraction limit; therefore, these devices propagated a transverse magnetic or a so-called gap-plasmon mode. Additionally slightly wider devices which propagated a transverse electric mode showed operation at room temperature, which is an important step for applications. Another group from University of California at San Diego had success with metal/semiconductor nanolaser structures, showing room-temperature operation for an optically pumped device which was less than a free space wavelength of light in all three dimensions (also in the near infrared) [6]. Others at the California Institute of Technology showed evidence of lasing in a microdisk cavity having one side coated with metal [7].

Meanwhile, researchers at the University of California at Berkeley, the Lawrence Berkeley National Laboratory, and Peking University showed lasing in a section of a hybrid dielectric/plasmonic waveguide [8]. The waveguide is constructed from a flat metal substrate (silver) coated with a thin dielectric layer on which a thin semiconductor nanowire is placed [9]. The optical mode propagating in the silver/dielectic/semiconductor waveguide has a significant amount of its energy squeezed into the thin dielectric gap between the nanowire and the metal substrate, leading to a highly localized mode which has, according to calculations, an area that is significantly below the diffraction limit. The tail of the propagating mode overlaps with the semiconductor nanowire, which acts as the gain medium. The nanowire forms a Fabry–Perot cavity, with the plasmonic modes resonating between its two ends (which are a few micrometers or more apart). Using short optical pulses to pump the semiconductor nanowire, lasing is shown in the Fabry–Perot cavity at low temperatures, in the blue part of the visible spectrum.

Even more remarkable, researchers at Norfolk State University, Purdue University, and Cornell University have shown lasing in a gold nanoparticle with a diameter of 14 nm that is surrounded by a silica shell containing dye molecules that exhibit optical gain (to give an overall diameter of 44 nm) [10]. The gold nanoparticle which forms the optical cavity has a plasmon resonance at a wavelength of $\sim$520 nm. When the dye molecules are pumped by short optical pulses, there is sufficient gain created to overcome the losses in the gold, and a coherent source of highly localized SPPs is created. It is truly remarkable to demonstrate such a laser-like device with a cavity, gain medium, and optical mode that are all an order of magnitude smaller than the wavelength of light in all three dimensions.

So how small can lasers be made? There is speculation that they could be made down to the size of few nanometers [11]. It appears plausible that both dye and semiconductor lasers could be made

down to a size of a few tens of nanometers in several dimensions [12], [13]. Certainly in the next few years, experiments will probe these incredible minimum size limits.

Will such small lasers have any use? With laser size now no longer limited by diffraction, the modulation or switching speed of these nanolasers can potentially reach into the terahertz region [14], at low power consumption, which will be of interest for short-range optical communication and switching applications. The availability of ultrasmall high-speed SPP sources will also open up the way to complex nanoscale optical systems based on plasmonics. Finally, now having independent lasers that can be formed into arrays of subwavelength pitch may open up new possibilities for subwavelength scanning and optical atom traps.

For many applications, there will be a requirement for continuous operation at room or higher temperatures with good device lifetimes and efficient electrical pumping of the laser gain medium. If these challenges can be met, then spasers [11] or plasmonic nanolasers will be widely employed diverse areas, including information processing, communications, sensing, and possibly many other new applications.

References

[1] O. Painter, R. K. Lee, A. Scherer, A. Yariv, J. D. O'Brien, P. D. Dapkus, and I. Kim, "Two-dimensional photonic band-gap defect mode laser," *Science*, vol. 284, no. 5421, pp. 1819–1821, Jun. 1999.

[2] H. A. Atwater, "The promise of plasmonics," *Sci. Amer.*, vol. 296, pp. 38–45, Apr. 2007.

[3] W. L. Barnes, A. Dereux, and T. W. Ebbesen, "Surface plasmon subwavelength optics," *Nature*, vol. 424, no. 6950, pp. 824–830, Aug. 2003.

[4] M. T. Hill, Y.-S. Oei, B. Smalbrugge, Y. Zhu, T. de Vries, P. J. van Veldhoven, F. W. M. van Otten, T. J. Eijkemans, J. P. Turkiewicz, H. de Waardt, E. J. Geluk, S.-H. Kwon, Y.-H. Lee, R. Nötzel, and M. K. Smit, "Lasing in metallic-coated nanocavities," *Nat. Photon.*, vol. 1, no. 10, pp. 589–594, Oct. 2007.

[5] M. T. Hill, M. Marell, E. S. P. Leong, B. Smalbrugge, Y. Zhu, M. Sun, P. J. van Veldhoven, E. J. Geluk, F. Karouta, Y.-S. Oei, R. Nötzel, C.-Z. Ning, and M. K. Smit, "Lasing in metal-insulator-metal sub-wavelength plasmonic waveguides," *Opt. Exp.*, vol. 17, no. 13, pp. 11 107–11 112, Jun. 2009.

[6] M. P. Nezhad, A. Simic, O. Bondarenko, B. A. Slutsky, A. Mizrahi, L. Feng, V. Lomakin, and Y. Fainman, "Room temperature lasing from subwavelength metal-insulator-semiconductor structures," presented at the Conf. Lasers Electro-Optics (CLEO), Baltimore, MD, 2009, Paper CMD2.

[7] R. Perahia, T. P. Mayer Alegre, A. H. Safavi-Naeini, and O. Painter, "Surface-plasmon mode hybridization in subwavelength microdisk lasers," *Appl. Phys. Lett.*, vol. 95, no. 20, p. 201 114, Nov. 2009.

[8] R. F. Oulton, V. J. Sorger, T. Zentgraf, R.-M. Ma, C. Gladden, L. Dai, G. Bartal, and X. Zhang, "Plasmon lasers at deep subwavelength scale," *Nature*, vol. 461, no. 7264, pp. 629–632, Oct. 2009.

[9] R. F. Oulton, V. J. Sorger, D. F. P. Pile, D. A. Genov, and X. Zhang, "A hybrid plasmonic waveguide for sub-wavelength confinement and long range propagation," *Nat. Photon.*, vol. 2, no. 8, pp. 496–500, Aug. 2008.

[10] M. A. Noginov, G. Zhu, A. M. Belgrave, R. Bakker, V. M. Shalaev, E. E. Narimanov, S. Stout, E. Herz, T. Suteewong, and U. Wiesner, "Demonstration of a spaser-based nanolaser," *Nature*, vol. 460, no. 7259, pp. 1110–1112, Aug. 2009.

[11] D. J. Bergman and M. I. Stockman, "Surface plasmon amplification by stimulated emission of radiation: Quantum generation of coherent surface plasmons in nanosystems," *Phys. Rev. Lett.*, vol. 90, no. 2, p. 027402, Jan. 2003.

[12] S. A. Maier, "Gain-assisted propagation of electromagnetic energy in subwavelength surface plasmon polariton gap waveguides," *Opt. Commun.*, vol. 258, no. 2, pp. 295–299, Feb. 2006.

[13] M. T. Hill, "Metallic nano-cavity lasers at near infrared wavelengths," *Proc. SPIE*, vol. 7394, pp. 739409-1–739409-6, Aug. 2009.

[14] H. Altug, D. Englund, and J. Vučković, "Ultrafast photonic crystal nanocavity laser," *Nat. Phys.*, vol. 2, no. 7, pp. 484–488, Jul. 2006.

Breakthroughs in Silicon Photonics 2009

Richard M. De La Rue

(Invited Paper)

Optoelectronics Research Group, Department of Electronics and Electrical Engineering, University of Glasgow, G12 8QQ Glasgow, U.K.

DOI: 10.1109/JPHOT.2010.2045646
1943-0655/$26.00 ©2010 IEEE

Manuscript received January 25, 2010. Current version published April 23, 2010. Corresponding author: R. M. De La Rue (e-mail: r.delarue@elec.gla.ac.uk).

Abstract: Silicon photonics research published in 2009 exhibited considerable dynamism. Significant progress was made in research on optomechanics, novel phenomena in Bragg gratings, bio-sensing, photo-detectors, and silicon-organic hybrid structures. Non-linearity was successfully exploited for third-harmonic generation, pulse steepening, waveform compression, and high-speed sampling. All three solid states of silicon–single-crystal, polycrystalline, and amorphous–featured. It was a good year for silicon photonics research!

2009 was a year of strong advances for research in silicon photonics. Despite—or perhaps even because of—its intrinsic passivity, silicon technology, primarily in the form of silicon-on-insulator (SOI), has proven to be the appropriate vehicle for exploration of novel device concepts and even of new physics. For the purposes of this brief review, the definition of silicon photonics has been restricted to cover only photonic devices and structures in which silicon is at the core of the photonic action. The silicon involved may be present in any one of its three solid manifestations—single-crystal, polycrystalline or amorphous—and could even be alloyed, for instance, with germanium.

Our first breakthrough is exemplified by two publications [1], [2] that appeared simultaneously in closely related journals. The subject of *opto-mechanics*—in which the radiation pressure associated with propagating, but strongly confined, light beams gives rise to gradient forces that are sufficient to produce readily observable mechanical deformations—is undoubtedly a trendy one, but developments that will lead to this version of a nano-opto-electro-mechanical system being usefully exploited are now happening [3].

The high refractive index of silicon makes it possible to obtain strong optical confinement in waveguides with well submicrometer cross-sectional dimensions, but such waveguides are also commensurately more vulnerable to light scattering caused by dimensional variations, leading to significant propagation losses for rms waveguide wall fluctuations below 1 nm. For some possible applications, propagation losses of 0.1 dB.cm^{-1} or lower will be required. A partial answer to this problem is not to etch the silicon core layer at all [4] but to use a combination of multiple thermal oxidation stages and etch-patterning of the resulting silicon oxide.

Although silicon has already been demonstrated to be an interesting nonlinear material, with substantial $\chi 3$, the idea of using it as a vehicle for the generation of *green light* by third harmonic generation might seem to be at least a little odd. However, notable aficionados of slow light in photonic crystal channel waveguides have succeeded in this task [5], with immediate extraction out of the waveguide making it possible partially to bypass the issue of fundamentally strong absorption. See Fig. 1. Two British phenomena (Bragg diffraction and Brewster's angle) have combined to provide another unexpected phenomenon—"the *disappearing stop-band*" [6]. The specifically restricted

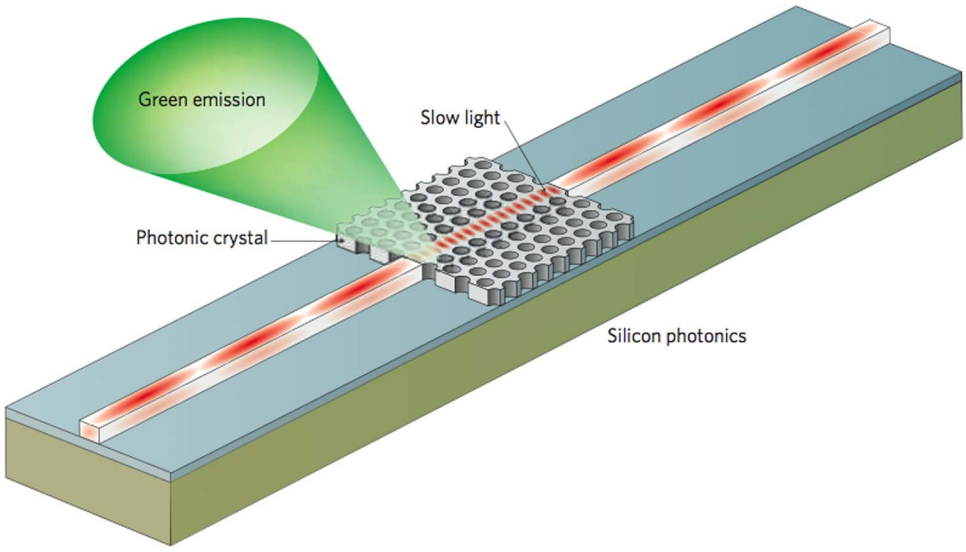

Fig. 1. Schematic of third-harmonic generation of green light from the infrared in SOI photonic crystal channel waveguide. *Courtesy of Nature Photonics*.

conditions under which the phenomenon becomes observable in a photonic wire Bragg grating suggest that it might find application in sensors.

The mention of sensors brings us logically to *bio-sensors*. A notable contribution [7] has been the engineered combination of a high-Q photonic wire ring resonator, which is specially deformed to enhance the interaction, with multichannel capability and micro-fluidic delivery of the bio-analyte. However, strongly defined band edges for photonic wire Bragg gratings have also been demonstrated to have potential in bio-sensing [8]. Simulation shows that the simple addition of a phase jump into such a grating [9] converts it into a high-Q and very compact sensor structure, although experimental demonstration will be required in due course.

While the intrinsic transparency of silicon at standard telecommunications wavelengths such as 1.3 μm and 1.55 μm is key to much of what is currently happening on the scene, *built-in photo-detection* at just those wavelengths is a very desirable capability. Ion implantation [10] offers both the possibility of electro-absorption-type modulation and photo-detection with useful quantum efficiency—and with the waveguide configuration enabling high performance via matching between the device length and the absorption wavelength.

As already remarked, silicon has a large value of $\chi 3$. Because of two-photon absorption, its figure of merit is much less impressive for operation at infrared wavelengths below about 2.2 μm. One approach that seems likely to be useful is the polymer-infilled "slot-guide," in which highly *nonlinear polymer* becomes, locally, the primary transport medium for the light [11]. This silicon/polymer combination makes it possible to take advantage of the continuity of the normal component of the electric flux density D of the light across the interface between the silicon and the polymer to enhance the field strength by approximately a factor of 4 and the strength of the resulting Kerr effect by $4^2 = 16$, i.e., by more than an order of magnitude.

The forward march of *amorphous* silicon as a waveguide device medium has been demonstrated in work on a grating triplexer [12] for cable TV applications with the three operating wavelengths being 1310 nm, 1490 nm, and 1550 nm. A device footprint of only 150 μm $\times$ 130 μm is a result of the high index contrast offered by silicon, while the absorption losses of around 1.5 dB/cm should have negligible impact at that size scale. Although not strongly exploited in this particular device, the fact that the thickness of the silicon waveguide core can readily be selected at the deposition stage is a potentially significant advantage. *Polycrystalline* silicon features in a ring-resonator photonic wire modulator described in Ref. [13]. Tradeoffs between recombination-time-limited device operating speed and propagation loss tend to favor polycrystalline silicon over single crystal.

The stage in the evolution of silicon (nano-)photonics has now arrived where the provision of complex signal-processing functionality using a silicon integrated photonic chip is becoming the norm. Recent examples include *optical sampling* [14] and *time-compression* [15]. Finally, mention should be made of impressive values predicted for high-Q cavity micro-/nano-resonators based on a combination of photonic wire and 1-D photonic crystal structuring [16]—and *shock-wave generation* [17]. *Suspended nano-beam*s [16] with both mechanically and optically resonant behavior should provide further (photon) momentum for research activity in 2010. As measured by the characteristic shock time, silicon photonic wires are typically more than an order of magnitude more shocking than photonic crystal fibers [17].

The above brief personal review is unavoidably incomplete and subject to randomness. It has tended to emphasize the micro/nano aspects of silicon photonics—and has been based solely on journal publications that have appeared in the calendar year 2009. I expect the year 2010 to bring with it at least as much interest and excitement.

References

[1] J. Roels, I. De Vlaminck, L. Lagae, B. Maes, D. Van Thourhout, and R. Baets, "Tunable optical forces between nanophotonic waveguides," *Nat. Nanotechnol.*, vol. 4, no. 8, pp. 510–513, Aug. 2009.

[2] M. Li, W. H. P. Pernice, and H. X. Tang, "Tunable bipolar optical interactions between guided lightwaves," *Nat. Photon.*, vol. 3, no. 8, pp. 464–468, Aug. 2009.

[3] J. Rosenberg, Q. Lin, and O. Painter, "Static and dynamic wavelength routing via the gradient optical force," *Nat. Photon.*, vol. 3, no. 8, pp. 478–483, Aug. 2009.

[4] J. Cardenas, C. B. Poitras, J. T. Robinson, K. Preston, L. Chen, and M. Lipson, "Low loss etchless silicon photonic waveguides," *Opt. Express*, vol. 17, no. 6, pp. 4752–4757, Mar. 16, 2009.

[5] B. Corcoran, C. Monat, C. Grillet, D. J. Moss, B. J. Eggleton, T. P. White, and T. F. Krauss, "Green light emission in silicon through slow-light enhanced third-harmonic generation in photonic-crystal waveguides," *Nat. Photon.*, vol. 3, no. 4, pp. 206–210, Apr. 2009.

[6] M. Gnan, W. C. L. Hopman, G. Bellanca, R. M. de Ridder, R. M. De La Rue, and P. Bassi, "Closure of the stop-band in photonic wire Bragg gratings," *Opt. Express*, vol. 17, no. 11, pp. 8830–8842, May 25, 2009.

[7] A. Densmore, M. Vachon, D.-X. Xu, S. Janz, R. Ma, Y.-H. Li, G. Lopinski, A. Delâge, J. Lapointe, C. C. Luebbert, Q. Y. Liu, P. Cheben, and J. H. Schmid, "Silicon photonic wire biosensor array for multiplexed real-time and label-free molecular detection," *Opt. Lett.*, vol. 34, no. 23, pp. 3598–3600, Dec. 1, 2009.

[8] A. Jugessur, J. Dou, J. S. Aitchison, R. M. De La Rue, and M. Gnan, "A photonic nano-Bragg grating device integrated with microfluidic channels for bio-sensing applications," *Microelectron. Eng.*, vol. 86, no. 4–6, pp. 1488–1490, Apr.–Jun. 2009.

[9] P. Prabhathan, V. M. Murukeshan, Z. Jing, and P. V. Ramana, "Compact SOI nanowire refractive index sensor using phase shifted Bragg grating," *Opt. Express*, vol. 17, no. 17, pp. 15 330–15 341, Aug. 17, 2009.

[10] D. Logan, P. E. Jessop, A. P. Knights, G. Wojcik, and A. Goebel, "Optical modulation in silicon waveguides via charge state control of deep levels," *Opt. Express*, vol. 17, no. 21, pp. 18 571–18 580, Oct. 12, 2009.

[11] C. Koos, P. Vorreau, T. Vallaitis, P. Dumon, W. Bogaerts, R. Baets, B. Esembeson, I. Biaggio, T. Michinobu, F. Diederich, W. Freude, and J. Leuthold, "All-optical high-speed signal processing with silicon–organic hybrid slot waveguides," *Nat. Photon.*, vol. 3, no. 4, pp. 216–219, Apr. 2009.

[12] N. Zhu, J. Song, L. Wosinski, S. He, and L. Thylen, "Experimental demonstration of a cross-order echelle grating triplexer based on an amorphous silicon nanowire platform," *Opt. Lett.*, vol. 34, no. 3, pp. 383–385, Feb. 1, 2009.

[13] K. Preston, S. Manipatruni, A. Gondarenko, C. B. Poitras, and M. Lipson, "Deposited silicon high-speed integrated electro-optic modulator," *Opt. Express*, vol. 17, no. 7, pp. 5118–5124, Mar. 30, 2009.

[14] R. Salem, M. A. Foster, A. C. Turner-Foster, D. F. Geraghty, M. Lipson, and A. L. Gaeta, "High-speed optical sampling using a silicon-chip temporal magnifier," *Opt. Express*, vol. 17, no. 6, pp. 4324–4329, Mar. 16, 2009.

[15] M. Foster, R. Salem, Y. Okawachi, A. C. Turner-Foster, M. Lipson, and A. L. Gaeta, "Ultrafast waveform compression using a time-domain telescope," *Nat. Photon.*, vol. 3, no. 10, pp. 581–585, Oct. 2009.

[16] P. Deotare, M. W. McCutcheon, I. W. Frank, M. Khan, and M. Lončar, "High quality factor photonic crystal nanobeam cavities," *Appl. Phys. Lett.*, vol. 94, no. 12, p. 121106, Mar. 23, 2009.

[17] N. Panoiu, X. Liu, and R. M. Osgood, Jr., "Self-steepening of ultrashort pulses in silicon photonic nanowires," *Opt. Lett.*, vol. 34, no. 7, pp. 947–949, Apr. 1, 2009.

III-Nitride Photonics

Nelson Tansu, Hongping Zhao, Guangyu Liu, Xiao-Hang Li, Jing Zhang, Hua Tong, and Yik-Khoon Ee

(Invited Paper)

Center for Optical Technologies, Department of Electrical and Computer Engineering, Lehigh University, Bethlehem, PA 18015 USA

DOI: 10.1109/JPHOT.2010.2045887
1943-0655/$26.00 ©2010 IEEE

Manuscript received January 27, 2010; revised February 23, 2010. Current version published April 23, 2010. Corresponding author: N. Tansu (e-mail: tansu@lehigh.edu).

Abstract: The progress in III-Nitride photonics research in 2009 is reviewed. The III-Nitride photonics research is a very active field with many important applications in the areas of energy, biosensors, laser devices, and communications. The applications of nitride semiconductors in energy-related technologies include solid-state lighting, solar cells, thermoelectric, and power electronics. Several new research areas in III-Nitride photonics related to terahertz photonics, intersubband quantum wells, nanostructures, and other devices are discussed.

Index Terms: III-Nitride, photonics, light-emitting diodes, lasers, solid state lighting, nanotechnology, energy, thermoelectric, photodetector, terahertz, intersubband quantum well.

The fields of III-Nitride photonics have made significant progress in the Year 2009. The applications of III-Nitride semiconductor photonics cover many different areas including visible diode lasers, solid-state lighting, solar cells, and biosensors. In addition to the progress of nitride semiconductor devices for these applications, new research areas in III-Nitride photonics have arisen such as terahertz generation, intersubband quantum well (QW) devices, nitride-based nanostructures, and other opto-electronics devices.

High-performance III-Nitride light-emitting diodes (LEDs) play significant role for solid-state lighting [1]. Recent significant progress in 2009 has focused on three important aspects limiting the performance applicable for solid-state lighting [2], [3], namely 1) "green gap" issue in nitride LEDs, 2) efficiency-droop in high-power LEDs, and 3) novel approaches for high light extraction efficiency.

To address "green gap" nitride LEDs, there are two important issues, namely 1) charge separation issues in InGaN/GaN QWs and 2) low material quality for high-In-content InGaN QWs required to achieve green emission. The existence of the strong electric field from both spontaneous and piezoelectric polarizations causes the charge separation in the InGaN QWs, which leads to a significant reduction of the electron-hole wavefunction overlap (Γ_{e_hh}). The significant reduction of Γ_{e_hh} in InGaN QW leads to significant reduction in its radiative recombination rate $(\sim|\Gamma_{e\_hh}|^2)$. The charge separation effect has been one of the most challenging factors leading to significant reduction in radiative efficiency in green-emitting nitride LEDs (a key technology for solid-state lighting). In order to address the charge separation issues in nitride QWs, several approaches have been pursued with the goal to achieve high-internal-quantum-efficiency InGaN QW LEDs to address the "green gap" in solid-state lighting devices. The use of nonpolar InGaN QW LEDs has been investigated as a potential approach to address charge separation issue [4]–[6], and significant progress on this

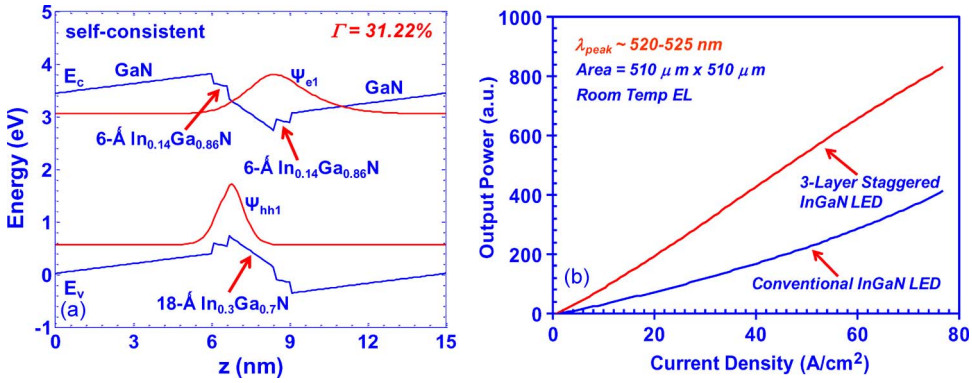

Fig. 1. (a) Schematic of band lineup for three-layer staggered InGaN QW active region with improved overalp emitting at green spectral regime. (b) Comparison of the light output power for green-emitting staggered InGaN QW LEDs and conventional InGaN QW LEDs.

exciting technology has been reported in 2009 [4]–[6]. One of the main issues for nonpolar InGaN QW LEDs is related to less mature material epitaxy and substrate availability; thus, the advances in improved epitaxy and nonpolar GaN substrate developments will have a tremendous impact on the progress of this technology.

In addition to the pursuit of nonpolar nitride QW technologies, there are significant efforts to engineer the polar InGaN QW structures with improved electron-hole wavefunction overlap [9]–[23]. By improving the electron-hole wavefunction overlap (Γ_{e_hh}) in the InGaN-based QW, several successful demonstration have been reported to increase the radiative recombination rate and radiative efficiency (and internal quantum efficiency) of nitride LEDs emitting in blue and green spectral regime. The concept of staggered InGaN QW LEDs was proposed and demonstrated previously [7]–[9], and recent experimental works on the growth of three-layer staggered InGaN QW LEDs have resulted in a 2.5–3 times enhancement in radiative efficiency and output power of the devices [10]–[12] emitting in the green spectral region, as shown in Fig. 1. Time-resolved photoluminescence from the staggered InGaN QW LEDs had also shown that the enhancement in output power can be attributed to the increase in radiative recombination rate [12]. Based on the comprehensive modeling of staggered InGaN QW, it is expected that the use of this active region will potentially result in internal quantum efficiency in the range of 50% for green-emitting devices [10]. In addition to the use of staggered InGaN QW LEDs, several other approaches have been pursued as follow: type-II InGaN-GaNAs QW [17], [18], strain-compensated InGaN-AlGaN QW [19], [20], triangular InGaN QW [21], InGaN QW with delta-AlGaN layer [22], [23], and dip-shape QWs [15]. Another issue on the "green-gap" LEDs is related to the material quality. Wetzel *et al.* identified the importance of improving the epitaxy of high-In-content InGaN QW to reduce the V-defect density [24], which will improve the radiative efficiency of the active region by suppressing the nonradiative process.

One of the major challenges for high-power nitride LEDs is the issue of "efficiency-droop." The use of c-plane InGaN-based QW LEDs suffers from the reduction in efficiency at high operating current density, which is referred as "efficiency-droop" [25]–[35]. Both the external (EQE) and internal (IQE) quantum efficiencies reach their maximum and start to drop at current densities of 10–60 $\mathrm{A/cm^2}$ [25]–[35]. The efficiency-droop is a very important limitation for achieving high-power LEDs, as these devices are required to operate at relatively high operating current density $(> 200-300\ \mathrm{A/cm^2})$. The origin and dominant mechanisms leading to efficiency-droop phenomenon in nitride LEDs are very controversial, and the understanding of the factors leading to the droop is lacking. Several factors have been suggested as potential reasons affecting the efficiency-droop in LEDs, however two leading theories have arisen, namely 1) carrier leakage process [27]–[30] or/and 2) Auger process in InGaN active region [34], [35]. Recent theoretical studies predicted Auger recombination coefficient in InGaN/GaN QW system as $C = 3.5 \times 10^{-34}\ \mathrm{cm^6/s}$ [36]. However, it is important to note that recent experimental studies have indicated the possibility of the Auger recombination coefficient in thick InGaN/GaN double-heterostructure active regions

($d_{\text{Active}} = 10-77$ nm) in the range of $C = 1.4 \times 10^{-30}$ cm^6/s up to $C = 2 \times 10^{-30}$ cm^6/s [34], [35]. Recent theoretical works have suggested the possibility of interband Auger recombination as the dominant process in InGaN bulk semiconductor [37]. Further studies are still required to clarify and confirm the Auger coefficients (C) for InGaN/GaN QW system, due to the large discrepancies for the reported Auger coefficients in the literatures [34]–[37]. Another leading theory has attributed the carrier leakage from the polarization field as the main factor in the efficiency-droop in the InGaN QW LEDs. Recently, InGaN QWs employing polarization matched quaternary AlInGaN barriers instead of GaN barriers have been demonstrated as a method to reduce the efficiency droop [29], [30]. Another interesting approach to suppress efficiency-droop is by employing very thin large bandgap barriers (i.e., AlInN or AlInGaN) to surround the InGaN QW active region [38]. The complete description of the current injection efficiency and radiative efficiency in nitride LEDs are important to provide complete understanding and indicate potential solutions to efficiency-droop in nitride LEDs [38]. The use of thin larger bandgap barrier materials in more mature GaAs-based diode lasers had resulted in significant carrier leakage suppression, leading to high-performance laser devices [39]–[44]. The accurate determination of internal quantum efficiency in nitride LEDs is still challenging, and recently, Getty *et al.* presented an approach to determine the IQE by taking into consideration the light extraction efficiency of the LEDs [45].

The coupling of the surface plasmon mode to the InGaN QW active region leads to an increase in density of states and to a Purcell enhancement factor, which in turn leads to significant increase in radiative recombination rate and radiative efficiency of the InGaN QW LEDs [46], [47]. The tuning of the surface plasmon mode by employing metallo-dielectric stacked layers was proposed [48], [49], and recently, the use of double metallic layer was also proposed as an approach to tune the surface plasmon frequency over a wide range of spectrum [50]. The demonstration of the electrical-injected surface plasmon InGaN QW LEDs was recently demonstrated [51]. However, significant works are still required to achieve optimized device structures.

Other important aspect of nitride LEDs focused on the pursuit of novel low-cost colloidal-based microlens arrays as an approach to enhance the light extraction efficiency of nitride LEDs [52]–[55]. The use of convex colloidal microlens arrays based on SiO_2/polystyrene microspheres had resulted in enhancement of more than 2.5 times in light output power, in comparison with that of conventional planar LEDs [52]–[54]. The use of concave microlens arrays have also been demonstrated with enhancement of 1.7 times [55], and the use of this approach have the potential to result in self-focusing in the far-field pattern. Recently, the use of photonic crystal have also resulted in significant enhancement in nitride LEDs [56], [57], with encapsulated light extraction efficiency as high as 73% [56].

In addition to the issues presented above for solid-state lighting, other interesting progress to realize white LEDs have been reported in 2009. The use of a phosphor-free approach to generate white LEDs have focused on the mixing of blue- and yellow-emitting QWs in a device structure [58]. Another approach has focused on the use of 1) patterning and selective area epitaxy or 2) *in situ* roughening to realize GaN with different planes, such that the different polarization fields will lead to emission from two different spectra [59], [60].

The availability of high-quality GaN substrate is important for the progress of GaN-based optoelectronics, and the issues related to research and development of this substrate technology is reviewed by Paskova *et al.* [61]. Another important aspect is the use of novel epitaxy technique to reduce the dislocation density in GaN material grown on sapphire substrate. The use of new "abbreviated growth mode" of GaN on nanopatterned sapphire [62], [63] leads to the growth of GaN material with significant reduction in dislocation density (2-order of magnitude), as well as a reduction in epitaxy time/cost. The experimental works have resulted in improvement in radiative efficiency of InGaN QW LEDs employing this growth technique by approximately 25% [62], [63].

The visible diode lasers have applications as light sources for DVD, medical, industrial, display, and laser mini projectors. The availability of green-emitting nitride diode lasers will be advantageous over current technology based on frequency-doubled sources. In order to overcome the detrimental effect from the polarization fields, nitride heterostructures and QWs grown along nonpolar or semipolar orientations have been attempted. Recently, nonpolar m-plane InGaN/GaN QW laser diodes (LDs) emitting at 404 nm without Al-containing waveguide cladding layers grown on free-standing m-plane

GaN substrates have been demonstrated [64]. The threshold current density and operating voltage of the nonpolar diode lasers are 6.8 kA/cm^2 and 5.6 V, respectively, and the devices operate under continuous-wave (CW) condition at room temperature for more than 15 h. More recently, asymmetric p-GaN/n-AlGaN-cladded InGaN-based pure blue (440–460 nm) LDs were fabricated on the nonpolar m-plane GaN substrate [65]. The lasing wavelengths are 443 nm and 465 nm, with threshold current densities of 14 kA/cm^2 and 19 kA/cm^2, respectively. Despite the theoretical promise of the higher optical gain for nonpolar InGaN QW resulting from the elimination of the polarization field in the active region, the performance of the nonpolar lasers is still limited by the epitaxy and material quality issues. The epitaxy and material quality of current nonpolar and semipolar materials are still less mature than the more established c-plane (0001) GaN, where nonpolar GaN films are found to contain high concentration of stacking faults and threading dislocations. The progress in the nonpolar InGaN–GaN QW active region is very promising, and it is expected that the nonpolar nitride materials and devices would have impacts in the field of diode lasers and solid-state lighting. However, the maturity of this technology is still at early stage, and a significant amount of research and development works are still required to enable this technology to compete with polar c-plane GaN materials.

Recently, InGaN-QW-based LDs grown on c-plane GaN substrate with lasing wavelength of 510–515 nm was demonstrated by Nichia with threshold current density of 4.4 kA/cm^2 at 25 °C and output power of 5 mW (at $I = 88$ mA and $V = 5.5$ V) [66]. Note that the laser structure [66] was fabricated by employing both facets coated with high-reflectivity (HR) dielectric films (HR/HR), which reduces the mirror loss and threshold gain. However, the HR/HR coatings on both facets limit the output power and external differential quantum efficiency of LDs, which leads to limitations of conventional InGaN QW as active regions for high-power LDs or other laser devices requiring high-gain active region (i.e., VCSELs). Recently, OSRAM reported the 500-nm electrically driven InGaN-based LDs grown on c-plane GaN substrate with threshold current density of 8.2 kA/cm^2 and output power of several tens of milliwatts [67], with mirror coatings of 50% and 95%. OSRAM also reported InGaN LDs emitting at 515 nm with threshold current density of $\sim$9 kA/cm^2 [68]. It is very challenging to extend the conventional InGaN-QW-based LDs to the green spectral regime with high output power and low-threshold current density. Further advances are still required to reduce the threshold current density from 4.4–8.2 kA/cm^2 down to more acceptable level. Significant reduction in threshold carrier density and threshold current density in green-emitting diode lasers are important, in particular, for enabling the nitride QW lasers as practical and reliable laser technology in the green spectral regimes. Polar novel InGaN-based QWs with improved overlap design are expected to reduce the threshold carrier density [18], [20], [69], which in turn have the potential to enable the realization of high-performance green-emitting LDs.

Significant progress on the theoretical description of the nitride quantum dots have been reported in 2009. Williams *et al.* [70] and Wu *et al.* [71] reported the simulations of nitride QDs as significantly different than those of GaAs-based QDs, due to the existence of the polarization fields and strong shape-dependent characteristics. One of the important challenges in the growth of self-assembled nitride QDs is the relatively low-density QD density for enabling realization of high-performance photonics devices [72]. The progress in the growths of high-quality and ultrahigh-density nitride QDs are still ongoing.

High-efficiency multijunction tandem solar cells of InGaN/InN material have the potential to compete with the traditional III–V tandem cells [73]–[75]. Recent progress on the InGaN-based single-junction solar cells has been exciting. Dahal *et al.* reported the use of $In_{0.3}Ga_{0.7}N$ multiple QWs resulting in open circuit voltage of about 2 V and fill factor of 60% [74]. Neufeld reported the use of 2.95 eV InGaN junction to achieve solar cells with open circuit voltage of 1.81 V and fill factor of 75% [75]. The pursuit of narrow bandgap junction by employing InN semiconductor with metalorganic chemical vapor deposition is important [76]–[78], and the use of pulsed MOCVD growth method has resulted in narrow-bandgap (0.77 eV) InN with relatively low V/III ratio [77], [78].

The pursuit of near-infrared intersubband QW devices require large conduction band offset, which can be accomplished by GaN/AlN heterostructure. Transition wavelengths in the spectral range of 2 μm had been reported for GaN/AlN QWs measured under optical pumping [79]. Sodabanlu *et al.* have reported the use of AlGaN interlayer to modify the strain in the GaN/AlN QWs

and shift the wavelength into the 1.54-μm spectral regime [80]. Significant works are still required to investigate the use of polar GaN/AlN-based QWs to realize intersubband QW lasers. The pursuit of intersubband devices by employing nitride quantum dots and nanowires are important to enable the realization of devices operating at room temperature.

The use of ultrafast laser pulses have led to efficient generation of broad terahertz pulses from InN films [81]–[83]. The average output power reached 0.93 μW based on result for 700-nm-thick InN film [83], and the mechanism can be attributed to the resonance enhanced optical rectification. Recently, a new results based on terahertz generation from pulsed-MOCVD grown have indicated the existence of destructive interference between optical rectification and photocurrent surge [84]. From the studies in reference [84], optical rectification is the primary mechanism for the terahertz generation in the frequencies of 300 GHz–2.5 THz, with ultrafast laser pulses at 782 nm. The highest output power reported is 2.4 μW at an average pump intensity of 176 W/cm^2 from the 220-nm-thick pulsed-MOCVD grown InN film [84].

In summary, significant progress and exciting research advances in III-Nitride photonics have been reported in 2009. The impacts of III-Nitride photonics are wide ranging with applications in solid-state lighting, solar cells, visible lasers, and biosensors, and the progress in these fields are expected to continue. Further growths in new research areas such as intersubband QW devices, surface plasmonic-based devices, novel nanostructures, Terahertz generation, and potential uses for thermoelectric applications are expected in the research areas of III-Nitride photonics and semiconductors. Nitride-based LEDs and lasers have been employed as light sources for probing biological materials in the visible and UV spectral regimes. Recently, AlGaN/GaN high-electron-mobility transistor (HEMT) has been demonstrated for solid-state biosensor application with excellent thermal, chemical, and mechanical stability, which suggests that nitride HEMTs are excellent candidates for pressure sensor and piezoelectric-related applications [85]. The avalanche photo diodes (APDs) based on GaN material have also been developed, and recently, first principle simulations have also provided accurate modeling of the properties of these devices [86].

References

[1] E. F. Schubert, *Light Emitting Diodes*. Cambridge, U.K.: Cambridge Univ. Press, 2006.

[2] N. Tansu, E. F. Schubert, P. M. Smowton, and H. C. Kuo, "Introduction to the issue on solid-state lighting," *IEEE J. Sel. Topics Quantum Electron.*, vol. 15, no. 4, pp. 1025–1027, Jul./Aug. 2009.

[3] M. H. Crawford, "LEDs for solid state lighting: Performance challenges and recent advances," *IEEE J. Sel. Topics Quantum Electron.*, vol. 15, no. 4, pp. 1028–1040, Jul./Aug. 2009.

[4] S. M. Hwang, Y. G. Seo, K. H. Baik, I. S. Cho, J. H. Baek, S. Jung, T. G. Kim, and M. Cho, "Demonstration of nonpolar a-plane InGaN/GaN light emitting diode on r-plane sapphire substrate," *Appl. Phys. Lett.*, vol. 95, no. 7, pp. 071101-1–071101-3, Aug. 2009.

[5] T. Detchprohm, M. Zhu, Y. Li, Y. Xia, L. Liu, D. Hanser, and C. Wetzel, "Growth and characterization of green GaInN-based light emitting diodes on free-standing non-polar GaN templates," *J. Cryst. Growth*, vol. 311, no. 10, pp. 2937–2941, May 2009.

[6] Y. D. Lin, A. Chakraborty, S. Brinkley, H. C. Kuo, T. Melo, K. Fujito, J. S. Speck, S. P. DenBaars, and S. Nakamura, "Characterization of blue-green m-plane InGaN light emitting diodes," *Appl. Phys. Lett.*, vol. 94, no. 26, pp. 261108-1–261108-3, Jul. 2009.

[7] R. A. Arif, Y. K. Ee, and N. Tansu, "Polarization engineering via staggered InGaN quantum wells for radiative efficiency enhancement of light emitting diodes," *Appl. Phys. Lett.*, vol. 91, no. 9, pp. 091110-1–091110-3, Aug. 2007.

[8] R. A. Arif, H. P. Zhao, Y. K. Ee, and N. Tansu, "Spontaneous emission and characteristics of staggered InGaN quantum wells light emitting diodes," *IEEE J. Quantum Electron.*, vol. 44, no. 6, pp. 573–580, Jun. 2008.

[9] R. A. Arif, Y. K. Ee, and N. Tansu, "Nanostructure engineering of InGaN-based active regions for improved III-nitride gain media emitting at 420–550 nm," *Phys. Stat. Sol. (C)*, vol. 205, no. 1, pp. 96–100, Jan. 2008.

[10] H. Zhao, R. A. Arif, and N. Tansu, "Design analysis of staggered InGaN quantum wells light-emitting diodes at 500–540 nm," *IEEE J. Sel. Topics Quantum Electron.*, vol. 15, no. 4, pp. 1104–1114, Jul./Aug. 2009.

[11] H. Zhao, G. S. Huang, G. Liu, X. H. Li, J. D. Poplawsky, S. Tafon Penn, V. Dierolf, and N. Tansu, "Growths of staggered InGaN quantum wells light-emitting diodes emitting at 520–525 nm employing graded growth-temperature profile," *Appl. Phys. Lett.*, vol. 95, no. 6, pp. 061104-1–061104-3, Aug. 2009.

[12] H. P. Zhao, G. Liu, X. H. Li, R. A. Arif, G. S. Huang, J. D. Poplawsky, S. Tafon Penn, V. Dierolf, and N. Tansu, "Design and characteristics of staggered InGaN quantum well light-emitting diodes in the green spectral regimes," *IET Optoelectron.*, vol. 3, no. 6, pp. 283–295, Dec. 2009.

[13] S. H. Park, D. Ahn, and J. W. Kim, "High-efficiency staggered 530 nm InGaN/InGaN/GaN quantum-well light-emitting diodes," *Appl. Phys. Lett.*, vol. 94, no. 4, pp. 041109-1–041109-3, Jan. 2009.

[14] S. H. Park, D. Ahn, B. H. Koo, and J. W. Kim, "Electronic and optical properties of staggered InGaN/InGaN quantum-well light-emitting diodes," *Phys. Stat. Sol. (A)*, vol. 206, no. 11, pp. 2637–2640, Nov. 2009.
[15] S. H. Park, D. Ahn, B. H. Koo, and J. W. Kim, "Dip-shaped InGaN/GaN quantum-well light-emitting diodes with high efficiency," *Appl. Phys. Lett.*, vol. 95, no. 6, pp. 063507-1–063507-3, Aug. 2009.
[16] S. H. Yen and Y. K. Kuo, "Improvement in piezoelectric effect of violet InGaN laser diodes," *Opt. Commun.*, vol. 281, no. 18, pp. 4735–4740, Sep. 2008.
[17] R. A. Arif, H. Zhao, and N. Tansu, "Type-II InGaN-GaNAs quantum wells active regions for lasers applications," *Appl. Phys. Lett.*, vol. 92, no. 1, pp. 011104-1–011104-3, Jan. 2008.
[18] H. Zhao, R. A. Arif, and N. Tansu, "Self consistent gain analysis of Type-II 'W' InGaN–GaNAs quantum well lasers," *J. Appl. Phys.*, vol. 104, no. 4, pp. 043104-1–043104-7, Aug. 2008.
[19] H. Zhao, R. A. Arif, Y. K. Ee, and N. Tansu, "Optical gain analysis of strain-compensated InGaN–AlGaN quantum well active regions for lasers emitting at 420–500 nm," *Opt. Quantum Electron.*, vol. 40, no. 5/6, pp. 301–306, Apr. 2008.
[20] H. Zhao, R. A. Arif, Y. K. Ee, and N. Tansu, "Self-consistent analysis of strain-compensated InGaN–AlGaN quantum wells for lasers and light emitting diodes," *IEEE J. Quantum Electron.*, vol. 45, no. 1, pp. 66–78, Jan. 2009.
[21] Z. Yang, R. Li, Q. Wei, T. Yu, Y. Zhang, W. Chen, and X. Hu, "Analysis of optical gain property in the InGaN/GaN triangular shaped quantum well under the piezoelectric field," *Appl. Phys. Lett.*, vol. 94, no. 6, pp. 061120-1–061120-3, Feb. 2009.
[22] J. Park and Y. Kawakami, "Photoluminescence property of InGaN single quantum well with embedded AlGaN δ layer," *Appl. Phys. Lett.*, vol. 88, no. 20, pp. 202107-1–202107-3, May 2006.
[23] S. H. Park, J. Park, and E. Yoon, "Optical gain in InGaN/GaN quantum well structures with embedded AlGaN delta layer," *Appl. Phys. Lett.*, vol. 90, no. 2, pp. 023508-1–023508-3, Jan. 2007.
[24] T. Detchprohm, M. Zhu, W. Zhao, Y. Wang, Y. Li, Y. Xia, and C. Wetzel, "Enhanced device performance of GaInN-based deep green light emitting diodes with V-defect-free active region," *Phys. Stat. Sol. (C)*, vol. 6, no. S2, pp. S840–S843, May 2009.
[25] S. F. Chichibu, T. Azuhata, M. Sugiyama, T. Kitamura, Y. Ishida, H. Okumura, H. Nakanishi, T. Sota, and T. Mukai, "Optical and structural studies in InGaN quantum well structure laser diodes," *J. Vac. Sci. Technol. B*, vol. 19, no. 6, pp. 2177–2183, Nov. 2001.
[26] A. A. Efremov, N. I. Bochkareva, R. I. Gorbunov, D. A. Lavrinovich, Y. T. Rebane, D. V. Tarkhin, and Y. G. Shreter, "Effect of the joule heating on the quantum efficiency and choice of thermal conditions for high-power blue InGaN/GaN LEDs," *Semiconductors*, vol. 40, no. 5, pp. 605–610, May 2006.
[27] M. H. Kim, M. F. Schubert, Q. Dai, J. K. Kim, E. F. Schubert, J. Piprek, and Y. Park, "Origin of efficiency droop in GaN-based light-emitting diodes," *Appl. Phys. Lett.*, vol. 91, no. 18, pp. 183507-1–183507-3, Oct. 2007.
[28] M. F. Schubert, S. Chhajed, J. K. Kim, E. F. Schubert, D. D. Koleske, M. H. Crawford, S. R. Lee, A. J. Fischer, G. Thaler, and M. A. Banas, "Effect of dislocation density on efficiency droop in GaInN/GaN light-emitting diodes," *Appl. Phys. Lett.*, vol. 91, no. 23, pp. 231114-1–231114-3, Dec. 2007.
[29] M. F. Schubert, J. Xu, J. K. Kim, E. F. Schubert, M. H. Kim, S. Yoon, S. M. Lee, C. Sone, T. Sakong, and Y. Park, "Polarization-matched GaInN/AlGaInN multi-quantum-well light-emitting diodes with reduced efficiency droop," *Appl. Phys. Lett.*, vol. 93, no. 4, pp. 041102-1–041102-3, Jul. 2008.
[30] J. Xu, M. F. Schubert, A. N. Noemaun, D. Zhu, J. K. Kim, E. F. Schubert, M. H. Kim, H. J. Chung, S. Yoon, C. Sone, and Y. Park, "Reduction in efficiency droop, forward voltage, ideality factor, and wavelength shift in polarization-matched GaInN/GaInN multi-quantum-well light-emitting diodes," *Appl. Phys. Lett.*, vol. 94, no. 1, pp. 011113-1–011113-3, Jan. 2009.
[31] J. Xie, X. Ni, Q. Fan, R. Shimada, U. Ozgur, and H. Morkoc, "On the efficiency droop in InGaN multiple quantum wells," *Appl. Phys. Lett.*, vol. 93, no. 12, pp. 121107-1–121107-3, Sep. 2008.
[32] X. Ni, Q. Fan, R. Shimada, U. Ozgur, and H. Morkoc, "Reduction of efficiency droop in InGaN light emitting diodes by coupled quantum wells," *Appl. Phys. Lett.*, vol. 93, no. 17, pp. 171113-1–171113-3, Oct. 2008.
[33] M. Maier, K. Kohler, M. Kunzer, W. Pletschen, and J. Wagner, "Reduced nonthermal rollover of wide-well GaInN light-emitting diodes," *Appl. Phys. Lett.*, vol. 94, no. 4, pp. 041 103-1–041 103-3, Jan. 2009.
[34] Y. C. Shen, G. O. Mueller, S. Watanabe, N. F. Gardner, A. Munkholm, and M. R. Krames, "Auger recombination in InGaN measured by photoluminescence," *Appl. Phys. Lett.*, vol. 91, no. 14, pp. 141101-1–141101-3, Oct. 2007.
[35] N. F. Gardner, G. O. Muller, Y. C. Shen, G. Chen, S. Watanabe, W. Gotz, and M. R. Krames, "Blue-emitting InGaN–GaN double-heterostructure light-emitting diodes reaching maximum quantum efficiency above 200A/cm^2," *Appl. Phys. Lett.*, vol. 91, no. 24, pp. 243506-1–243506-3, Dec. 2007.
[36] J. Hader, J. V. Moloney, B. Pasenow, S. W. Koch, M. Sabathil, N. Linder, and S. Lutgen, "On the importance of radiative and Auger losses in GaN-based quantum wells," *Appl. Phys. Lett.*, vol. 92, no. 26, pp. 261103-1–261103-3, Jun. 2008.
[37] K. T. Delaney, P. Rinke, and C. G. Van de Walle, "Auger recombination rates in nitrides from first principles," *Appl. Phys. Lett.*, vol. 94, no. 19, pp. 191109-1–191109-3, May 2009.
[38] H. P. Zhao, G. Y. Liu, R. A. Arif, and N. Tansu, "Effect of current injection efficiency on efficiency-droop in InGaN quantum well light-emitting diodes," in *Proc. IEEE ISDRS*, College Park, MD, Nov. 2009, pp. 1–2.
[39] N. Tansu, J. Y. Yeh, and L. J. Mawst, "Physics and characteristics of 1200-nm InGaAs and 1300–1400 nm InGaAsN quantum-well lasers by metalorganic chemical vapor deposition," *J. Phys.: Condens. Matter*, vol. 16, no. 31, pp. S3277–S3318, Aug. 2004.
[40] N. Tansu and L. J. Mawst, "Current injection efficiency of 1300-nm InGaAsN quantum-well lasers," *J. Appl. Phys.*, vol. 97, no. 5, pp. 054502-1–054502-18, Mar. 2005.
[41] N. Tansu, J. Y. Yeh, and L. J. Mawst, "Improved photoluminescence of InGaAsN–(In)GaAsP quantum well by organometallic vapor phase epitaxy using growth pause annealing," *Appl. Phys. Lett.*, vol. 82, no. 18, pp. 3008–3010, May 2003.
[42] N. Tansu, J. Y. Yeh, and L. J. Mawst, "Experimental evidence of carrier leakage in InGaAsN quantum well lasers," *Appl. Phys. Lett.*, vol. 83, no. 11, pp. 2112–2114, Sep. 2003.

[43] A. Thranhardt, I. Kuznetsova, C. Schlichenmaier, S. W. Koch, L. Shterengas, G. Belenky, J. Y. Yeh, L. J. Mawst, N. Tansu, J. Hader, J. V. Moloney, and W. W. Chow, "Nitrogen incorporation effects on gain properties in GaInNAs lasers: Experiment and theory," *Appl. Phys. Lett.*, vol. 86, no. 20, pp. 201117-1–201117-3, May 2005.
[44] N. Tansu, N. J. Kirsch, and L. J. Mawst, "Low-threshold-current-density 1300-nm dilute-nitride quantum well lasers," *Appl. Phys. Lett.*, vol. 81, no. 14, pp. 2523–2525, Sep. 2002.
[45] A. Getty, E. Matioli, M. Iza, C. Weisbuch, and J. S. Speck, "Electroluminescent measurement of the internal quantum efficiency of light emitting diodes," *Appl. Phys. Lett.*, vol. 94, no. 18, pp. 181102-1–181102-3, May 2009.
[46] K. Okamoto, I. Niki, A. Shvartser, Y. Narukawa, T. Mukai, and A. Scherer, "Surface-plasmon-enhanced light emitters based on InGaN quantum wells," *Nat. Mater.*, vol. 3, no. 9, pp. 601–605, Sep. 2004.
[47] K. Okamoto and Y. Kawakami, "High-efficiency InGaN/GaN light emitters based on nanophotonics and plasmonics," *IEEE J. Sel. Topics Quantum Electron.*, vol. 15, no. 4, pp. 1199–1209, Jul./Aug. 2009.
[48] R. Paiella, "Tunable surface plasmons in coupled metallo-dielectric multiple layers for light-emission efficiency enhancement," *Appl. Phys. Lett.*, vol. 87, no. 11, pp. 111104-1–111104-3, Sep. 2005.
[49] J. Henson, A. Bhattacharyya, T. D. Moustakas, and R. Paiella, "Controlling the recombination rate of semiconductor active layers via coupling to dispersion-engineered surface plasmons," *J. Opt. Soc. Amer. B, Opt. Phys.*, vol. 25, no. 8, pp. 1328–1335, Aug. 2008.
[50] H. Zhao, G. Liu, and N. Tansu, "Surface plasmon dispersion engineering utilizing double-metallic Ag/Au layers for InGaN quantum wells light emitting diodes," in *Proc. SPIE Photon. West, LEDs: Mater., Devices, Appl. Solid State Lighting XIV*, San Francisco, CA, Jan. 2010.
[51] D. M. Yeh, C. F. Huang, C. Y. Chen, Y. C. Lu, and C. C. Yang, "Localized surface plasmon-induced emission enhancement of a green light-emitting diode," *Nanotechnol.*, vol. 19, no. 34, p. 345 201, Aug. 2008.
[52] Y. K. Ee, R. A. Arif, N. Tansu, P. Kumnorkaew, and J. F. Gilchrist, "Enhancement of light extraction efficiency of InGaN quantum wells light emitting diodes using SiO_2/polystyrene microlens arrays," *Appl. Phys. Lett.*, vol. 91, no. 22, pp. 221107-1–221107-3, Nov. 2007.
[53] P. Kumnorkaew, Y. K. Ee, N. Tansu, and J. F. Gilchrist, "Deposition of microsphere monolayers for fabrication of microlens arrays," *Langmuir*, vol. 24, no. 21, pp. 12 150–12 157, Nov. 2008.
[54] Y. K. Ee, P. Kumnorkaew, R. A. Arif, H. Tong, H. P. Zhao, J. F. Gilchrist, and N. Tansu, "Optimization of light extraction efficiency of III-nitride light emitting diodes with self-assembled colloidal-based microlenses," *IEEE J. Sel. Topics Quantum Electron.*, vol. 15, no. 4, pp. 1218–1225, Jul./Aug. 2009.
[55] Y. K. Ee, P. Kumnorkaew, R. A. Arif, H. Tong, J. F. Gilchrist, and N. Tansu, "Light extraction efficiency enhancement of InGaN quantum wells light-emitting diodes with polydimethylsiloxane concave microstructures," *Opt. Express*, vol. 17, no. 16, pp. 13 747–13 757, Aug. 2009.
[56] J. J. Wierer, A. David, and M. M. Megens, "III-nitride photonic-crystal light-emitting diodes with high extraction efficiency," *Nat. Photon.*, vol. 3, no. 3, pp. 163–169, May 2009.
[57] K. McGroddy, A. David, E. Matioli, M. Iza, S. Nakamura, S. DenBaars, J. S. Speck, C. Weisbuch, and E. L. Hu, "Directional emission control and increased light extraction in GaN photonic crystal light emitting diodes," *Appl. Phys. Lett.*, vol. 93, no. 10, pp. 103502-1–103502-3, Sep. 2008.
[58] C. F. Lu, C. H. Huang, Y. S. Chen, W. Y. Shiao, C. Y. Chen, Y. C. Lu, and C. C. Yang, "Phosphor-free monolithic white-light LED," *IEEE J. Sel. Topics Quantum Electron.*, vol. 15, no. 4, pp. 1210–1217, Jul./Aug. 2009.
[59] M. Funato, K. Hayashi, M. Ueda, Y. Kawakami, Y. Narukawa, and T. Mukai, "Emission color tunable light-emitting diodes composed of InGaN multifacet quantum wells," *Appl. Phys. Lett.*, vol. 93, no. 2, pp. 021126-1–021126-3, Jul. 2008.
[60] T. Jung, L. K. Lee, and P. C. Ku, "Novel epitaxial nanostructures for the improvement of InGaN LEDs efficiency," *IEEE J. Sel. Topics Quantum Electron.*, vol. 15, no. 4, pp. 1073–1079, Jul./Aug. 2009.
[61] T. Paskova and K. Evans, "GaN substrates—Progress, status, and prospects," *IEEE J. Sel. Topics Quantum Electron.*, vol. 15, no. 4, pp. 1041–1052, Jul./Aug. 2009.
[62] Y. K. Ee, J. M. Biser, W. Cao, H. M. Chan, R. P. Vinci, and N. Tansu, "Metalorganic vapor phase epitaxy of III-nitride light-emitting diodes on nano-patterned AGOG sapphire substrate by abbreviated growth mode," *IEEE J. Sel. Topics Quantum Electron.*, vol. 15, no. 4, pp. 1066–1072, Jul./Aug. 2009.
[63] Y. K. Ee, X. H. Li, J. E. Biser, W. Cao, H. M. Chan, R. P. Vinci, and N. Tansu, "Abbreviated MOVPE nucleation of III-nitride light-emitting diodes on nano-patterned sapphire," *J. Cryst. Growth*, vol. 312, no. 8, pp. 1311–1315, Apr. 2010. DOI:10.1016/j.jcrysgro.2009.10.029.
[64] R. M. Farrell, D. F. Feezell, M. C. Schmidt, D. A. Haeger, K. M. Kelchner, K. Iso, H. Yamada, M. Saito, K. Fujito, D. A. Cohen, J. S. Speck, S. P. DenBaars, and S. Nakamura, "Continuous-wave operation of AlGaN-cladding-free nonpolar m-plane InGaN/GaN laser diodes," *Jpn. J. Appl. Phys.*, vol. 46, no. 29–32, pp. L761–L763, Aug. 2007.
[65] Y. D. Lin, C. Y. Huang, M. T. Hardy, P. S. Hsu, K. Fujito, A. Chakraborty, H. Ohta, J. S. Speck, S. P. DenBaars, and S. Nakamura, "m-plane pure blue laser diodes with p-GaN/n-AlGaN-based asymmetric cladding and InGaN-based wave-guiding layers," *Appl. Phys. Lett.*, vol. 95, no. 8, pp. 081110-1–081110-3, Aug. 2009.
[66] T. Miyoshi, S. Masui, T. Okada, T. Yanamoto, T. Kozaki, S. Nagahama, and T. Mukai, "510–515 nm InGaN-based green laser diodes on c-plane GaN substrate," *Appl. Phys. Express*, vol. 2, no. 6, p. 062201, May 2009.
[67] D. Queren, A. Avramescu, G. Bruderl, A. Breidenassel, M. Schillgalies, S. Lutgen, and U. Strau, "500 nm electrically driven InGaN based laser diodes," *Appl. Phys. Lett.*, vol. 94, no. 8, pp. 081119-1–081119-3, Feb. 2009.
[68] A. Avramescu, T. Lermer, J. Muller, S. Tautz, D. Queren, S. Lutgen, and U. Strau, "InGaN laser diodes with 50 mW output power emitting at 515 nm," *Appl. Phys. Lett.*, vol. 95, no. 7, pp. 071103-1–071103-3, Aug. 2009.
[69] H. P. Zhao, R. A. Arif, and N. Tansu, "Design of staggered InGaN quantum wells for green diode lasers," in *Proc. SPIE Photon. West, Novel In-Plane Semicond. Lasers VIII*, San Jose, CA, Jan. 2009.
[70] D. P. Williams, S. Schulz, A. D. Andreev, and E. P. O'Reilly, "Theory of GaN quantum dots for optical applications," *IEEE J. Sel. Topics Quantum Electron.*, vol. 15, no. 4, pp. 1092–1103, Jul./Aug. 2009.
[71] Y. R. Wu, Y. Y. Lin, H. H. Huang, and J. Singh, "Electronic and optical properties of InGaN quantum dot based emitters for light emitting diodes," *J. Appl. Phys.*, vol. 105, no. 1, pp. 013117-1–013117-7, Jan. 2009.

[72] Y. K. Ee, H. P. Zhao, R. A. Arif, M. Jamil, and N. Tansu, "Self-assembled InGaN quantum dots on GaN grown by metalorganic vapor phase epitaxy," *J. Cryst. Growth*, vol. 310, no. 7–9, pp. 2320–2325, Apr. 2008.
[73] O. Jani, I. Ferguson, C. Honsberg, and S. Kurtz, "Design and characterization of GaN/InGaN solar cells," *Appl. Phys. Lett.*, vol. 91, no. 13, pp. 132117-1–132117-3, Sep. 2007.
[74] R. Dahal, B. Pantha, J. Li, J. Y. Lin, and H. X. Jiang, "InGaN/GaN multiple quantum well solar cells with long operating wavelengths," *Appl. Phys. Lett.*, vol. 94, no. 6, pp. 063505-1–063505-3, Feb. 2009.
[75] C. J. Neufeld, N. G. Toledo, S. C. Cruz, M. Iza, S. P. DenBaars, and U. K. Mishra, "High quantum efficiency InGaN/GaN solar cells with 2.95 eV band gap," *Appl. Phys. Lett.*, vol. 93, no. 14, pp. 143502-1–143502-3, Oct. 2008.
[76] M. Jamil, R. A. Arif, Y. K. Ee, H. Tong, J. B. Higgins, and N. Tansu, "MOCVD epitaxy of InN films on GaN templates grown on sapphire and silicon (111) substrates," *Phys. Stat. Sol. (A)*, vol. 205, no. 7, pp. 1619–1624, Jul. 2008.
[77] M. Jamil, H. P. Zhao, J. Higgins, and N. Tansu, "Influence of growth temperature and V/III ratio on the optical characteristics of narrow-band gap (0.77 eV) InN grown on GaN/sapphire using pulsed MOVPE," *J. Cryst. Growth*, vol. 310, no. 23, pp. 4947–4953, Nov. 2008.
[78] M. Jamil, H. P. Zhao, J. Higgins, and N. Tansu, "MOVPE and photoluminescence of narrow band gap (0.77 eV) InN on GaN/sapphire by pulsed growth mode," *Phys. Stat. Sol. (A)*, vol. 205, no. 12, pp. 2886–2891, Dec. 2008.
[79] K. Driscoll, Y. Liao, A. Bhattacharyya, L. Zhou, D. J. Smith, T. D. Moustakas, and R. Paiella, "Optically pumped intersubband emission of short-wave infrared radiation with GaN/AlN quantum wells," *Appl. Phys. Lett.*, vol. 94, no. 8, pp. 081120-1–081120-3, Feb. 2009.
[80] H. Sodabanlu, J. S. Yang, M. Sugiyama, Y. Shimogaki, and Y. Nakano, "Strain effects on the intersubband transitions in GaN/AlN multiple quantum wells grown by low-temperature metal organic vapor phase epitaxy with AlGaN interlayer," *Appl. Phys. Lett.*, vol. 95, no. 16, pp. 161908-1–161908-3, Oct. 2009.
[81] R. Ascazubi, I. Wilke, K. Denniston, H. Lu, and W. J. Schaff, "Terahertz emission by InN," *Appl. Phys. Lett.*, vol. 84, no. 23, pp. 4810–4812, May 2004.
[82] G. D. Chern, E. D. Readinger, H. Shen, M. Wraback, C. S. Gallinat, G. Koblmuller, and J. S. Speck, "Excitation wavelength dependence of terahertz emission from InN and InAs," *Appl. Phys. Lett.*, vol. 89, no. 14, pp. 141115-1–141115-3, Oct. 2006.
[83] X. Mu, Y. J. Ding, K. Wang, D. Jena, and Y. B. Zotova, "Resonant terahertz generation from InN thin films," *Opt. Lett.*, vol. 32, no. 11, pp. 1423–1425, Apr. 2007.
[84] G. Xu, Y. J. Ding, H. P. Zhao, M. Jamil, G. Y. Liu, N. Tansu, I. B. Zotova, C. E. Stutz, D. E. Diggs, N. Fernelius, F. K. Hopkins, C. S. Gallinat, G. Koblmüller, and J. S. Speck, "THz generation from InN films due to destructive interference between optical rectification and photocurrent surge," *Semicond. Sci. Technol.*, vol. 25, no. 1, p. 015004, Jan. 2010.
[85] S. J. Pearton, F. Ren, Y. L. Wang, B. H. Chu, K. H. Chen, C. Y. Chang, W. Lim, J. Lin, and D. P. Norton, "Recent advances in wide bandgap semiconductor biological and gas sensors," *Prog. Mater. Sci.*, vol. 55, no. 1, pp. 1–59, Jan. 2010.
[86] F. Bertazzi, M. Moresco, and E. Bellotti, "Theory of high field carrier transport and impact ionization in wurtzite GaN. Part I: A full band Monte Carlo model," *J. Appl. Phys.*, vol. 106, no. 6, pp. 063718-1–063718-12, Sep. 2009.

Photonic Metamaterials: Science Meets Magic

Ekmel Ozbay

(Invited Paper)

Nanotechnology Research Center, Bilkent University, Bilkent, Ankara 06800, Turkey

DOI: 10.1109/JPHOT.2010.2047100
1943-0655/$26.00 ©2010 IEEE

Manuscript received February 2, 2010. Current version published April 23, 2010. Corresponding author: E. Ozbay (e-mail: ozbay@fen.bilkent.edu.tr).

Abstract: The word "magic" is usually associated with movies, fiction, children stories, etc., but seldom with the natural sciences. Recent advances in metamaterials have changed this notion, in which we can now speak of "almost magical" properties that scientists could only dream about a decade ago. In this paper, we review some of the recent "almost magical" progress in the field of photonic metamaterials.

Starting in high school physics, we learn that light is made of a combination of electric and magnetic fields. As light propagates through matter, conventional materials only react to the electric field, and this interaction results in most of the optical effects that we know of, such as refraction, diffraction, lensing, imaging, etc. Forty years ago, Veselago asked the question "What if matter also interacts with the magnetic field of light?" [1]. He showed that when both electric and magnetic properties were negative ($\varepsilon < 0$ and $\mu < 0$), the solution of the Maxwell equations resulted in an index of refraction with a negative sign.

The theoretical predictions of Veselago had to wait about 30 years for the first experimental realization of these engineered materials that are also called metamaterials. The seminal work of Pendry [2] provided the blueprints for the experimental realization of metallic-based resonant structures that are called split ring resonators (SRRs), which exhibit $\mu < 0$ at the resonance frequencies. Smith *et al.* [3] combined an array of SRRs $(\mu < 0)$ and an array of metallic wires $(\varepsilon < 0)$ in order to create double negative composite metamaterials. In such a case, the famous "right-handed rule" between the electric and magnetic fields becomes left handed, in which these materials are known as left-handed materials (LHMs) or negative index materials (NIMs).

Besides negative refraction, scientists have shown that metamaterials can also be used to achieve "almost magical" applications such as subwavelength imaging, superlenses, perfect lenses, cloaking, chirality etc. Although the early experiments were performed at microwave frequencies, it took only a few years for the scientists to downscale these structures to optical frequencies [4]. These nanoscale metamaterials are now called photonic metamaterials.

As shown in Fig. 1, SRRs can be fabricated with dimensions reaching nanometer scales. The nanoscale SRR acts as an LC resonator with a resonance frequency at optical frequencies [5]. More importantly, the typical size of these resonant inclusions is approximately 10 times smaller than the vacuum wavelength of the light at the resonance frequency. Although a single-layer SRR structure can easily be fabricated on a dielectric surface, it is relatively difficult to stack these structures due to the tight alignment tolerance requirements. Giessen and his group have reported a new method where metamaterials in the near-infrared spectral region can be fabricated using a layer-by-layer technique [6].

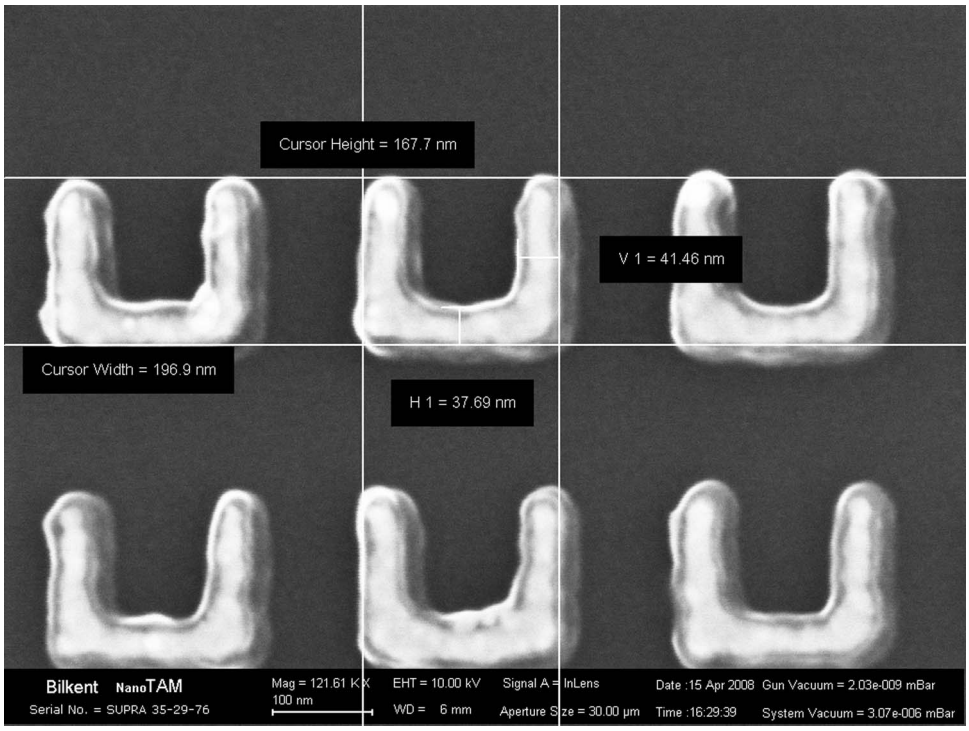

Fig. 1. Nanoscale SRR structures fabricated in Bilkent University.

Conventional SRRs provide a neat way to achieve magnetism at optical frequencies. In order to excite the magnetic resonance of the SRR, the incoming light should propagate in a direction that is parallel to the SRR plane. Shalaev *et al.* at Purdue University came up with a solution to this problem, where they modified the classical SRR into a coupled nanostrip structure [7]. Using the coupled nanostructures with various dimensions, the Purdue researchers were able to create metamaterials exhibiting optical magnetic responses across the entire visible spectrum: from red to blue.

Although the coupled nanostrip structure results in magnetism at even shorter wavelengths, they still do not possess the desired negative index behavior. If the metallic nanowires are fabricated on the same plane with the coupled nanorods, the structure resembles that of a fishnet. Professor Zhang's group at the University of California at Berkeley reported a 10-layer fishnet metamaterial structure [8]. Instead of relying on numerical retrieval methods, measurements of the refractive index of the structures were carried out by observing the refraction angle of the light passing through the prism by "Snell's Law." This method provides a direct and unambiguous determination of the refractive index [9], as the refraction angle depends solely on the phase gradient that the light beam experiences when refracted from the angled output face. The refractive index varied from $n = 0.63$ at 1200 nm to $n = -1.23$ at 1775 nm.

Photonic-crystal-based metamaterials also possess "almost magical" properties, including negative refraction and subwavelength imaging [10]. In a *Science* article, the Berkeley group reported observations of negative refraction in metallic-photonic-crystal-based metamaterials composed of silver nanowires embedded in alumina [11]. The group refractive indices of the metallic-photonic-crystal-based metamaterial are then shown to be -4.0 and 2.2 for TM and TE light, respectively. Similar to dielectric-based photonic crystals [12], metallic-photonic-crystal-based metamaterials can support propagating waves with large wave vectors that are evanescent in air or dielectrics, enabling the manipulation of visible light at the subwavelength scale. Such a property will be rather useful in various photonic applications including waveguiding, imaging, and optical communications.

Thanks to the popularity of the magic presented in the Harry Potter series of books and films, cloaking has also emerged as another "almost magical" application of metamaterials. The early experiments have shown that it is possible to design a metamaterial around an object such that an incoming wave can be totally reconstructed on the other side of the same object [13]. In a sense, the metamaterial acts like a cloak that makes the object inside invisible to the outside. Canonical spiral particles can also be used to achieve cloaking for both polarizations of the electromagnetic waves [14]. Spirals are optimized to exhibit equal permittivity and permeability response so that the cloak consisting of these spirals will work for both the TE and TM polarizations. Researchers at Berkeley have designed an optical "carpet" cloak using quasi-conformal mapping to conceal an object that is placed under a curved reflecting surface by imitating the reflection of a flat surface [15]. The cloak consists only of isotropic dielectric materials, which enables broadband and low-loss invisibility at a wavelength range of 1400–1800 nm. Another approach to obtain cloaking at optical frequencies is recently demonstrated by Cornell researchers [16]. The cloak operates in the near infrared at a wavelength of 1550 nm and it is composed of nanometer-size silicon structures with spatially varying densities across the cloak. The cloak conceals a deformation on a flat reflecting surface, under which an object can be hidden. The density variation is defined using transformation optics to define the effective index distribution of the cloak.

Although Chirality can be observed in nature, this effect is usually very weak, and to observe a significant polarization rotation effect, the light would have to propagate more than several centimeters (tens of thousands of visible wavelengths). Metamaterials can boost this effect by several orders of magnitude. In place of molecules, one can engineer tiny, subwavelength resonant electromagnets that act as magnetic dipoles [17]. Instead of using a resonant particle with a very narrow bandwidth, researchers at Karlsruhe University developed a uniaxial photonic metamaterial composed of 3-D gold helices arranged on a 2-D square lattice [18]. For propagation of light along the helix axis, the structure blocks the circular polarization with the same handedness as the helices, whereas it transmits the other, for a frequency range exceeding one octave. The structure is scalable to other frequency ranges and can be used as a compact broadband circular polarizer.

Photonic metamaterials are definitely one of the most active research areas within the photonics research community. Thanks to the recent experimental and theoretical demonstrations, the optical magic behind these structures has already been partially unveiled, in which we will definitely see more magic appear from photonic metamaterials in the coming years. The true magic behind photonic metamaterials is to create optical materials with new and unusual optical properties, and our imagination and creativity will continue to shape and advance this new research area.

References

[1] V. G. Veselago, "The electrodynamics of substances with simultaneously negative values of ϵ and μ," *Sov. Phys.—Usp.*, vol. 10, no. 4, pp. 509–514, 1968.

[2] J. Pendry, "Negative refraction makes a perfect lens," *Phys. Rev. Lett.*, vol. 85, no. 18, pp. 3966–3969, Oct. 2000.

[3] D. R. Smith, W. J. Padilla, D. C. Vier, S. C. Nemat-Nasser, and S. Schultz, "Composite medium with simultaneously negative permeability and permittivity," *Phys. Rev. Lett.*, vol. 84, no. 18, pp. 4184–4187, May 2000.

[4] C. M. Soukoulis, S. Linden, and M. Wegener, "Negative refractive index at optical wavelengths," *Science*, vol. 315, no. 5808, pp. 47–49, Jan. 2007.

[5] S. Linden, C. Enkrich, M. Wegener, J. Zhou, T. Koschny, and C. M. Soukoulis, "Magnetic response of metamaterials at 100 terahertz," *Science*, vol. 306, no. 5700, pp. 1351–1353, Nov. 2004.

[6] N. Liu, H. Guo, L. Fu, S. Kaiser, H. Schweizer, and H. Giessen, "Three-dimensional photonic metamaterials at optical frequencies," *Nat. Mater.*, vol. 7, no. 1, pp. 31–37, Jan. 2008.

[7] W. Cai, U. K. Chettiar, H.-K. Yuan, V. C. de Silva, A. V. Kildishev, V. P. Drachev, and V. M. Shalaev, "Metamagnetics with rainbow colors," *Opt. Express*, vol. 15, no. 6, pp. 3333–3341, Mar. 2007.

[8] J. Valentine *et al., Nature*, vol. 454, p. 7247, 2008.

[9] E. Ozbay, "Plasmonics: Merging photonics and electronics at nanoscale dimensions," *Science*, vol. 311, no. 5758, pp. 189–193, Jan. 2006.

[10] E. Cubukcu, K. Aydin, E. Ozbay, S. Foteinopoulou, and C. M. Soukoulis, "Electromagnetic waves: Negative refraction by photonic crystals," *Nature*, vol. 423, no. 6940, pp. 604–605, Jun. 2003.

[11] J. Yao, Z. Liu, Y. Liu, Y. Wang, C. Sun, G. Bartal, A. M. Stacy, and X. Zhang, "Optical negative refraction in bulk metamaterials of nanowires," *Science*, vol. 321, no. 5891, p. 930, Aug. 2008.

[12] E. Cubukcu *et al., Phys. Rev. Lett.*, vol. 91, p. 2140, 2003.

[13] D. Schurig, J. J. Mock, B. J. Justice, S. A. Cummer, J. B. Pendry, A. F. Starr, and D. R. Smith, "Metamaterial electromagnetic cloak at microwave frequencies," *Science*, vol. 314, no. 5801, pp. 977–980, Nov. 2006.
[14] K. Guven, E. Saenz, R. Gonzalo, E. Ozbay, and S. Tretyakov, "Electromagnetic cloaking with canonical spiral inclusions," *New J. Phys.*, vol. 10, p. 115 037, Nov. 2008.
[15] J. Valentine, J. Li, T. Zentgraf, G. Bartal, and X. Zhang, "An optical cloak made of dielectrics," *Nat. Mater.*, vol. 8, no. 7, pp. 568–571, Jul. 2009.
[16] L. H. Gabrielli, J. Cardenas, C. B. Poitras, and M. Lipson, "Silicon nanostructure cloak operating at optical frequencies," *Nat. Photon.*, vol. 3, no. 8, pp. 461–463, Aug. 2009.
[17] E. Plum *et al., Phys. Rev. Lett.*, vol. 79, p. 035407, 2009.
[18] J. K. Gansel, M. Thiel, M. S. Rill, M. Decker, K. Bade, V. Saile, G. von Freymann, S. Linden, and M. Wegener, "Gold helix photonic metamaterial as broadband circular polarizer," *Science*, vol. 325, no. 5947, pp. 1513–1515, Sep. 2009.

Major Accomplishments in 2009 on Femtosecond Laser Fabrication: Fabrication of Bio-Microchips

Koji Sugioka and Katsumi Midorikawa

(Invited Paper)

Advanced Science Institute, RIKEN, Wako 351-0198, Japan

DOI: 10.1109/JPHOT.2010.2047252
1943-0655/$26.00 ©2010 IEEE

Manuscript received February 12, 2010. Current version published April 23, 2010. Corresponding author: K. Sugioka (e-mail: ksugioka@riken.jp).

Abstract: Femtosecond (fs) lasers have become common tools for microfabrication and nanofabrication, and a large amount of research has been carried out in this field in 2009. This paper reviews the major areas of achievement in 2009 relating to bio-microchips such as the so-called lab-on-a-chip (LOC) and optofluidics.

Index Terms: Femtosecond laser, microfabrication, bio-microchip, lab-on-a-chip, optofludics.

Over the past few decades, the rapid development of femtosecond (fs) lasers has opened up new avenues for materials processing, and they have already become common tools for microfabrication and nanofabrication. Fabrication using fs lasers is still a highly active research field in material science from the standpoint of both fundamental physics and the development of practical applications. One important recent advancement is the development of both spatial and temporal beam-shaping techniques that allow higher efficiency, quality, and resolution during fabrication [1]. Using the ISI Web of Knowledge, a search for scientific papers published in 2009 with the keywords "femtosecond laser" and "fabrication" produced 157 hits in subjects including micromachining [2], surface modification [3], surface nanostructuring [4], waveguide writing [5], photonic device fabrication [6], 3-D microfabrication and nanofabrication [7], two-photon polymerization [8], nanomaterial synthesis [9], and bio-tissue treatment [10]. Among these research areas, the number of papers describing fabrication of bio-microchips, such as the so-called lab-on-a-chip (LOC), optofluidics, and micro total analysis systems (μ-TAS), is significantly increasing. In this review, some relevant accomplishments related to the fabrication of bio-microchips using fs lasers in 2009 are introduced.

Optofludic devices have been fabricated by integrating optical waveguides into commercial fused-silica LOCs for photonic biosensing [11]. High-quality waveguides intersecting the microfluidic channel in the LOC were written by internal modification of the refractive index using a focused scanned fs laser beam. The fabricated devices had the capability to excite fluorescent molecules flowing in the microfluidic channels with high spatial selectivity. Further, the optofluidic devices were fabricated using only an fs laser [12], [13]. 3-D microfluidic channels were first formed in fused silica by fs laser direct writing followed by selective wet etching in a hydrofluoric (HF) acid solution [14]. The optical waveguides intersecting the microchannel were subsequently integrated into the microchannels by refractive-index modification using the fs laser beam. A single red blood cell (RBC) in diluted human blood introduced into the microchannel was detected by two different

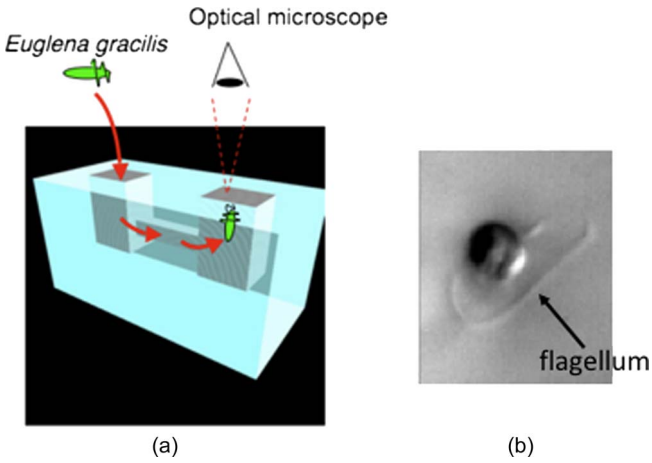

Fig. 1. (a) Schematic illustration of the concept of a nanoaquarium and (b) microscopic image of the front view of *Euglena gracilis* swimming upward in the microchannel in the nanoaquarium.

optical methods. In the first, the transmitted light intensity of an He-Ne laser beam coupled into the optical waveguides was measured. When the cell arrived at a specific region in the microchannel where the waveguides crossed, a decrease occurred in the intensity of the transmitted light due to scattering by the cell, resulting in detection of the cell. The second method involved detection of fluorescence emission from a dyed RBC excited by an Ar laser beam delivered through the optical waveguide.

A more sophisticated demonstration of the capabilities of fs lasers in the fabrication of optofluidics was the integration of a Mach–Zehnder interferometer into a microfluidic channel for label-free sensing of liquid samples [15]. The simple 3-D microfluidic channel was fabricated in fused silica by fs laser direct writing followed by HF etching. A Mach–Zehnder unbalanced interferometer was then integrated with the fabricated microchannel. The interferometer had two optical-waveguide arms of slightly different length, one of which intersected the microchannel, while the other passed above it. The interferometer can produce fringes when a sufficiently large spectral region is scanned with a tunable laser. When the light propagating through one of arms travels through a different medium, the fringe pattern becomes shifted due to the slight change in refractive index. Thus, variations in the refractive index of the content of the microchannel can be detected by measuring the shift in wavelength of the fringes. The sensitivity of the integrated interferometer was tested by filling the microchannel with glucose-D solutions of different concentrations. The fabricated optofluidic devices succeeded in clearly distinguishing solutions with concentration differences of just 50 mM, which was equivalent to a sensitivity of 1×10^{-3} in refractive index.

Another interesting application of bio-microchips is dynamic observation of aquatic microorganisms [16], [17]. Some species of microorganisms have survived almost unchanged for more than 500 million years. Some of them undergo extremely rapid motion, which is unusual in the macroworld in which we live, and display unique 3-D patterns of movement defying gravity. Most of these microorganisms are single-celled, and thereby, it is very important to explore the dynamics of their movement and their physiological energy-generation mechanisms in order to fully understand the functioning and potential abilities of the individual cells that make up multicellular organisms, including human beings. Therefore, observation of microorganisms is currently a challenging subject for cell biologists. However, using the conventional observation method, in which the microorganisms are placed in a Petri dish with water and are observed using an optical microscope with a high-numerical-aperture objective lens, it is often difficult to capture clear images due to their rapid movement and their small size. The use of a microchip with a 3-D microfluidic structure, which is referred to as a nanoaquarium, scales down the observation site, that is, the microorganisms become three-dimensionally encapsulated within a limited volume, which still provides sufficient space for movement. This makes it much easier to capture images of their movements, as shown in Fig. 1(a). The nanoaquarium was fabricated in a photosensitive glass microchip by fs laser direct

writing followed by thermal treatment, HF etching, and additional thermal treatment. It enabled us, for the first time, to obtain an image of the front view of *Euglena gracilis* swimming upward in the microchannel, as shown in Fig. 1(b). The rapid motion of the flagellum, whose diameter was several hundred nanometers, was also clearly observed. To date, several kinds of nanoaquariums with different structures and functionalities have been successfully fabricated for specific purposes, including the analysis of flagellum motion of *Euglena gracilis*, determining the information-transmission process used by *Pleurosira laevis*, observations of high-speed motion of Cryptomonas, and Phormidium assemblage to seedling roots for the promotion of vegetable growth.

Fabrication using fs lasers allows the 3-D integration of various functions in a single glass microchip with easy assembly of each microcomponent and without the need for cumbersome processes for stacking and joining substrates. Such direct fabrication of truly 3-D microstructures can be realized only by fs laser fabrication. Finally, we emphasize that such 3-D microfabrication techniques will have a significant impact on the manufacture of integrated microchips that are highly efficient for on-chip biosensing and analysis.

References

[1] C. Mauclair, G. Cheng, N. Huot, E. Audouard, A. Rosenfeld, I. V. Hertel, and R. Stoian, "Dynamic ultrafast laser spatial tailoring for parallel micromachining of photonic devices in transparent materials," *Opt. Express*, vol. 17, no. 5, pp. 3531–3542, 2009.

[2] D. K. Das and T. M. Pollock, "Femtosecond laser machining of cooling holes in thermal barrier coated CMSX4 superalloy," *J. Mater. Process. Technol.*, vol. 209, p. 5661, 2009.

[3] Y. Izawa, S. Tokita, M. Fujita, M. Nakai, T. Norimatsu, and Y. Izawa, "Ultrathin amorphization of single-crystal silicon by ultraviolet femtosecond laser pulse irradiation," *J. Appl. Phys.*, vol. 105, no. 6, p. 064909, Mar. 2009.

[4] M. Zamfirescu, M. Ulmeanu, F. Jipa, O. Cretu, A. Moldovan, G. Epurescu, M. Dinescu, and R. Dabu, "Femtosecond laser induced periodic surface structures on ZnO thin films," *J. Laser Micro/Nanoeng.*, vol. 4, p. 7, 2009.

[5] S. Z. Xu, J. R. Qiu, C. B. Li, H. Y. Sun, and Z. Z. Xu, "Direct writing waveguides inside YAG crystal by femtosecond laser," *Opt. Commun.*, vol. 282, no. 24, pp. 4810–4814, Dec. 2009.

[6] G. D. Marshall, A. Politi, J. C. F. Matthews, P. Dekker, M. Ams, M. J. Withford, and J. L. O'Brien, "Laser written waveguide photonic quantum circuits," *Opt. Express*, vol. 17, no. 15, pp. 12 564–12 554, Jul. 2009.

[7] S. Matsuo, H. Sumi, S. Kiyama, T. Tomita, and S. Hashimoto, "Femtosecond laser-assisted etching of Pyrex glass with aqueous solution of KOH," *Appl Surf. Sci.*, vol. 255, no. 24, pp. 9758–9760, Sep. 2009.

[8] D. Wu, Q. D. Chen, L. G. Niu, J. N. Wang, J. Wang, R. Wang, H. Xia, and H. B. Sun, "Femtosecond laser rapid prototyping of nanoshells and suspending components towards microfluidic devices," *Lab Chip*, vol. 9, no. 16, pp. 2391–2394, Aug. 2009.

[9] N. Barsch, A. Gatti, and S. Barcikowski, "Improving laser ablation of zirconia by liquid films: Multiple influence of liquids on surface machining and nanoparticle generation," *J. Laser Micro/Nanoeng.*, vol. 4, p. 66, 2009.

[10] R. Le Harzic, K. König, C. Wullner, K. Vogler, and C. Donitzky, "Ultraviolet femtosecond laser creation of corneal flap," *J. Refractive Surgery*, vol. 25, p. 383, 2009.

[11] R. M. Vazquez, R. Osellame, D. Nolli, C. Dongre, H. van den Vlekkert, R. Ramponi, M. Pollnaub, and G. Cerullo, "Integration of femtosecond laser written optical waveguides in a lab-on-chip," *Lab Chip*, vol. 9, no. 1, pp. 91–96, Jan. 2009.

[12] M. Kim, D. J. Hwang, H. Jeon, K. Hiromatsu, and C. P. Grigoropoulos, "Single cell detection using a glass-based optofluidic device fabricated by femtosecond laser pulses," *Lab Chip*, vol. 9, no. 2, pp. 311–318, Jan. 2009.

[13] D. J. Hwang, M. Kim, K. Hiromatsu, H. Jeon, and C. P. Grigoropoulos, "Three-dimensional opto-fluidic devices fabricated by ultrashort laser pulses for high throughput single cell detection and processing," *Appl. Phys. A, Mater. Sci. Process.*, vol. 96, p. 385, 2009.

[14] A. Marcinkevicius, S. Juodkazis, M. Watanabe, M. Miwa, S. Matsuo, H. Misawa, and J. Nishii, "Femtosecond laser-assisted three-dimensional microfabrication in silica," *Opt. Lett.*, vol. 26, no. 5, pp. 277–279, 2001.

[15] R. Osellame, R. Martinez, P. Laporta, R. Ramponi, and G. Cerullo, "Integration of micro-optics and microfluidics in a glass chip by fs-laser for optofluidic applications," *Proc. SPIE*, vol. 7202, p. 720 202, Feb. 2009.

[16] Y. Hanada, K. Sugioka, H. Kawano, I. Shihira Ishikawa, A. Miyawaki, and K. Midorikawa, "Nano-aquarium with microfluidic structures for dynamic analysis of *Cryptomonas* and *Phormidium* fabricated by femtosecond laser direct writing of photostructurable glass," *Appl Surf. Sci.*, vol. 255, no. 24, pp. 9893–9897, Sep. 2009.

[17] K. Sugioka, Y. Hanada, and K. Midorikawa, *Laser Photon. Rev.*, 2009, DOI 10.1002/lpor.200810074 (early view publication).

Three-Dimensional Holographic Imaging for Identification of Biological Micro/Nanoorganisms

B. Javidi,[1] *Fellow, IEEE*, M. Daneshpanah,[1] *Member, IEEE*, and I. Moon,[2] *Member, IEEE*

(Invited Paper)

[1]Electrical and Computer Engineering Department, University of Connecticut, Storrs, CT 06269-2157 USA
[2]School of Computer Engineering, Chosun University, Gwangju 501-759, Korea

DOI: 10.1109/JPHOT.2010.2044876
1943-0655/$26.00 ©2010 IEEE

Manuscript received February 12, 2010. Current version published April 23, 2010. Corresponding author: B. Javidi (e-mail: bahram@engr.uconn.edu).

Abstract: The integration of information photonics and 3-D imaging systems for low-cost automated screening and characterization of biological specimen is presented. In particular, 3-D holographic imaging and computational models are described that provide potentially powerful tools for rapid noninvasive 3-D sensing, identification, and tracking of biological micro/nanoorganisms.

Index Terms: Digital holography, 3-D microscopy, cell analysis, computational imaging, medical and biological imaging.

Traditionally, 3-D imaging, visualization, and displays have been investigated with broad applications in entertainment, manufacturing, medical diagnosis, robotics, defense, and security [1], [2]. Recently, information photonics based 3-D imaging systems have been utilized for automated identification of unicellular microorganisms [3]–[5]. Low-cost, rapid and automated detection and identification of biological micro/nanoorganisms can play a central role in future point of care health solutions, environmental monitoring, food safety, early detection of pandemics, and combating biological terrorism [5]. Although morphologically simple and minute, biological micro/nanoorganisms exhibit complex machinery resulting in sophisticated behavior and interaction with their environment. These properties make such organisms difficult to inspect and characterize with automated systems. Here, we overview some of recent advances in 3-D imaging systems integrated with information photonics for rapid, high-throughput sensing, visualization and identification of micro/nanoorganisms [3]–[8].

Interface between information photonics and 3-D imaging has been enabled by advances in sensors, sources, electronic hardware, and complex computational algorithms that can interpret the data provided by sensor for task-specific applications. In this capacity, computers are used to interpret sensor information according to physical laws governing the imaging system (e.g., diffraction), as well as performing various information processing algorithms for the desired task at hand (e.g., identification). Digital Holographic Microscopy is one such system in which digital holograms are processed by computer to recover specimen information in 3-D [9]–[11].

Microorganisms are usually semitransparent resulting in low contrast when imaged with conventional bright-field microscopes. It is thus a common practice to stain the cells or label them with

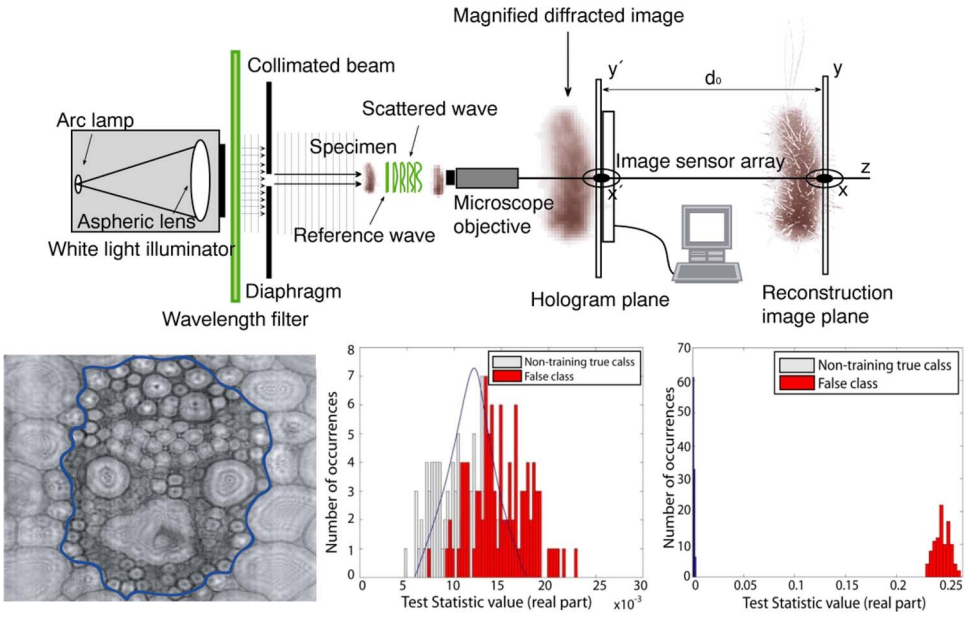

Fig. 1. (a) Three-dimensional imaging microscopy system under partially coherent illumination in Gabor configuration provides a compact and stable tool for characterization of biological specimen. A laser diode or laser-emitting diode source provides quasi-coherent illumination. The object wavefront is magnified with a microscope objective, and the interference pattern is recorded at the sensor plane. (b) Computational reconstruction of a corn stem cell sample at 25 μm from the hologram plane. (c) Real part of the test statistic in between nontraining true class and false class. (d) Same as (c) with Gabor-transformed digital holograms [3], [6].

fluorescent markers to image them in detail. This process is invasive for cells and can adversely affect their viability or disturb their natural life cycle, which can be undesirable for certain studies where noninvasiveness is required, e.g., stem-cell screening. Although semitransparency of microorganisms results in low contrast in intensity-based imaging techniques, the phase of the light can be significantly modulated by these specimen due to sensitivity of phase of light to refractive index variation inside the organism [9], [10]. Hence, complex amplitude wavefront modulated by the specimen contains a rich data set for quantitative characterization and recognition of micro/nanoorganisms [3].

Among various 3-D microscopy techniques [12], digital holography (DH) captures the complex amplitude of the object wavefront interferometrically in a coherent optical system. The four components recorded by a sensor are [13]

$$I(x,y) = |R + O(x,y)|^2 = |R|^2 + |O(x,y)|^2 + R^* O(x,y) + RO^*(x,y) \quad (1)$$

in which R and O denote the plane reference wave and the object wave, respectively. The recorded holograms convey the information of intricate interactions of incident light with the specimen in 3-D. Digital holograms can be used to computationally reconstruct the in-focus images of microorganisms at different depths with no mechanical scanning, hence extending the depth of field of the imaging system (e.g., microscope objective) [3], [13], [14].

For dynamic objects, single exposure DH microscopy has been adapted to biological imaging in on-axis and off-axis configurations [3], [9]–[11]. Off-axis configuration allows for quantitative phase measurement by separating real and conjugate terms [see eq. (1)] in expense of larger requirements on the space-bandwidth product of the sensor [14]. Nevertheless, it has been shown

that crosstalk between real and conjugate terms are bound to low spatial frequencies in Fresnel on-axis DH [14].

In certain applications where recognition of semitransparent micro/nanoorganisms is the primary objective, the two arms of an on-axis interferometer can collapse into a single path in Gabor geometry as shown in Fig. 1. The ballistic photons that pass through the specimen (and its surrounding medium) without any scattering provide the necessary reference wavefront for interferometery. In this configuration, the system can be drastically simplified and built with low-cost components. In particular, in Gabor geometry, the laser can be replaced with inexpensive, spatially incoherent and temporally quasi-coherent LEDs [8], [15], [16]. The coherence length of a typical 600-nm (red) LED of 25-nm bandwidth is 15 μm, thus reducing the speckle noise while retaining the sought-after information about the specimen, within the coherence length, at the hologram plane (see Fig. 1) [8]. After recording the hologram, a number of methods can be used for computational reconstruction including Fresnel transformation, convolution, and angular spectrum approaches [13].

Involvement of computational algorithms can be extended further into task-specific decision-making process based on information rich digital holograms of the specimen. It has been shown that digital holograms can be used for recognition and classification of macro objects [17] and biological micro/nanoorganisms [3]–[5], as well as for tracking them in 3-D [7]. In [3] it has been shown that statistical hypothesis testing can be applied to distinguish between different classes of microorganisms. By applying Gabor transformation and filtering at computationally reconstructed image plane, one can selectively target specific features of recorded diffraction patterns that are mostly discriminating between different classes of microorganisms. Fig. 1(c) and (d) illustrates how Gabor transformation can help in separating nontraining true class from false class on plant stem cells as a model.

In summary, 3-D holographic imaging and information photonics provide a potentially powerful tool for low-cost 3-D sensing, visualization, and rapid identification of biological micro/nanoorganisms. The applications range from detection of diseased cells, marker-less cell sorting and pathogen identification, among others.

References

[1] B. Javidi, F. Okano, and J.-Y. Son, Eds., *Three-Dimensional Imaging, Visualization, and Display (Signals and Communication Technology),* 1st ed. New York: Springer-Verlag, Dec. 2008.

[2] S. A. Benton and V. M. Bove, *Holographic Imaging*. New York: Wiley-Interscience, Apr. 2008.

[3] I. Moon, M. Daneshpanah, B. Javidi, and A. Stern, "Automated three-dimensional identification and tracking of micro/nanobiological organisms by computational holographic microscopy," *Proc. IEEE*, vol. 97, no. 6, pp. 990–1010, Jun. 2009.

[4] B. Javidi, S. Yeom, I. Moon, and M. Daneshpanah, "Real-time automated 3D sensing, detection, and recognition of dynamic biological micro-organic events," *Opt. Exp.*, vol. 14, no. 9, pp. 3806–3829, May 2006.

[5] B. Javidi, I. Moon, S. Yeom, and E. Carapezza, "Three-dimensional imaging and recognition of micro-organism using single-exposure on-line (SEOL) digital holography," *Opt. Exp.*, vol. 13, no. 12, pp. 4492–4506, Jun. 2005.

[6] I. Moon and B. Javidi, "3D identification of stem cells by computational holographic imaging," *J. R. Soc. Interface*, vol. 4, no. 13, pp. 305–313, Apr. 2007.

[7] M. Daneshpanah and B. Javidi, "Tracking biological microorganisms in sequence of 3D holographic microscopy images," *Opt. Exp.*, vol. 15, no. 17, pp. 10 761–10 766, Aug. 2007.

[8] I. Moon and B. Javidi, "3D visualization and identification of biological microorganisms using partially temporal incoherent light in-line computational holographic imaging," *IEEE Trans. Med. Imag.*, vol. 27, no. 12, pp. 1782–1790, Dec. 2008.

[9] J. Kühn, F. Montfort, T. Colomb, B. Rappaz, C. Moratal, N. Pavillon, P. Marquet, and C. Depeursinge, "Submicrometer tomography of cells by multiple-wavelength digital holographic microscopy in reflection," *Opt. Lett.*, vol. 34, no. 5, pp. 653–655, Mar. 2009.

[10] Y. Sung, W. Choi, C. Fang-Yen, K. Badizadegan, R. R. Dasari, and M. S. Feld, "Optical diffraction tomography for high resolution live cell imaging," *Opt. Exp.*, vol. 17, no. 1, pp. 266–277, Jan. 2009.

[11] F. Charrière, A. Marian, F. Montfort, J. Kuehn, T. Colomb, E. Cuche, P. Marquet, and C. Depeursinge, "Cell refractive index tomography by digital holographic microscopy," *Opt. Lett.*, vol. 31, no. 2, pp. 178–180, Jan. 2006.

[12] M. Martínez-Corral and G. Saavedra, "The resolution challenge in 3D optical microscopy," *Prog. Opt.*, vol. 53, pp. 1–67, 2009.

[13] U. Schnars and W. Jüptner, "Digital recording and numerical reconstruction of holograms," *Meas. Sci. Technol.*, vol. 13, no. 9, pp. R85–R101, Sep. 2002.
[14] A. Stern and B. Javidi, "Theoretical analysis of three-dimensional imaging and recognition of microorganism technique using single-exposure on-line (SEOL) digital holography," *J. Opt. Soc. Amer. A, Opt. Image Sci. Vis.*, vol. 24, no. 1, pp. 163–168, Jan. 2007.
[15] F. Dubois, M.-L. N. Requena, C. Minetti, O. Monnom, and E. Istasse, "Partial spatial coherence effects in digital holographic microscopy with a laser source," *Appl. Opt.*, vol. 43, no. 5, pp. 1131–1139, Feb. 2004.
[16] U. Gopinathan, G. Pedrini, and W. Osten, "Coherence effects in digital in-line holographic microscopy," *J. Opt. Soc. Amer. A, Opt. Image Sci. Vis.*, vol. 25, no. 10, pp. 2459–2466, Oct. 2008.
[17] B. Javidi and E. Tajahuerce, "Three-dimensional object recognition by use of digital holography," *Opt. Lett.*, vol. 25, no. 9, pp. 610–612, May 2000.

Imaging Nanoscale Magnetic Structures With Polarized Soft X-Ray Photons

Peter Fischer and Mi-Young Im

(Invited Paper)

Center for X-ray Optics, Lawrence Berkeley National Laboratory, Berkeley, CA 94720 USA

DOI: 10.1109/JPHOT.2010.2043666
1943-0655/$26.00 ©2010 IEEE

Manuscript received January 25, 2010; revised February 12, 2010. Current version published April 23, 2010. This work was supported by the Director, Office of Science, Office of Basic Energy Sciences, Materials Sciences and Engineering Division of the U.S. Department of Energy. Corresponding author: P. Fischer (e-mail: PJFischer@lbl.gov).

Abstract: Imaging nanoscale magnetic structures and their fast dynamics is scientifically interesting and technologically of highest relevance. The combination of circularly polarized soft X-ray photons, which provide a strong X-ray magnetic circular dichroism effect at characteristic X-ray absorption edges, with a high-resolution soft X-ray microscope utilizing Fresnel zone plate optics allows, in a unique way, the study of the stochastical behavior in the magnetization reversal process of thin films and the ultrafast dynamics of magnetic vortices and domain walls in confined ferromagnetic structures. Future sources of femtosecond-short and highly intense soft X-ray photon pulses hold the promise of magnetic imaging down to fundamental magnetic length and time scales.

Index Terms: Magnetic domain imaging, magnetophotonics, picosecond phenomena, synchrotron sources, time-resolved imaging, ultrafast, X-ray imaging, X-ray optics.

The magnetic properties of matter are one of the most vibrant research areas [1], [2], not only because the phenomenon of magnetism itself is scientifically very attractive, but it also has immense implications to modern magnetic storage and sensor device technologies. Nanomagnetism investigates magnetism approaching fundamental magnetic length scales which are given by material specific properties such as exchange lengths or anisotropy constants being in the few-nanometer regime for common materials.

To minimize the competing magnetic interactions, e.g., exchange and anisotropy, in ferromagnetic systems, the ground state is often not the single domain state, where all spins are aligned parallel, but breaks up into multiple magnetic domains [3]. The transition region between domains is referred to as a domain wall (DW). In confined geometries, e.g., micrometer-sized disk structures, the spin configuration forms a magnetic vortex (MV) [4], [5], with a singularity occurring at the center, i.e., the MV core, which overcomes shape anisotropy and points perpendicular to the disk plane. The sizes of DWs and vortex cores are proportional to magnetic exchange lengths.

With a typical bit size of only a few tens of nanometers in high-density magnetic storage media of 1 Tb/in^2 and the capability to artificially fabricate nanoscale magnetic structures either top-down or bottom-up, e.g., by state-of-the-art lithographical techniques [6], an abundance of analytical tools to characterize the magnetic behavior of these structures has been developed. Imaging methods are very attractive, since they give detailed and direct insight into the mechanisms involved.

There are several interaction mechanisms to control and manipulate the spin structure on a nanoscale. For example, reversal of the magnetic moments can be achieved by applying an

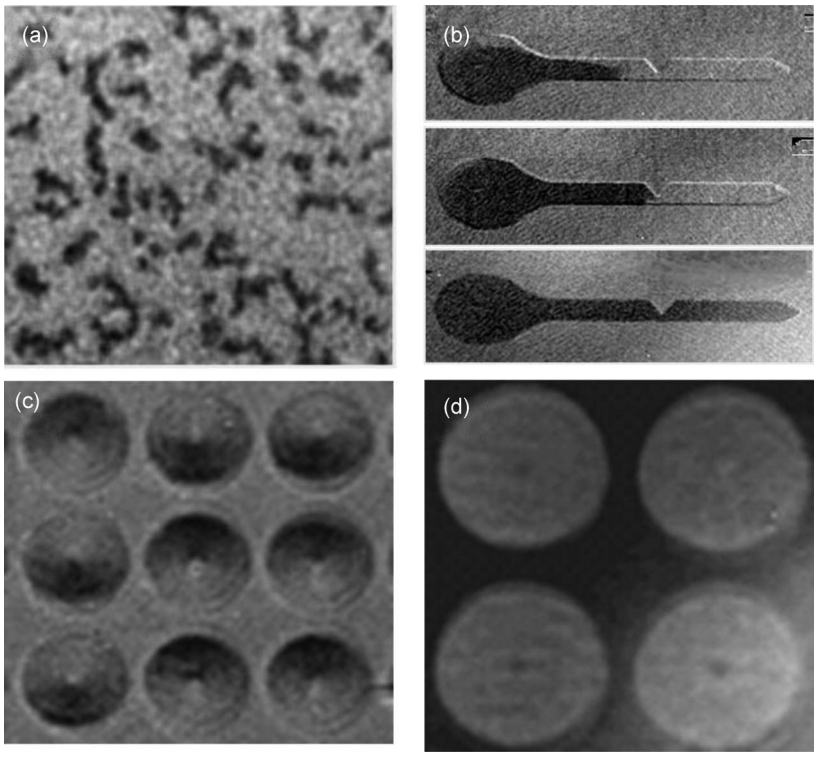

Fig. 1. Images of various magnetic nanostructures obtained with magnetic soft X-ray transmission microscopy. (a) Magnetic domains of a nanogranular 50-nm-thin $(Co_{82}Cr_{18})_{87}Pt_{13}$ alloy film exhibiting a pronounced perpendicular magnetic anisotropy during nucleation and reversal process [38]. Spatial resolution better than 15 nm. (b) Study of the field-driven depinning process of a magnetic DW in a 450-nm-wide notched Permalloy $(Fe_{20}Ni_{80})$ nanowire [39]. Spatial resolution better than 25 nm. (c) Circulating in-plane MV structure (chirality) of a 3×3 array of Permalloy disks with a diameter of 850 nm. Spatial resolution better than 25 nm. (d) In perpendicular geometry the images show directly the MV cores (polarity) in a 2×2 array of Permalloy disks with a diameter of 850 nm. Spatial resolution better than 25 nm.

external magnetic field pointing in opposite direction. Although discovered in the 1820's, Oersted switching is still used in magnetic storage. In the realm of spintronics, where in addition to the charge also the electron spin is exploited, the torque created by a spin polarized current on the spins can be used to reverse the magnetization [7]–[9]. In the future, the torque created by a photon onto the spins (opto-magnetics) is considered as the fastest way to switch the spins [10], [11].

The functionality of a spin system is determined by its dynamic behavior and therefore the spin dynamics of nanoscale magnetic structures down to fundamental time scales, which are again determined by inherent magnetic interactions has received significant scientific interest recently [12]–[19].

Powerful imaging techniques have been developed utilizing various probes. To name but a few, there are optical Kerr microscopies, electron microscopies, e.g., SEM with polarization analysis (SEMPA) [20], [21], Lorentz TEM [22], [23], spin-polarized LEEM [24], [25], or spin-polarized STM [26], [27], as well as scanning probe microscopies, such as Magnetic Force microscopy (MFM) or Magnetic resonant force microscopy (MRFM) [28]–[30].

The counterpart to the Kerr effect in the X-ray regime is X-ray magnetic circular dichroism (XMCD) [31], which describes the difference in X-ray absorption for circular polarized photons, depending on the relative orientation between helicity and magnetization of the sample. XMCD serves as large and element specific magnetic contrast mechanism for several magnetic X-ray microscopies. Photoemission electron microscopy (X-PEEM) [32] detects the secondary electrons generated in the X-ray absorption process, while Fresnel zone plates [33] provide high-spatial-resolution optics for both scanning (STXM) [34] and full-field transmission X-ray microscopy for

magnetic imaging (MTXM) [35]. State-of-the-art zone plates have demonstrated a better than 12-nm spatial resolution [36]. While X-PEEM is surface sensitive, STXM and MTXM give access to the bulk and particularly to buried layers. External parameters such as magnetic fields or radio-frequency current pulses can be applied easily during the data acquisition process which enables studies of nucleation, swiching, or DW motion upon spin injection [37].

Recently, MTXM has addressed the fundamental scientific question as to whether the magnetic behavior on the nanoscale exhibits a deterministic character in nanogranular thin magnetic films [38] [see Fig. 1(a)], DW depinning in nanowires [39] [see Fig. 1(b)], and in MV structures [see Fig. 1(c) and (d)]. A stochastic component has been identified in all those systems, which could be traced back to thermal fluctuations in the nanogranular system, geometrical, and multiplicity effects for the DW depinning in the nanowires and a Dzyaloshinsky–Moriya coupling effect for the switching of MV cores.

X-rays pulses from synchrotron sources have an inherent time structure with less than 100-ps length at typically megahertz frequencies. This matches perfectly magnetization dynamics such as precession and relaxation time of MVs and DW motion. Due to the low intensity per photon pulse at third-generation sources, stroboscopic pump–probe schemes are used, which requires the dynamic processes to be fully repeatable [40]. Fine details of MV motion [41], switching of a MV core by a single pulse [42], dynamics of a constricted DW [43], but also quantitative measurements of the spin polarization of currents [44] have been reported. The excellent agreement with micromagnetic simulations [45] indicates that a description by micromagnetic theory is still valid at these length scales. While this is good news for potential applications of e.g., MV cores [46], there is increased interest to explore the nonlinear regime of magnetization dynamics on the nanoscale [47].

Although the spatial resolution with X-ray microscopies is close to fundamental length scales, the fundamental femtosecond time scale is still far away. In the few picosecond regime, which is accessible already today e.g., with slicing sources, albeit at largely reduced photon intensities, first, spectroscopic XMCD experiments have shown the evolution of orbital moments as function of time [48], which helps to understand magnetic anisotropies. On the femtosecond time scale, one expects to explore the very origin of exchange interaction. This will be the realm at X-ray FELs [49] which are planned or have started operation very recently. HHG lab sources could serve as an alternative. Today, they are already capable of addressing femtosecond dynamics at M edges in transition metals covering the transient regime between delocalized bands and localized atomic levels [50].

At these highly brilliant and highly coherent femtosecond sources, lensless imaging techniques using XMCD [51], [52] hold great promise as a reciprocal space alternative to lens-based techniques for single shot and femtosecond magnetic X-ray imaging.

References

[1] S. D. Bader, "Colloquium: Opportunities in nanomagnetism," *Rev. Mod. Phys.*, vol. 78, no. 1, pp. 1–15, Jan. 2006.
[2] J. Stoehr and H. C. Siegmann, *Magnetism*. Berlin, Germany: Springer-Verlag, 2006.
[3] A. Hubert and R. Schäfer, *Magnetic Domains: The Analysis of Magnetic Microstructure*. Berlin, Germany: Springer-Verlag, 1998.
[4] T. Shinjo, T. Okuno, R. Hassdorf, K. Shigeto, and T. Ono, "Magnetic vortex core observation in circular dots of permalloy," *Science*, vol. 289, no. 5481, pp. 930–932, Aug. 2000.
[5] A. Wachowiak, J. Wiebe, M. Bode, O. Pietzsch, M. Morgenstern, and R. Wiesendanger, "Direct observation of internal spin structure of magnetic vortex cores," *Science*, vol. 298, no. 5593, pp. 577–580, Oct. 2002.
[6] B. D. Terris and T. Thomson, "Nanofabricated and self-assembled magnetic structures as data storage media," *J. Phys. D, Appl. Phys.*, vol. 38, no. 12, pp. R199–R222, Jun. 2005.
[7] L. Berger, "Emission of spin waves by a magnetic multilayer traversed by a current," *Phys. Rev. B, Condens. Matter*, vol. 54, no. 13, pp. 9353–9358, Oct. 1996.
[8] J. Slonczewski, "Current-driven excitation of magnetic multilayers," *J. Magn. Magn. Mater.*, vol. 159, no. 1/2, pp. L1–L7, Jun. 1996.
[9] K. Yamada, S. Kasai, Y. Nakatani, K. Kobayashi, H. Kohno, A. Thiaville, and T. Ono, "Electrical switching of the vortex core in a magnetic disk," *Nat. Mater.*, vol. 6, no. 4, p. 270, Apr. 2007.
[10] C. D. Stanciu, F. Hansteen, A. V. Kimel, A. Kirilyuk, A. Tsukamoto, A. Itoh, and T. Rasing, "All-optical magnetic recording with circularly polarized light," *Phys. Rev. Lett.*, vol. 99, no. 4, p. 047601, Jul. 2007.

[11] A. V. Kimel, B. A. Ivanov, R. V. Pisarev, P. A. Usachev, A. Kirilyuk, and T. Rasing, "Inertia-driven spin switching in antiferromagnets," *Nat. Phys.*, vol. 5, no. 10, pp. 727–731, Oct. 2009.
[12] E. Beaurepaire, J.-C. Merle, A. Daunois, and J.-Y. Bigot, "Ultrafast spin dynamics in ferromagnetic nickel," *Phys. Rev. Lett.*, vol. 76, no. 22, pp. 4250–4253, May 1996.
[13] J. P. Park, P. Eames, D. M. Engebretson, J. Berezovsky, and P. A. Crowell, "Imaging of spin dynamics in closure domain and vortex structures," *Phys. Rev. B, Condens. Matter*, vol. 67, no. 2, p. 020403(R), Jan. 2003.
[14] S. B. Choe, Y. Acremann, A. Scholl, A. Bauer, A. Doran, J. Stöhr, and H. A. Padmore, "Vortex core-driven magnetization dynamics," *Science*, vol. 304, no. 5669, pp. 420–422, Apr. 2004.
[15] H. Stoll, A. Puzic, B. van Waeyenberge, P. Fischer, J. Raabe, M. Buess, T. Haug, R. Höllinger, C. Back, D. Weiss, and G. Denbeaux, "High-resolution imaging of fast magnetization dynamics in magnetic nanostructures," *Appl. Phys. Lett.*, vol. 84, no. 17, p. 3328, Apr. 2004.
[16] J. Raabe, C. Quitmann, C. H. Back, F. Nolting, S. Johnson, and C. Buehler, "Quantitative analysis of magnetic excitations in landau flux-closure structures using synchrotron-radiation microscopy," *Phys. Rev. Lett.*, vol. 94, no. 21, p. 217 204, Jun. 2005.
[17] K. Buchanan, P. E. Roy, M. Grimsditch, F. Y. Fradin, K. Y. Guslienko, S. D. Bader, and V. Novosad, "Soliton-pair dynamics in patterned ferromagnetic ellipses," *Nat. Phys.*, vol. 1, no. 3, pp. 172–176, Dec. 2005.
[18] B. Van Waeyenberge, A. Puzic, H. Stoll, K. W. Chou, T. Tyliszczak, R. Hertel, M. Fähnle, H. Brückl, K. Rott, G. Reiss, I. Neudecker, D. Weiss, C. H. Back, and G. Schütz, "Magnetic vortex core reversal by excitation with short bursts of an alternating field," *Nature*, vol. 444, no. 7118, pp. 461–464, Nov. 2006.
[19] S.-K. Kim, K.-S. Lee, Y.-S. Yu, and Y.-S. Choi, "Reliable low-power control of ultrafast vortex-core switching with the selectivity in an array of vortex states by in-plane circular-rotational magnetic fields and spin-polarized currents," *Appl. Phys. Lett.*, vol. 92, no. 2, p. 022509, Jan. 2008.
[20] M. R. Scheinfein, J. Unguris, M. H. Kelley, D. T. Pierce, and R. J. Celotta, "Scanning electron microscopy with polarization analysis (SEMPA)," *Rev. Sci. Instrum.*, vol. 61, no. 10, p. 2501, Oct. 1990.
[21] R. Allenspach, "Spin-polarized scanning electron microscopy," *IBM J. Res. Develop.*, vol. 44, no. 4, p. 553, Jul. 2000.
[22] J. N. Chapman, A. B. Johnston, L. J. Heyderman, S. McVitie, W. A. P. Nicholson, and B. Bormans, "Coherent magnetic imaging by TEM," *IEEE Trans. Magn.*, vol. 30, no. 6, pp. 4479–4484, Nov. 1994.
[23] C. Phatak, M. Tanase, A. K. Petford-Long, and M. De Graef, "Determination of magnetic vortex polarity from a single Lorentz Fresnel image," *Ultramicroscopy*, vol. 109, no. 3, pp. 264–267, Feb. 2009.
[24] E. Bauer, "Low energy electron microscopy," *Rep. Prog. Phys.*, vol. 57, no. 9, pp. 895–938, Sep. 1994.
[25] J. Choi, J. Wu, F. El Gabaly, A. K. Schmid, C. Hwang, and Z. Q. Qiu, "Quantum well states in Au/Ru(0001) and their effect on the magnetic properties of a Co overlayer," *New J. Phys.*, vol. 11, p. 043016, Apr. 2009.
[26] M. Bode, "Spin-polarized scanning tunnelling microscopy," *Rep. Prog. Phys.*, vol. 66, no. 4, pp. 523–582, Mar. 2003.
[27] A. Heinrich, "Applied physics: Looking below the surface," *Science*, vol. 323, no. 5918, pp. 1178–1179, Feb. 2009.
[28] D. Rugar, "Single spin detection by magnetic resonance force microscopy," *Nature*, vol. 430, no. 6997, pp. 329–332, Jul. 2004.
[29] P. C. Hammel, "Imaging: Nanoscale MRI," *Nature*, vol. 458, no. 7240, pp. 844–845, Apr. 2009.
[30] C. L. Degen, M. Poggio, H. J. Mamin, C. T. Rettner, and D. Rugar, "Nanoscale magnetic resonance imaging," in *Proc. Nat. Acad. Sci.*, Feb. 2009, vol. 106, no. 5, pp. 1313–1317.
[31] C. T. Chen, F. Sette, Y. Ma, and S. Modesti, "Soft-x-ray magnetic circular dichroism at the $L_{2,3}$ edges of nickel," *Phys. Rev. B, Condens. Matter*, vol. 42, no. 11, pp. 7262–7265, Mar. 1990.
[32] J. Stoehr, "Element specific magnetic microscopy using circularly polarized X-rays," *Science*, vol. 259, p. 658, 1993.
[33] D. T. Attwood, *Soft X-rays and Extreme Ultraviolet Radiation: Principles and Applications*. Cambridge, U.K.: Cambridge Univ. Press, 1999.
[34] J. B. Kortright, S.-K. Kim, H. Ohldag, G. Meigs, and A. Warwick, "Magnetization imaging using scanning transmission x-ray microscopy," in *Proc. 6th Int. Conf. X-Ray Microscopy*, 2000, vol. 507, pp. 49–54.
[35] P. Fischer, G. Schütz, G. Schmahl, P. Guttmann, and D. Raasch, "Imaging of magnetic domains with the X-ray microscope at BESSY using X-ray magnetic circular dichroism," *Z.f. Phys. B*, vol. 101, pp. 313–316, 1996.
[36] W. Chao, J. Kim, S. Rekawa, P. Fischer, and E. H. Anderson, "Demonstration of 12 nm resolution fresnel zone plate lens based soft x-ray microscopy," *Opt. Express*, vol. 17, no. 20, pp. 17 669–17 677, Sep. 2009.
[37] P. Fischer, "Studying nanoscale magnetism and its dynamics with soft x-ray microscopy," *IEEE Trans. Magn.*, vol. 44, no. 7, pp. 1900–1904, Jun. 2008.
[38] M.-Y. Im, P. Fischer, D. H. Kim, K. D. Lee, S. H. Lee, and S. C. Shin, "Direct real-space observation of stochastic behavior in domain nucleation process on a nanoscale," *Adv. Mater.*, vol. 20, no. 9, pp. 1750–1754, 2008.
[39] M.-Y. Im, L. Bocklage, P. Fischer, and G. Meier, "Direct observation of stochastic domain-wall depinning in magnetic nanowires," *Phys. Rev. Lett.*, vol. 102, no. 14, p. 147 204, Apr. 2009.
[40] P. Fischer, "Celebrating 20 years of CMR—Past, present, and future (II)," in *Proc. AAPPS Bull.*, C.-R. Chang and B. Terris, Eds., 2008, vol. 18, p. 12.
[41] J.-H. Shim, D.-H. Kim, B. L. Mesler, J.-H. Moon, K.-J. Lee, E. Anderson, and P. Fischer, "Magnetic vortex dynamics on a picoseconds timescale in a hexagonal Permalloy pattern," *J. Appl. Phys.*, 2010, to be published.
[42] B. Van Waeyenberge, A. Puzic, H. Stoll, K. W. Chou, T. Tyliszczak, R. Hertel, M. Fähnle, H. Brückl, K. Rott, G. Reiss, I. Neudecker, D. Weiss, C. H. Back, and G. Schütz, "Magnetic vortex core reversal by excitation with short bursts of an alternating field," *Nature*, vol. 444, no. 7118, pp. 461–464, Nov. 2006.
[43] L. Bocklage, B. Krüger, R. Eiselt, M. Bolte, P. Fischer, and G. Meier, "Time-resolved imaging of current-induced domain-wall oscillations," *Phys. Rev. B, Condens. Matter*, vol. 78, no. 18, p. 180 405(R), Nov. 2008.
[44] S. Kasai, P. Fischer, M.-Y. Im, K. Yamada, Y. Nakatani, K. Kobayashi, H. Kohno, and T. Ono, "Probing the spin polarization of current by soft x-ray imaging of current-induced magnetic vortex dynamics," *Phys. Rev. Lett.*, vol. 101, no. 23, p. 237 203, Dec. 2008.

[45] K.-S. Lee, S.-K. Kim, Y.-S. Yu, Y.-S. Choi, K. Y. Guslienko, H. Jung, and P. Fischer, "Universal criterion and phase diagram for switching a magnetic vortex core in soft magnetic nanodots," *Phys. Rev. Lett.*, vol. 101, no. 26, p. 267 206, Dec. 2009.
[46] A. Drews, B. Krüger, G. Meier, S. Bohlens, L. Bocklage, T. Matsuyama, and M. Bolte, "Current- and field-driven magnetic antivortices for nonvolatile data storage," *Appl. Phys. Lett.*, vol. 94, no. 6, p. 062504, Feb. 2009.
[47] K. S. Buchanan, M. Grimsditch, F. Y. Fradin, S. D. Bader, and V. Novosad, "Driven dynamic mode splitting of the magnetic vortex translational resonance," *Phys. Rev. Lett.*, vol. 99, no. 26, p. 267 201, Dec. 2007.
[48] C. Stamm, T. Kachel, N. Pontius, R. Mitzner, T. Quast, K. Holldack, S. Khan, C. Lupulescu, E. F. Aziz, M. Wietstruk, H. A. Dürr, and W. Eberhardt, "Femtosecond modification of electron localization and transfer of angular momentum in nickel," *Nat. Mater.*, vol. 6, no. 10, pp. 740–743, Oct. 2007.
[49] K. A. Nugent and William A. Barletta, "Short-wavelength free-electron lasers," *IEEE Photonics J.*, to be published.
[50] C. La-O-Vorakiat, "Ultrafast demagnetization dynamics at the *M* edges of magnetic elements observed using a tabletop high-harmonic soft x-ray source," *Phys. Rev. Lett.*, vol. 103, no. 25, p. 257 402, Dec. 2009.
[51] S. Eisebitt *et al., Nature*, vol. 432, p. 885, 2004.
[52] S. Streit-Nierobisch, D. Stickler, C. Gutt, L.-M. Stadler, H. Stillrich, C. Menk, R. Frömter, C. Tieg, O. Leupold, H. P. Oepen, and G. Grübel, "Magnetic soft x-ray holography study of focused ion beam-patterned Co/Pt multilayers," *J. Appl. Phys.*, vol. 106, no. 8, p. 083909, Oct. 2009.

Solution-Processed Light Sensors and Photovoltaics

D. Aaron R. Barkhouse and Edward H. Sargent

(Invited Paper)

Edward S. Rogers Sr. Department of Electrical and Computer Engineering, University of Toronto, Toronto, ON M5S 3G4, Canada

DOI: 10.1109/JPHOT.2010.2045368
1943-0655/$26.00 ©2010 IEEE

Manuscript received February 14, 2010; revised March 3, 2010. Current version published April 23, 2010. This publication was supported in part by Award KUS-I1-009-21, made by King Abdullah University of Science and Technology. Corresponding author: E. H. Sargent (e-mail: ted.sargent@utoronto.ca).

Abstract: Solution processed solar cells and photodetectors have been investigated extensively due to their potential for low-cost, high throughput fabrication. Colloidal quantum dots (CQDs) and conjugated polymers are two of the most promising materials systems for these applications, due to their processibility and their tunability, the latter achieved by varying their size or molecular structure. Several breakthroughs in the past year highlight the rapid progress that continues to be made in understanding these materials and engineering devices to realize their full potential. CQD photodiodes, which had already shown greater detectivity than commercially available photodetectors, have now reached MHz bandwidths. Polymer solar cells with near-perfect internal quantum efficiencies have been realized, and improved 3-D imaging of these systems has allowed theorists to link structure and function quantitatively. Organic photodetectors with sensitivities at wavelengths longer than 1 μm have been achieved, and multiexciton generation has been unambiguously observed in a functioning CQD device, indicating its viability in further improving detector sensitivity.

Solution-processed semiconductors are fabricated with ease, at low cost, and on any reasonable substrate including a flexible one. Both polymer and colloidal quantum-dot-based devices continue to show promise to replace current commercially available technologies, and a number of breakthroughs in the past year have brought them significantly closer to that goal by advancing our understanding of device operation and by highlighting ways to harness absorbed photons more efficiently.

Photodetectors, which underpin the sensitive capture of digital images, saw several major leaps forward in the past year. First, 2009 saw the advent of the first sensitive megahertz-bandwidth solution-processed photodetectors [1]. Earlier years had seen huge advances in sensitivity but, by exploiting photoconductivity, often did so at the expense of speed [2]. The realization of a fully depleted Schottky photodiode employing 1.55-um-bandgap colloidal quantum dots overcame slow diffusive transport in these materials. The resultant devices exhibited D^* (normalized detectivity) in the 10^{12} Jones, competing with sensitivities achieved by room-temperature InGaAs detectors. The colloidal quantum dot devices provided light sensing across the entire spectrum spanning 400 nm to 1.6 um (see Fig. 1).

A new avenue to even further-enhanced sensitivity—one distinctive to quantum solids—was proven in device form. Multiple-exciton generation (MEG), a process in which a single photon creates more than one excited electron-hole pair, has gained attention due to its potential for increasing the sensitivity and efficiency of photodetectors and photovoltaics. Despite this interest, evidence for MEG has so far been confined to spectroscopic signatures in ultrafast experiments which probe the relaxation dynamics of excitons in order to infer the presence of MEG [3]. An optoelectronic device

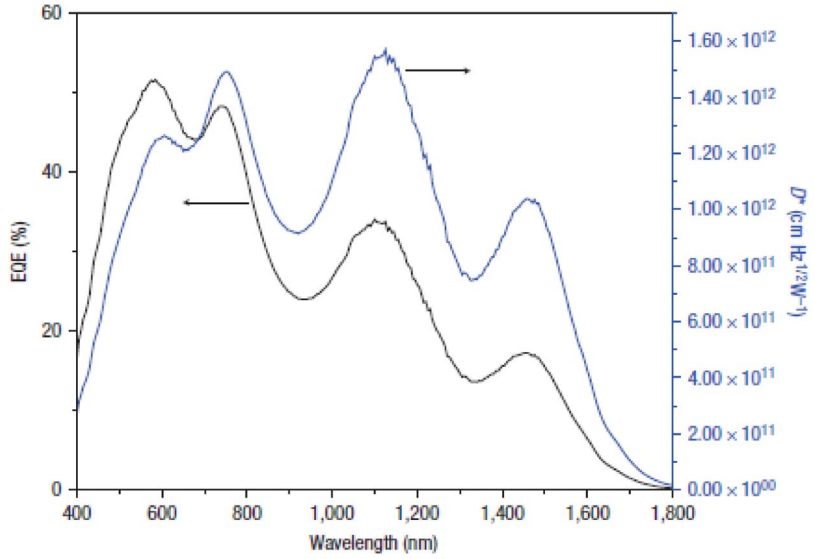

Fig. 1. Spectral responsivity of a solution processed quantum dot photodetector.

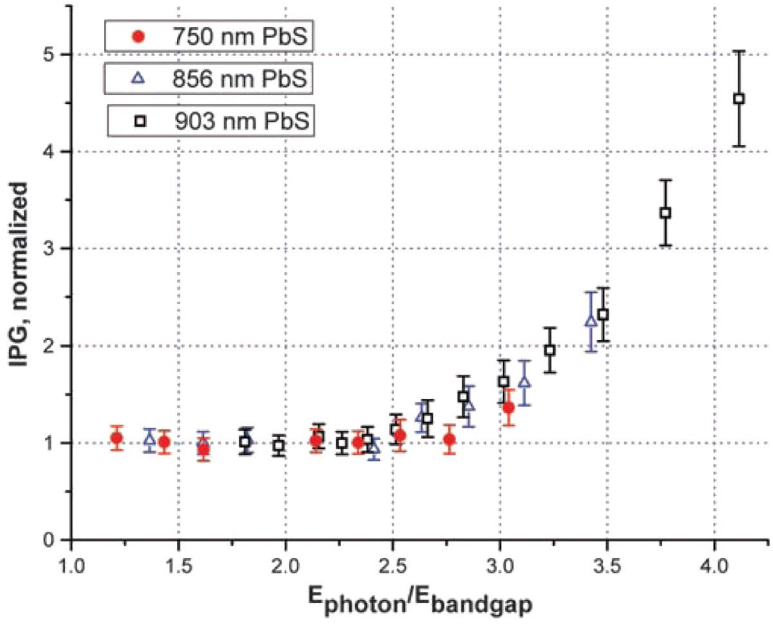

Fig. 2. Internal photoconductive gain as a function of photon energy for CQDs of three different sizes, showing increased sensitivity for photon energies above $2.7E_g$ as a result of MEG.

showing increased photocurrent at photon energies of more than twice the bandgap $(2E_g)$ could help prove not only the existence of MEG but its usefulness in enhancing device performance as well. 2009 saw the arrival of such a device in the form of a solution-processed photoconductive photodetector [4]. Consisting of a film of infrared-bandgap colloidal quantum dots addressed using coplanar electrical contacts, the device showed constant internal photoconductive gain as a function of photon energy for photon energies below $2E_g$. As the photon energy was increased to $2.7E_g$ and beyond, which is the MEG threshold in these materials, the internal gain grew significantly, reaching nearly four times the long-wavelength value when the photon energy reached $4.1E_g$ (see Fig. 2). MEG was thus harnessed to create a more sensitive photodetector.

Because they offer convenient integration combined with exceptional sensitivity and speed, these materials became poised for incorporation into commercial imaging arrays. This dream became a reality [5], with a multimegapixel light imager being created based on a CMOS silicon integrated circuit providing pixel read-out and a continuous 100%-fill-factor top-surface colloidal quantum dot layer providing high-performance low-light imaging.

Photovoltaics for energy conversion saw major advances as well. Polymer bulk heterojunction solar cells had seen many years of rapid progress, reaching 5% solar-power-conversion efficiencies in 2008. In 2009, three separate groups reported a significant further advance, creating bulk heterojunction solar cells with efficiencies above 6% [6]–[8]. All of the groups exercised careful control over nanoscale separation between electron-donating and electron-accepting phases to achieve optimal exciton dissociation and charge transport, *emphasizing the crucial role these two processes play in efficient device operation*. The best devices achieved near-perfect internal quantum efficiency (electrons collected for every photon absorbed). Combined with careful manipulation of the optical field in the device by the introduction of a transparent TiO_x spacer layer, this resulted in impressive short-circuit current densities greater than 10 mA/cm^2.

These findings put an even sharper focus on the critical importance of nanoscale morphology in polymer photovoltaics—and as such mandated further advances in its detailed characterization. Rough estimates of morphology from AFM [9], [10], TEM [11], or various photocurrent mapping techniques [12]–[14] are instructive, but the direct morphological information obtained from these techniques tends to be confined to surface or in-plane morphology of the films, while both exciton dissociation and carrier transport depend sensitively on the bulk and out-of-plane domain morphology as well. 2009 heralded nanometer-scale mapping of the 3-D morphology of polymer/ZnO bulk heterojunction solar cells, enabling quantitative correlation of device performance with nanoscale morphology [15]. The roles of transport and exciton dissociation in limiting device performance are today much better quantified.

Colloidal quantum dot photovoltaics saw a similarly brisk pace of progress. These materials offer the potential to absorb not only the visible but the infrared half of the sun's spectrum reaching the earth [16] as well. These devices, which were first reported in 2005 with subpercent efficiencies, [17] rose to multipercent efficiencies in 2009 [18]–[20].

In both polymers and colloidal quantum dots, one of the major outstanding questions is the stability of devices and materials. It is known that, with rigorous encapsulation, commercially relevant device lifetimes may be achieved in organic semiconductor materials and devices [21], [22]. *Polymer solar cells already have shown illumination stability over hundreds of hours, but degrade quickly on exposure to moisture or oxygen,* [23] *while early quantum dot devices exhibited exceptionally short lifetimes upon exposure to air* [24]. It is of interest to build materials that are amenable to processing in minimally controlled environments (ideally room air) and that survive either under ambient conditions or with low-cost encapsulation. One recent report [25] introduces a new concept: the idea of building active photovoltaic semiconductor materials that—rather than being resistant to oxidation—are tolerant of oxidation. Specifically, the materials employed cation-rich surfaces that form oxides that produced shallow, rather than deep, traps, enabling the extension of photocarrier lifetimes without excessively compromising their extraction times [26].

In sum, optoelectronic devices based on printable materials advanced in 2009 both in concept and in quantitative performance. Light sensors achieved photodetection capability comparable with that of their single-crystal counterparts, and photovoltaics made significant progress toward the 10% solar power conversion efficiency often touted as the threshold for commercial competitiveness of low-cost solar technologies. *There remains a great deal of work to do to reach this goal, including understanding and controlling degradation mechanisms to achieve long-term device stability and making devices that absorb fully, and convert efficiently, the IR portion of the spectrum. Finally*, two important issues have shown recent promise and demand further development. Colloidal quantum dots based on heavy-metal-free constituents have shown encouraging initial performance [27] and merit further optimization. In addition, there are initial indications that organic semiconductors can harness infrared light at wavelengths not previously addressed by such materials [28], potentially paving the way to polymer solar cells converting a greater fraction of the sun's broad spectrum.

References

[1] J. P. Clifford, G. Konstantatos, K. W. Johnston, S. Hoogland, L. Levina, and E. H. Sargent, "Fast, sensitive and spectrally tuneable colloidal-quantum-dot photodetectors," *Nat. Nanotechnol.*, vol. 4, no. 1, pp. 40–44, Jan. 2009.

[2] G. Konstantatos, I. Howard, A. Fischer, S. Hoogland, J. Clifford, E. Klem, L. Levina, and E. H. Sargent, "Ultrasensitive solution-cast quantum dot photodetectors," *Nature*, vol. 442, no. 7099, pp. 180–183, Jul. 2006.

[3] R. D. Schaller and V. I. Klimov, "High efficiency carrier multiplication in PbSe nanocrystals: Implications for solar energy conversion," *Phys. Rev. Lett.*, vol. 92, no. 18, p. 186 601, May 2004.

[4] V. Sukhovatkin, S. Hinds, L. Brzozowski, and E. H. Sargent, "Colloidal quantum-dot photodetectors exploiting multiexciton generation," *Science*, vol. 324, no. 5934, pp. 1542–1544, Jun. 2009.

[5] E. H. Sargent, "Connecting the quantum dots," *IEEE Spectr.*, vol. 47, no. 2, pp. 48–52, Feb. 2010.

[6] S. H. Park, A. Roy, S. Beaupre, S. Cho, N. Coates, J. S. Moon, D. Moses, M. Leclerc, K. Lee, and A. J. Heeger, "Bulk heterojunction solar cells with internal quantum efficiency approaching 100%," *Nat. Photon.*, vol. 3, no. 5, pp. 297–302, May 2009.

[7] Y. Y. Liang, D. Q. Feng, Y. Wu, S. T. Tsai, G. Li, C. Ray, and L. P. Yu, "Highly efficient solar cell polymers developed via fine-tuning of structural and electronic properties," *J. Amer. Chem. Soc.*, vol. 131, no. 22, pp. 7792–7799, Jun. 2009.

[8] H. Y. Chen, J. H. Hou, S. Q. Zhang, Y. Y. Liang, G. W. Yang, Y. Yang, L. P. Yu, Y. Wu, and G. Li, "Polymer solar cells with enhanced open-circuit voltage and efficiency," *Nat. Photon.*, vol. 3, no. 11, pp. 649–653, Nov. 2009.

[9] D. Gebeyehu, C. J. Brabec, F. Padinger, T. Fromherz, J. C. Hummelen, D. Badt, H. Schindler, and N. S. Sariciftci, "The interplay of efficiency and morphology in photovoltaic devices based on interpenetrating networks of conjugated polymers with fullerenes," *Synth. Met.*, vol. 118, no. 1–3, pp. 1–9, Mar. 2001.

[10] C. Y. Kwong, A. B. Djurisic, P. C. Chui, K. W. Cheng, and W. K. Chan, "Influence of solvent on film morphology and device performance of poly(3-hexylthiophene):TiO_2 nanocomposite solar cells," *Chem. Phys. Lett.*, vol. 384, no. 4–6, pp. 372–375, Jan. 2004.

[11] X. N. Yang, J. K. J. van Duren, R. A. J. Janssen, M. A. J. Michels, and J. Loos, "Morphology and thermal stability of the active layer in poly(p-phenylenevinylene)/methanofullerene plastic photovoltaic devices," *Macromolecules*, vol. 37, no. 6, pp. 2151–2158, Mar. 2004.

[12] H. Frohne, C. R. McNeill, G. G. Wallace, and P. C. Dastoor, "Enhancement of polymer electronics via surface states on highly doped polymeric anodes," *J. Phys. D, Appl. Phys.*, vol. 37, no. 2, pp. 165–170, Jan. 2004.

[13] D. C. Coffey, O. G. Reid, D. B. Rodovsky, G. P. Bartholomew, and D. S. Ginger, "Mapping local photocurrents in polymer/fullerene solar cells with photoconductive atomic force microscopy," *Nano Lett.*, vol. 7, no. 3, pp. 738–744, Mar. 2007.

[14] B. J. Leever, M. F. Durstock, M. D. Irwin, A. W. Hains, T. J. Marks, L. S. C. Pingree, and M. C. Hersam, "Spatially resolved photocurrent mapping of operating organic photovoltaic devices using atomic force photovoltaic microscopy," *Appl. Phys. Lett.*, vol. 92, no. 1, p. 013302, 2008.

[15] S. D. Oosterhout, M. M. Wienk, S. S. van Bavel, R. Thiedmann, L. J. A. Koster, J. Gilot, J. Loos, V. Schmidt, and R. A. J. Janssen, "The effect of three-dimensional morphology on the efficiency of hybrid polymer solar cells," *Nat. Mater.*, vol. 8, no. 10, pp. 818–824, Oct. 2009.

[16] E. H. Sargent, "Infrared photovoltaics made by solution processing," *Nat. Photon.*, vol. 3, no. 6, pp. 325–331, Jun. 2009.

[17] S. A. McDonald, G. Konstantatos, S. G. Zhang, P. W. Cyr, E. J. D. Klem, L. Levina, and E. H. Sargent, "Solution-processed PbS quantum dot infrared photodetectors and photovoltaics," *Nat. Mater.*, vol. 4, no. 2, pp. 138–142, Feb. 2005.

[18] W. Ma, J. M. Luther, H. M. Zheng, Y. Wu, and A. P. Alivisatos, "Photovoltaic devices employing ternary PbS_xSe_{1-x} nanocrystals," *Nano Lett.*, vol. 9, no. 4, pp. 1699–1703, Apr. 2009.

[19] B. P. Rand, J. Xue, F. Yang, and S. R. Forrest, "Organic solar cells with sensitivity extending into the near infrared," *Appl. Phys. Lett.*, vol. 87, no. 23, p. 233508, Dec. 2005.

[20] J. J. Choi, Y. F. Lim, M. B. Santiago-Berrios, M. Oh, B. R. Hyun, L. F. Sung, A. C. Bartnik, A. Goedhart, G. G. Malliaras, H. D. Abruna, F. W. Wise, and T. Hanrath, "PbSe nanocrystal excitonic solar cells," *Nano Lett.*, vol. 9, no. 11, pp. 3749–3755, Nov. 2009.

[21] J. A. Hauch, P. Schilinsky, S. A. Choulis, S. Rajoelson, and C. J. Brabec, "The impact of water vapor transmission rate on the lifetime of flexible polymer solar cells," *Appl. Phys. Lett.*, vol. 93, no. 10, p. 103 306, Sep. 2008.

[22] F. L. Wong, M. K. Fung, S. L. Tao, S. L. Lai, W. M. Tsang, K. H. Kong, W. M. Choy, C. S. Lee, and S. T. Lee, "Long-lifetime thin-film encapsulated organic light-emitting diodes," *J. Appl. Phys.*, vol. 104, no. 1, pp. 014509-1–014509-4, Jul. 2008.

[23] F. C. Krebs, S. A. Gevorgyan, and J. Alstrup, "A roll-to-roll process to flexible polymer solar cells: Model studies, manufacture and operational stability studies," *J. Mater. Chem.*, vol. 19, no. 30, pp. 5442–5451, 2009.

[24] J. M. Luther, M. Law, M. C. Beard, Q. Song, M. O. Reese, R. J. Ellingson, and A. J. Nozik, "Schottky solar cells based on colloidal nanocrystal films," *Nano Lett.*, vol. 8, no. 10, pp. 3488–3492, Oct. 2008.

[25] J. Tang, L. Brzozowski, D. A. R. Barkhouse, X. Wang, R. Debnath, R. Wolowiec, E. Palmiano, L. Levina, A. G. Pattantyus-Abraham, D. Jamakosmanovic, and E. H. Sargent, "Quantum dot photovoltaics in the extreme quantum confinement regime: The surface-chemical origins of exceptional air- and light-stability," *ACS Nano*, vol. 4, no. 11, pp. 869–878, Jan. 2010.

[26] D. A. R. Barkhouse, A. G. Pattantyus-Abraham, L. Levina, and E. H. Sargent, "Thiols passivate recombination centers in colloidal quantum dots leading to enhanced photovoltaic device efficiency," *ACS Nano*, vol. 2, no. 11, pp. 2356–2362, Nov. 2008.

[27] J. Tang, G. Konstantatos, S. Hinds, S. Myrskog, A. G. Pattantyus-Abraham, J. Clifford, and E. H. Sargent, "Heavy-metal-free solution-processed nanoparticle-based photodetectors: Doping of intrinsic vacancies enables engineering of sensitivity and speed," *ACS Nano*, vol. 3, pp. 331–338, 2009.

[28] X. Gong, M. H. Tong, Y. J. Xia, W. Z. Cai, J. S. Moon, Y. Cao, G. Yu, C. L. Shieh, B. Nilsson, and A. J. Heeger, "High-detectivity polymer photodetectors with spectral response from 300 nm to 1450 nm," *Science*, vol. 325, no. 5948, pp. 1665–1667, Sep. 2009.

Photonic Integration Technologies for Large-Capacity Telecommunication Networks

Yoshinori Hibino

(Invited Paper)

NTT Photonics Laboratories, NTT Corporation, Atsugi 243-0198, Japan

DOI: 10.1109/JPHOT.2010.2047387
1943-0655/$26.00 ©2010 IEEE

Manuscript received February 14, 2010; revised March 4, 2010. Current version published April 23, 2010. Corresponding author: Y. Hibino (e-mail: hibino.yoshinori@lab.ntt.co.jp).

Abstract: Photonic integration technologies, which have been developed since the deployment of optical communications, are essential for increasing the network capacity at a low cost and with efficient power consumption. This paper reviews recent progress on photonic integrated devices for higher bit-rate and long-distance transmission technologies with advanced modulation formats.

Internet protocol (IP) data traffic has increased hugely with the increased access to such broadband access environments as fiber to the home (FTTH) and asynchronous digital subscriber lines (ADSLs), which have enabled the provision of video on demand, video chat, and other similar services. In Japan, IP data traffic doubles annually, and if this trend continues, in 10 years, the traffic will be 100 to 1000 times that of today.

A very-large-capacity backbone network is needed to support the huge traffic volume generated by access networks. For this purpose, various technologies, including time-division multiplexing (TDM) up to 40 Gb/s per channel, wavelength-division multiplexing (WDM), and a phase-shift keying (PSK) modulation method, have been developed and installed to support the existing IP traffic demand. In the near future, we will require WDM transmission systems with even greater transmission capacity. Recently, optical transmission technologies combined with coherent detection and digital signal processing technologies (digital coherent technologies) have been attracting a great deal of attention with a view to improving optical transmission performance.

Various optical components have been developed to construct telecommunication systems with large capacities and a variety of functions including WDM, FTTH, and ROADM using silica-based planar lightwave circuits (PLCs) [1], InP-based active components [2], and micro-optics technologies. PLC-based integrated devices have the advantages of high stability, reliability, and excellent optical performance, and we have recently been developing PLC-based components for high-bit-rate and large-capacity transmission systems [1]. InP-based active devices such as laser diodes and photodiodes are essential for optical telecommunications. Integration technologies based on InP active components have progressed greatly and can be used to construct highly functional devices. Micro-optics devices have continued to provide high levels of performance over many years. Photonic network systems are becoming more complicated, thus making it necessary to integrate more passive and active optical components on PLC platforms to achieve low cost and high flexibility. This paper reviews recent progress on such integrated components for large-capacity transmission technologies with advanced modulation formats.

Non-return-to-zero (NRZ) modulation formats have generally been used for systems operating at up to 10 Gb/s. However, advanced modulation formats are needed if we are to increase the capacity of transmission systems with high-bit-rate technologies of 40 Gb/s or more in WDM systems. Especially, the combination of advanced modulation formats and digital coherent detection techniques is emerging as one of the most promising solutions for these high-bit-rate transmission systems, because of the high tolerance to fiber dispersion and band filtering in the add/drop nodes [3]. With regard to advanced modulation formats, there have been reports on polarization-division multiplexing (PDM) and spectrally efficient modulation formats such as quadrature PSK (QPSK), orthogonal frequency-division multiplexing (OFDM), and multilevel quadrature amplitude multiplexing (QAM). By employing digital coherent detection techniques, the transmission performance, namely the product of transmission capacity and fiber length, has been greatly improved compared with direct detection methods such as RZ-DQPSK. The top data was currently obtained as about 112 Pb/s $\times$ km (15.5 Tb/s $\times$ 7200 km) [4].

Recently, transmission technologies with a PDM-QPSK modulation format and digital coherent detection have been extensively developed for 100-Gb/s-class WDM systems [5]–[7]. A transceiver for the 100G-level PDM-QPSK format consists of a digital signal processor (DSP), analog–digital converters (ADCs), and optical components. The role of digital signal processing in digital coherent technology is to recover the received signal data, which are degraded owing to such factors as chromatic dispersion and PMD during signal propagation through optical fibers. At the receiver, the data are digitally sampled by the ADCs. The ADC requires at least two samples per symbol. For instance, the ADC sampling speed for the PDM-QPSK modulation format with 112 Gb/s (28 GBd) is more than 56 GS/s. The digitized signal data are transported to the DSP and processed to compensate for the chromatic dispersion, polarization-mode dispersion (PMD), frequency offsets, and phase offsets. The digital coherent techniques have the advantages of being able to extract phase-modulation formats, utilize polarization modes, and increase sensitivity with a high power local oscillator.

It will become essential to integrate modulators and PDM components in the transmitter part in the transceiver for the PDM-QPSK schemes. To integrate two QPSK modulators and a PDM circuit with practical performance levels, we have developed a hybrid assembly technique with silica-based planar PLCs and $LiNbO_3$ (LN) phase modulators [8], in which we use a simple straight-line phase modulator array with LN, and butt joint it with PLCs on either side. Thus, we can achieve interferometer-type high-speed modulators with low losses and various circuit designs. We constructed the PDM-QPSK modulator using the PLC and LN hybrid-integration technique. The modulator consists of three chips: two 1.5%-δ PLCs, PLC-L and PLC-R, and an eight-channel array of LN phase modulators. This multichip circuit integrates two QPSK modulators (QPSK1 and 2) with two sub-MZMs (I and Q) nested in each, a polarization rotator using a half-wavelength plate (HWP), and a polarization beam combiner (PBC). The performance of the module is acceptable for the 100G-level PDM-QPSK. Using the modulator, we obtained the transmission data of 84 Pb/s $\times$ km (13.5 Tb/s $\times$ 6200 km) [9].

Higher order multilevel modulation formats are indispensable if we are to achieve systems with higher bit rates of more than 100 Gb/s and large capacities of over 10 Tb/s [10]–[15]. We have demonstrated the signal modulation and detection of a 240-Gb/s PDM 64-QAM signal [16]. A 20-GBd PDM 64-QAM signal was successfully generated by employing the optical synthesis technique with the PLC-LN hybrid modulator, in which six MZMs and low-loss asymmetric couplers are integrated with the PLC-LN hybrid configuration. The modulator generates a 64QAM signal through an optical signal synthesis with QPSK signals [28]–[30]. Fig. 1(a) shows the circuit configuration of the 64-QAM modulator. The modulator consists of two 1.5%-Δ PLCs, PLC-L and PLC-R, and a X-cutLN chip with an array of 12 high-speed phase modulators and six signal electrodes (coplanar waveguides). The asymmetric 1 $\times$ 3 splitter and 3 $\times$ 1 combiner (cascaded 4 : 3 and 2 : 1 Y-branches) were fabricated in PLC-L and PLC-R, respectively.

In the transmission experiment, the 64-QAM signal was generated by superposing three QPSK signals with an amplitude ratio of 4 : 2 : 1. The 20-GBd 64-QAM signals were then polarization multiplexed to form a 240-Gb/s PDM 64-QAM signal and were detected with a digital storage oscilloscope at 50 GS/s and postprocessed offline. Fig. 1(b) shows the constellation diagrams after equalization when the independent LO was used. The 64 signal points are clearly distinguished in

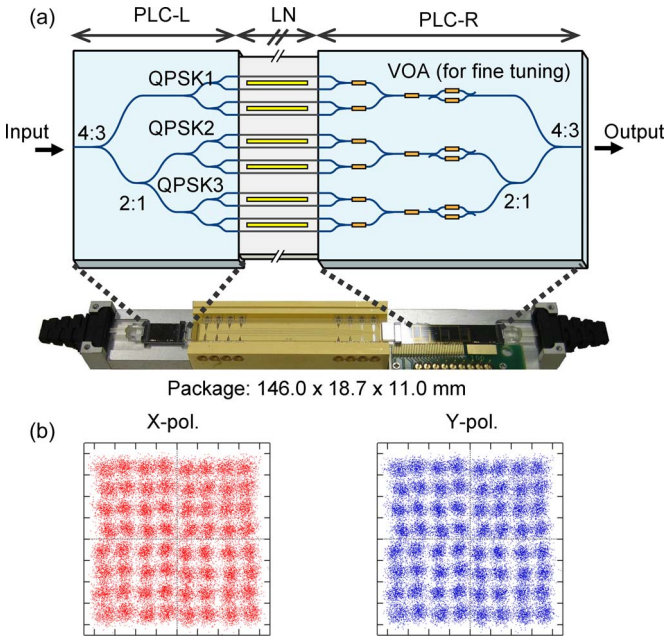

Fig. 1. (a) Configuration of 64-QAM modulator. (b) Constellation diagrams of 64-QAM modulation.

both polarizations, confirming that we achieved successful polarization demultiplexing and equalization. The spectral width of the main lobe of this modulation format was 40 GHz, which was one sixth of the line rate. Because of this narrow spectral width, an SE of 8 b/s/Hz, which is the highest so far, can be expected for WDM transmission with a spacing of 25 GHz.

This review described photonics-integrated devices for the high-bit-rate transmission technologies with advanced modulation formats such as 100G-class PDM-QPSK and 64-QAM. The devices exhibited sufficiently high levels of performance for practical use. Since they provide the advantages of mass producibility, dense integration, and high stability, photonics-integrated devices will contribute to further advances in high-bit-rate transmission.

References

[1] A. Himeno, K. Kato, and T. Miya, "Silica-based planar lightwave circuits," *IEEE J. Sel. Topics Quantum Electron.*, vol. 4, no. 6, pp. 913–924, Nov./Dec. 1998.
[2] R. Nagarajan, M. Kato, S. Hurtt, A. Dentai, J. Pleumeekers, P. Evans, M. Missey, R. Muthiah, A. Chen, D. Lambert, P. Chavarkar, A. Mathur, J. Bäck, S. Murthy, R. Salvatore, C. Joyner, J. Rossi, R. Schneider, M. Ziari, F. Kish, and D. Welch, "Monolithic, 10 and 40 channel InP receiver photonic integrated circuits with on-chip amplification," presented at the Optical Fiber Commun. Conf. Expo., Anaheim, CA, 2007, PDP 32.
[3] K. Roberts, M. O'Sullivan, K.-T. Wu, H. Sun, A. Awadalla, D. J. Krause, and C. Laperle, "Performance of dual-polarization QPSK for optical transport systems," *J. Lightw. Technol.*, vol. 27, no. 16, pp. 3546–3559, Aug. 2009.
[4] M. Salsi *et al.,* presented at the Eur. Conf. Optical Commun., 2009, PD2.5.
[5] E. Yamada *et al.,* presented at the Optical Fiber Commun. Conf. Expo., 2008, Paper PDP8.
[6] A. Sano *et al.,* presented at the Eur. Conf. Optical Commun., 2008, PD 1.7.
[7] P. J. Winzer, G. Raybon, S. Chandrasekhar, C. R. Doerr, T. Kawanishi, T. Sakamoto, and K. Higuma, "10 × 107 Gb/s NRZ-DQPSK transmission at 1.0 b/s/Hz over 12 × 100 km including 6 optical routing nodes," presented at the Optical Fiber Commun. Conf. Expo./NFOEC, Anaheim, CA, 2007, PDP24.
[8] H. Yamazaki *et al.,* presented at the Eur. Conf. Optical Commun., 2008, Mo.3.C.1.
[9] H. Matsuda *et al.,* presented at the Optical Fiber Commun. Conf. Expo., 2009, PDPB5.
[10] M. Nakazawa *et al.,* presented at the Eur. Conf. Optical Commun., 2008, Tu1.E.1.
[11] N. Kikuchi *et al.,* presented at the Optical Fiber Commun. Conf. Expo., 2009, OWG1.
[12] M. Nakamura and Y. Kamio, "30-Gbps (5-Gsymbol/s) 64-QAM self-homodyne transmission over 60-km SSMF using phase-noise cancelling technique and ISI-suppression based on electronic digital processing," presented at the Optical Fiber Commun. Conf. Expo., San Diego, CA, 2009, OWG4.

[13] H. Takahashi, A. Al Amin, S. L. Jansen, I. Morita, and H. Tanaka, "DWDM transmission with 7.0-bit/s/Hz spectral efficiency using 8 × 65.1-Gbit/s coherent PDM-OFDM signals," presented at the Optical Fiber Commun. Conf. Expo., San Diego, CA, 2009, PDPB7.
[14] A. H. Gnauck, P. J. Winzer, C. R. Doerr, and L. L. Buhl, "10 × 112 Gb/s PDM 16-QAM transmission over 630 km of fiber with 6.2-b/s/Hz spectral efficiency," presented at the Optical Fiber Commun. Conf. Expo., San Diego, CA, 2009, PDPB8.
[15] H. Yamazaki, T. Yamada, T. Goh, Y. Sakamaki, and A. Kaneko, "64QAM modulator with a hybrid configuration of silica PLCs and LiNbO3 phase modulators for 100-Gb/s applications," in *Proc. ECOC*, 2009, pp. 1–4.
[16] A. Sano *et al.,* presented at the Eur. Conf. Optical Commun., 2009, PD2.2.

Ultrafast VCSELs for Datacom

Dieter Bimberg

(Invited Paper)

Institut für Festkörperphysik und Zentrum für Nanophotonik,
Technische Universität Berlin, 10623 Berlin, Germany

DOI: 10.1109/JPHOT.2010.2047386
1943-0655/$26.00 ©2010 IEEE

Manuscript received February 2, 2010; revised March 26, 2010. Current version published April 23, 2010. The work at TU Berlin was supported by EU FP7 under Grant 224211 (the "VISIT" Project), the DFG (Sfb 787), and the State of Berlin (100 x 100 Optics). Corresponding author: D. Bimberg (e-mail: bimberg@physik.tu-berlin.de).

Abstract: Vertical-cavity surface-emitting lasers (VCSELs) are broadly used as low-cost reliable light sources for high-speed data communication in local area and storage area networks (LANs/SANs), as well as for computer and consumer applications. The rapid increase of the serial transmission speed and the limitations of copper-based links at bit rates beyond 10 Gb/s and distances beyond 1 m extend the applications of fiber-optic interconnects to progressively shorter distances. The wavelength of 850 nm is standard for LAN/SAN applications over OM3 and OM4 multimode fibers and will continue playing an important role in future standards. In the last year, impressive results were achieved with oxide-confined VCSELs emitting at 850 nm. The data transmission rate could be shifted from 30 to 38 Gb/s, which is presently the highest data rate for any oxide-confined VCSELs.

Index Terms: Data communication, interconnections, local area networks, optical interconnects, semiconductor lasers, storage area networks, vertical cavity surface emitting lasers.

Our modern communication society is increasingly hungry for bandwidth. Over the past few years, this hunger has been a driver for fast increases of memory capacity, in particular of flash memories, of the computational power of microprocessors, and the rapidly increasing demand for higher bit rates of data communication links. Interfaces for serial transmission at rates beyond 10 Gb/s are presently standardized for a variety of applications, including (with an expected data rate) Fibre Channel FC32G (34 Gb/s), InfiniBand (20 Gb/s), common electrical interface CEI (25–28 Gb/s), and universal serial bus protocol USB 4.0 (25 Gb/s or beyond). Because of the fundamental electro-magnetic limitations of copper-based links for bit rates beyond 10 Gb/s and distances beyond 1 m, fiber-based optics has now become indispensable for ultrafast data communication [1]–[4]. The rapidly increasing acceptance of short-reach optical interconnects and their penetration into traditional copper interconnect markets is enabled by the unique properties of advanced vertical-cavity surface-emitting lasers (VCSELs) such as a near-circular output beam with a small divergence angle, low threshold current and power consumption, planar processing and on-wafer characterization enabling inexpensive production and testing, high reliability, and easy packaging.

Oxide-confined VCSELs dominate today [5], [6]. Such devices have been available on the market for about 10 years, having established themselves as being very reliable, with impressive possibilities for high-volume, high-yield, and inexpensive manufacturing. Currently, up to 10-Gb/s oxide-confined VCSELs can be acquired from a variety of companies. Higher bit rates created a need for further research, and development in this area focused on increasing the modulation bandwidth, while

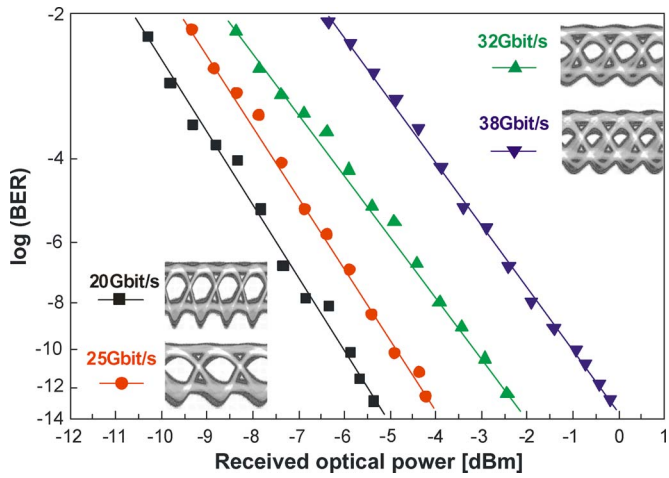

Fig. 1. Bit-error-rate measurements at 20 °C in a back-to-back configuration for the oxide-confined InGaAlAs VCSEL with the aperture diameter of 9 μm at 20, 25, 32, and 38 Gb/s for a bias current of 9 mA; the inset shows the corresponding optical eye diagrams.

simultaneously improving device reliability, power efficiency, modal and spectral characteristics, thermal management, and other figures of merit. The development of VCSELs at a few standard wavelengths (primarily around 850, 980, 1100, 1300 and 1550 nm) are presently in focus. The wavelength of 850 nm is particularly important, since it is the standard wavelength for local area and storage area networks (LANs/SANs) and is expected to play an increasingly important role for other standards.

Rate equation theory [7] predicts that the high-frequency properties of a semiconductor laser are described by the small-signal modulation transfer function, which depends on three parameters: relaxation oscillation frequency, damping, and the cutoff frequency of electric parasitics. Consequently, three types of limits exist, which can prevent high-speed operation: the thermal limit, the damping or internal limit, and the limit caused by electrical parasitics. Commonly, all three types of limitations are of importance, such that combined concepts must be developed to increase the laser bandwidth. Additionally, practical requirements like device reliability and simple fabrication technology must be considered as well.

Over the past few years, immense progress has been made and concepts have been developed to shift the limits to ever higher speed. Small-signal modulation bandwidths of 21 GHz and 24 GHz have been demonstrated for 4-μm-aperture-diameter VCSELs emitting at 850-nm [8] and 1100-nm devices based on a buried tunnel junction [9]. Thermal, intrinsic, and parasitic properties of the VCSELs were improved simultaneously. Large signal modulation at 35 Gb/s using 980-nm VCSELs with a tapered oxide aperture and deep oxidation layers [10] at 40 Gb/s using 1100-nm VCSELs with tunnel junctions [11] and at 22 Gb/s using 1550-nm VCSELs with a buried tunnel junction [12] have been reported. No data rates at or beyond 30 Gb/s were reported until 2008 for the commercially most relevant wavelength of 850 nm. Progress at 850 nm is more difficult to achieve, since e.g., the depth of the potential localizing the carriers is minimal.

Eventually, in 2008, large signal modulation at 30 Gb/s was demonstrated for oxide-confined VCSELs emitting at 850 nm [13]. Data rates higher than 30 Gb/s with 850-nm oxide-confined VCSELs were then reported last year by the group of A. Larsson the Chalmers University of Technology and by the Technical University of Berlin. 32-Gb/s error-free operation was demonstrated at sensationally low current densities of $\sim$10 kA/cm^2 [14], [15]. The main concepts used for these devices were double oxide apertures to reduce parasitic capacitance and InGaAs strained quantum wells (QWs) for the active layer to increase the differential gain and binary alloys in most of the bottom mirror to decrease the thermal resistance of the laser. It appeared that the 40-Gb/s directly modulated VCSELs were still a long way off.

A little bit later, a big step forward followed. The Technical University of Berlin and VI Systems GmbH demonstrated 38-Gb/s error-free operation of 850-nm oxide-confined VCSELs [16], [17]. By applying several concepts, among other strained InGaAs QWs in the active region, optimized

device design with thick dielectric layers for smaller parasitic capacitances, and two mesas for better thermal conductivity, it was possible to demonstrate the first oxide-confined VCSELs ever operating at data rates up to 38 Gb/s (see Fig. 1). These are the fastest 850-nm VCSELs in use today. Electrical parasitics and the thermal resistance of the laser were appreciably reduced, and the internal properties of the gain medium were improved. Optimization of both epitaxial structure and design has led to high-speed operation without increasing the current density beyond the range of $\sim$10 kA/cm^2, which is an important consideration for device reliability. Cutoff frequencies of electrical parasitics up to 27 GHz were extracted from the measurements, showing the positive impact of applying thick dielectric layers and small mesa sizes.

Thus, 2009 has seen great progress in the field of high-speed 850-nm VCSELs for datacom applications. Large-signal operation of oxide-confined VCSELs at or beyond 40 Gb/s, which seemed hardly possible at the beginning of the year, is now within reach. Oxide-confined VCSELs operating reliably at 25 and 40 Gb/s will be on the market in a few years time. This development will serve the need of society for faster communication and drive progress for a better future.

Acknowledgment

The author would like to thank A. Mutig for his assistance with this manuscript and J. A. Lott, S. A. Blokhin, G. Fiol, N. N. Ledentsov, and A. M. Nadtochiy for contributing to the work at TU Berlin.

References

[1] D. Collins, N. Li, D. Kuchta, F. Doany, C. Schow, C. Helms, and L. Yang, "Development of high-speed VCSELs: 10 Gb/s serial links and beyond," *Proc. SPIE*, vol. 6908, pp. 690809-1–690809-9, 2008.

[2] F. E. Doany, L. Schares, C. L. Schow, C. Schuster, D. M. Kuchta, and P. K. Pepeljugoski, "Chip-to-chip optical interconnects," presented at the Optical Fiber Communication Conf. (OFC), Anaheim, CA, 2006, Paper OFA3.

[3] D. G. Kam, M. B. Ritter, T. J. Beukema, J. F. Bulzacchelli, P. K. Pepeljugoski, Y. H. Kwark, L. Shan, X. Gu, C. W. Baks, R. A. John, G. Hougham, C. Schuster, R. Rimolo-Donadio, and B. Wu, "Is 25 Gb/s on-board signaling viable?" *IEEE Trans. Adv. Packag.*, vol. 32, no. 2, pp. 328–344, May 2009.

[4] J. A. Kash, F. Doany, D. Kuchta, P. Pepeljugoski, L. Schares, J. Schaub, C. Schow, J. Trewhella, C. Baks, Y. Kwark, C. Schuster, L. Shan, C. Parel, C. Tsang, J. Rosner, F. Libsch, R. Budd, P. Chiniwall, D. Guckenberger, D. Kucharski, R. Dangel, B. Offrein, M. Tan, G. Trott, D. Lin, A. Tandon, and M. Nystrom, "Terabus: A chip-to-chip parallel optical interconnect," in *Proc. 18th Annu. Meeting IEEE LEOS*, Sydney, Australia, 2005, pp. 363–364, Paper TuW3.

[5] D. L. Huffaker, D. G. Deppe, K. Kumar, and T. J. Rogers, "Native-oxide defined ring contact for low threshold vertical-cavity lasers," *Appl. Phys. Lett.*, vol. 65, no. 1, pp. 97–99, Jul. 1994.

[6] K. D. Choquette, R. P. Schneider, Jr., K. L. Lear, and K. M. Geib, "Low threshold voltage vertical-cavity lasers fabricated by selective oxidation," *Electron. Lett.*, vol. 30, no. 24, pp. 2043–2044, Nov. 24, 1994.

[7] L. A. Coldren and S. W. Corzine, *Diode Lasers and Photonic Integrated Circuits*. New York: Wiley, 1995.

[8] K. L. Lear, V. M. Hietala, H. Q. Hou, M. Ochiai, J. J. Banas, B. E. Hammons, J. Zolper, and S. P. Kilcoyne, "Small and large signal modulation of 850 nm oxide-confined vertical cavity surface emitting lasers," in *Advances in Vertical Cavity Surface Emitting Lasers. Washington, DC: OSA, 1997, pp. 69–74.*

[9] T. Anan, N. Suzuki, K. Yashiki, K. Fukatsu, H. Hatakeyama, T. Akagawa, K. Tokutome, and M. Tsuji, "High-speed InGaAs VCSELs for optical interconnections," in *Proc. Int. Symp. VCSELs Integr. Photon.*, Tokyo, Japan, Dec. 17–18, 2007, pp. 76–78.

[10] Y.-C. Chang, C. S. Wang, and L. A. Coldren, "High-efficiency, high-speed VCSELs with 35 Gbit/s error-free operation," *Electron. Lett.*, vol. 43, no. 19, pp. 1022–1023, Sep. 2007.

[11] N. Suzuki, T. Anan, H. Hatakeyama, K. Fukatsu, K. Yashiki, K. Tokutome, T. Akagawa, and M. Tsuji, "High speed 1.1-μm-range InGaAs-based VCSELs," *IEICE Trans. Electron.*, vol. E92-C, no. 7, pp. 942–949, Jul. 2009.

[12] W. Hofmann, M. Müller, A. M. Nadtochiy, C. Meltzer, A. Mutig, G. Böhm, J. Rosskopf, D. Bimberg, M.-C. Amann, and C. Chang-Hasnain, "22 Gb/s long wavelength VCSELs," *Opt. Express*, vol. 17, no. 20, pp. 17 547–17 554, Sep. 28, 2009.

[13] R. Johnson and D. Kuchta, "30 Gb/s directly modulated 850 nm datacom VCSELs," presented at the Conf. Lasers Electro-Optics (CLEO), San Jose, CA, 2008, post-deadline Paper CPDB2.

[14] P. Westbergh, J. S. Gustavsson, Å. Haglund, A. Larsson, F. Hopfer, D. Bimberg, and A. Joel, "32 Gbit/s transmission experiments using high speed 850 nm VCSELs," presented at the Conf. Lasers Electro-Optics/Int. Quantum Electronics Conf. (CLEO/IQEC), Baltimore, MD, Jun. 1, 2009, Paper CMGG6.

[15] P. Westbergh, J. S. Gustavsson, Å. Haglund, A. Larsson, F. Hopfer, G. Fiol, D. Bimberg, and A. Joel, "32 Gbit/s multimode fiber transmission using high-speed, low current density 850 nm VCSEL," *Electron. Lett.*, vol. 45, no. 7, pp. 366–368, Mar. 26, 2009.

[16] S. A. Blokhin, J. A. Lott, A. Mutig, G. Fiol, N. N. Ledentsov, M. V. Maximov, A. M. Nadtochiy, V. A. Shchukin, and D. Bimberg, "Oxide-confined 850 nm VCSELs operating at bit rates up to 40 Gbit/s," *Electron. Lett.*, vol. 45, no. 10, pp. 501–503, May 7, 2009.

[17] A. Mutig, S. A. Blokhin, A. M. Nadtochiy, G. Fiol, J. A. Lott, V. A. Shchukin, N. N. Ledentsov, and D. Bimberg, "Frequency response of large aperture oxide-confined 850 nm vertical cavity surface emitting lasers," *Appl. Phys. Lett.*, vol. 95, no. 13, p. 131 101, Sep. 2009.